AN ARM SIMULATOR FOR BLOOD PRESSURE MEASUREMENT

A dissertation submitted in partial fulfilment of the requirements for the degree of

Master of Technology

by

Omer Motasim Alim Mostafa

(163072001)

under the supervision of

Prof. P. C. Pandey

Department of Electrical Engineering

Indian Institute of Technology Bombay

June 2018

Left blank

Indian Institute of Technology Bombay
Department of Electrical Engineering

M. Tech. Dissertation Approval

This dissertation entitled "**An arm simulator for blood pressure measurement**" by **Omer Motasim Alim Mostafa** (Roll No.**163072001**) is approved, after the successful completion of *viva voce* examination, for the award of the degree of **Master of Technology** in **Electrical Engineering** with specialization in **Electronic Systems**.

Supervisor:	PCPandey 30/06/2018	(Prof. P. C. Pandey)
Examiners:	V. Rajbabu	(Prof. V. Rajbabu)
		(Prof. J. John)
Chairman:		(Prof. J. John)

Date: 30 June 2018
Place: Mumbai

Left blank

DECLARATION

I declare that this written submission represents my ideas in my own words and where ideas or words are taken from others, I have adequately cited and referenced the original sources. I also declare that I have adhered to all principles of academic honesty and integrity and I have not misrepresented or fabricated or falsified any idea/data/fact/source in my submission. I understand that any violation of the above will be cause for disciplinary action by the Institute and can also evoke penal action from the sources which have thus not been properly cited or from whom proper permission has not been taken when needed.

Omer Motasim Alim Mostafa

(Roll No. 163072001)

Date: 30 June 2018

Place: Mumbai

Left blank

Omer Mostafa / Prof. P. C. Pandey (Supervisor), “An arm simulator for blood pressure measurement,” *M.Tech. dissertation*, Department of Electrical Engineering, Indian Institute of Technology Bombay, July 2018.

ABSTRACT

Arm simulator for blood pressure (BP) measurement is an instrument that mimics the behavior of the human arm during the noninvasive BP measurement. It can be useful for training of the healthcare workers by getting them exposed to a wide range of normal and abnormal cardiovascular conditions and can also be used for calibration and evaluation of automatic BP monitors. The objective of the project is to develop a compact arm simulator for both auscultatory and oscillometric methods of BP measurement. It is in the form of a cylinder for wrapping the cuff of the BP monitor around it. The pressure of the cuff is measured using a pressure sensor connected to the tube between the cuff and the BP monitor. It is designed as a microcontroller-based instrument with a facility for wirelessly setting the simulation parameters including the systolic pressure, diastolic pressure, heart rate, arrhythmia level, and the pulse volume, using a graphical user interface (GUI) on a PC or a handheld computing device with Bluetooth interface. The simulation of the arm for the blood pressure measurement is carried out by generating the Korotkoff sounds for auscultatory method and pulsatile vibrations for the oscillometric method at each heartbeat with the amplitude and timing in accordance with the measured value of the cuff pressure and the set simulation parameters.

Left blank

CONTENTS

Left blank

LIST OF FIGURES

LIST OF TABLES

Left blank

LIST OF SYMBOLS

A	The arrhythmia level as a percentage with the range [0, 50].
ACLK	The source clock of DAC that is scaled down by 16 to give F_{DAC}.
F_{CY}	The frequency of the main system clock of the microcontroller.
F_{DAC}	The operating frequency of the DAC.
$F_{Sampling}$	The sampling frequency of the DAC.
F_{VCO}	The frequency of the PPL output clock.
F_1	The scaling factor for the generated Korotkoff sounds.
F_2	The scaling factor for the generated oscillations.
K-sound	Korotkoff sound.
N_{TB}	The mean heartbeat interval T_B represented in number of samples.
N_{TB0}	The mean heartbeat interval T_{B0} represented in number of samples.
R	The magnitude of the random number generated from the feedback shift register with the range [0, 127].
r	Random variable uniformly distributed in the range [–1,1].
S	The sign of the random number generated from the feedback shift register.
T_B	Heartbeat interval.
T_{B0}	Heartbeat interval with regular heartbeats.
T_{CY}	The period of the main system clock of the microcontroller.
$T_{Interrupt}$	The time interval between two consecutive interrupts of Timer 3.
T_{off}	The off-period during which no sound is produced.
T_{on}	The on-period during which the Korotkoff sound is output.
T_{Timer3}	The period of the clock of Timer 3.
V_S	The supply voltage of the pressure sensor.
a	Arrhythmia level representing the maximum deviation as a fraction of the mean interval T_{B0} with the range [0, 0.5].
ΔT_{B0}	Maximum variation in T_B.

Left blank

LIST OF ABBREVIATIONS

ADC	Analog-to-digital convertor.
AL	Arrhythmia level.
ANSI	American national standards institute.
AV	Atrioventricular
BHS	British hypertension society.
BP	Blood pressure.
bpm	Beats per minute.
BTL	Bridge-tied load.
Ch	Channel
COM	Communication.
CP	Cuff pressure.
DAC	Digital-to-Analog convertor.
DP	Diastolic pressure.
DSO	Digital oscilloscope.
ECG	Electrocardiogram.
ESH	European society of hypertension.
GUI	Graphical user interface.
HR	Heart rate.
I/O	Input/output.
ISR	Interrupt service routine.
LED	Light emitting diode.
MAP	Mean arterial pressure.
Min	Minimum.
NIBP	Non-invasive blood pressure.
PCB	Printed circuit board.
PLA	Polylactic acid.
PLL	Phase-locked loop.
PV	Pulse volume.
PWM	Pulse width modulation.
SA	Sino-atrial
SP	Systolic pressure.
UART	Universal asynchronous receiver-transmitter.
USB	Universal serial bus.

Left blank

Chapter 1

INTRODUCTION

1.1 Overview

Measurement of blood pressure (BP) is a basic tool in the diagnosis and management of cardiovascular diseases. It is particularly important because hypertension (high BP) and hypotension (low BP) may not show any symptoms in the initial stages. For the BP measurement to be accurate, the instrument used should be calibrated and tested, and the healthcare worker carrying out the measurement should be well trained.

It is difficult to compare two non-simultaneous BP measurements due to beat-to-beat variations. Further, as the BP also varies from site to site, human subjects are considered a poor reference for calibration of BP measurement instruments [1]. Currently, the calibration is carried out by taking measurements from a large number of human subjects to average out the errors [2]. During training of healthcare workers, the instructor needs to take measurements and compare it with the trainee's measurements. As the two measurements are not simultaneously carried out, they may not correspond to the same value. The available subjects often belong to the healthy population and may not represent the BP characteristics observed in the patients. Therefore, practicing on normal subjects does not give the trainee enough exposure to the difficulties in measuring the BP of patients with abnormal cardiac conditions like hypertension and arrhythmia [3].

Several arm simulators [4], [5], [6], [7], [8], [9], [10], [11], [12], [13], [14] that mimic the behavior of the human arm for BP measurement have been developed as an alternative method for calibration and evaluation of noninvasive blood pressure (NIBP) monitors and for training purposes. Most of these simulators lack the ability to simulate a wide range of abnormal conditions and the flexibility in setting the simulation parameters.

1.2 Project objective

The objective of this project is to develop a compact instrument to serve as an arm simulator for BP measurement. It is to be in the shape of a rigid cylinder for wrapping the cuff of the BP monitor around it. It is to be useable for both auscultatory and oscillometric methods. The instrument is to be designed so that the cuff pressure is measured using a pressure sensor connected to the tube between the cuff and the monitor via a T-connector. A microcontroller, with an on-chip analog-to-digital converter (ADC) and a digital-to-analog converter (DAC), is to be used to generate the Korotkoff sound and the pressure pulses with settable amplitude. A user-friendly GUI for use on a PC and Android-based handheld computing devices is to be developed so that the simulation parameters can be set wirelessly. This approach of the

instrument design is selected to reduce the cost involved in providing a user interface through specialized hardware in the instrument and to simplify the instrument packaging.

1.3 Report outline

The second chapter provides a description of the physiological origins of blood pressure, some of the noninvasive techniques of BP measurement, and a comparison between some of the previously developed arm simulators. Chapter 3 describes the design approach and provides a detailed description of the hardware. Chapter 4 describes the software for the GUIs and the microcontroller program for controlling the instrument operation. Chapter 5 presents the test results. The last chapter summarizes the work done with some suggestions for further development.

Chapter 2

NONINVASIVE BLOOD PRESSURE MEASUREMENT AND ARM SIMULATORS

2.1 Physiology of the heart

The cardiovascular system has three main components: blood, blood vessels through which the blood is circulated throughout the whole body, and the heart, which acts as a pump that generates the driving force for blood to flow [16], [17]. The heart, as shown in Figure 2.1, functions as a pump. It comprises the left heart and the right heart, both having two chambers known as the atrium and the ventricle. The atrium of the right heart receives the de-oxygenated blood from the head and upper extremity through the superior vena cava and from the trunk and lower extremity through the inferior vena cava. The blood is pumped by the ventricle of the right heart to the lungs through the pulmonary arteries. The atrium of the left heart receives the oxygenated blood from the lungs through the pulmonary veins. The blood is pumped by the ventricle of the left heart through the aorta to the peripheral organs.

The events that occur from the beginning of one heartbeat to the beginning of the next one are known as the cardiac cycle [16]. The cardiac cycle for the left heart is shown in Figure 2.2. It starts when a cardiac impulse is generated in the sino-atrial (SA) node and the resulting depolarization spreads through the left and right atriums. It causes the P wave to appear in the electrocardiogram (ECG). The atriums contract, which causes a slight rise in the atrial pressure curve marked as the ‘a’ wave and the blood is pushed into the ventricles. There is a plateau in the ventricle volume during this period of ventricle filling. After some delay, the cardiac impulse reaches the ventricles through the atrioventricular (AV) node. The ventricular depolarization occurs resulting in appearance of the QRS complex in the ECG diagram. As a result, the ventricles contract, resulting in the closure of the AV valves (tricuspid and mitral valves) due to the backward pressure. The pressure inside the ventricles is yet not enough to push the semilunar (aortic and pulmonary) valves open. Subsequently, the pressure in the ventricles rises rapidly as shown in the ventricle pressure curve in Figure 2.2. The second rise in the atrial pressure curve, marked as the ‘c’ wave, occurs mainly due to bulging of the AV valves into the atriums when the ventricles pressure increases.

The first heart sound shown in the phonocardiogram is caused by the closure of the AV valves. It lasts for a relatively long time and it has a low pitch. This period when the ventricles are contracted but all the valves are closed is known as the isovolumic contraction period. When the pressure inside the left ventricle exceeds that inside the aorta, the aortic valve is forced open and the blood is ejected into the aorta. At this time, the aortic pressure starts increasing and the rapidness of the ventricle pressure rise decreases considerably. The volume of the ventricles

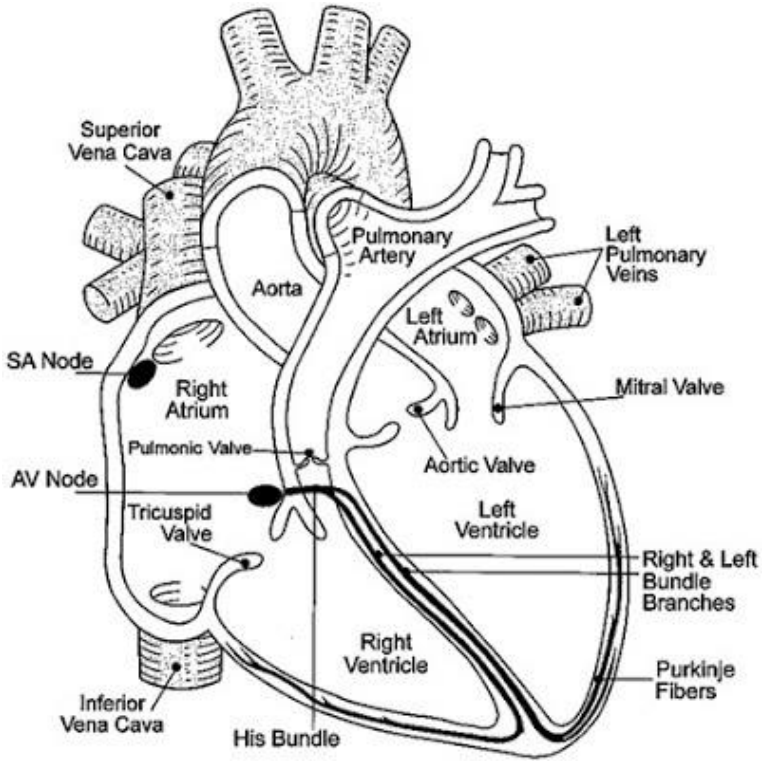

Figure 2.1: Anatomy of the heart (adapted from [17]).

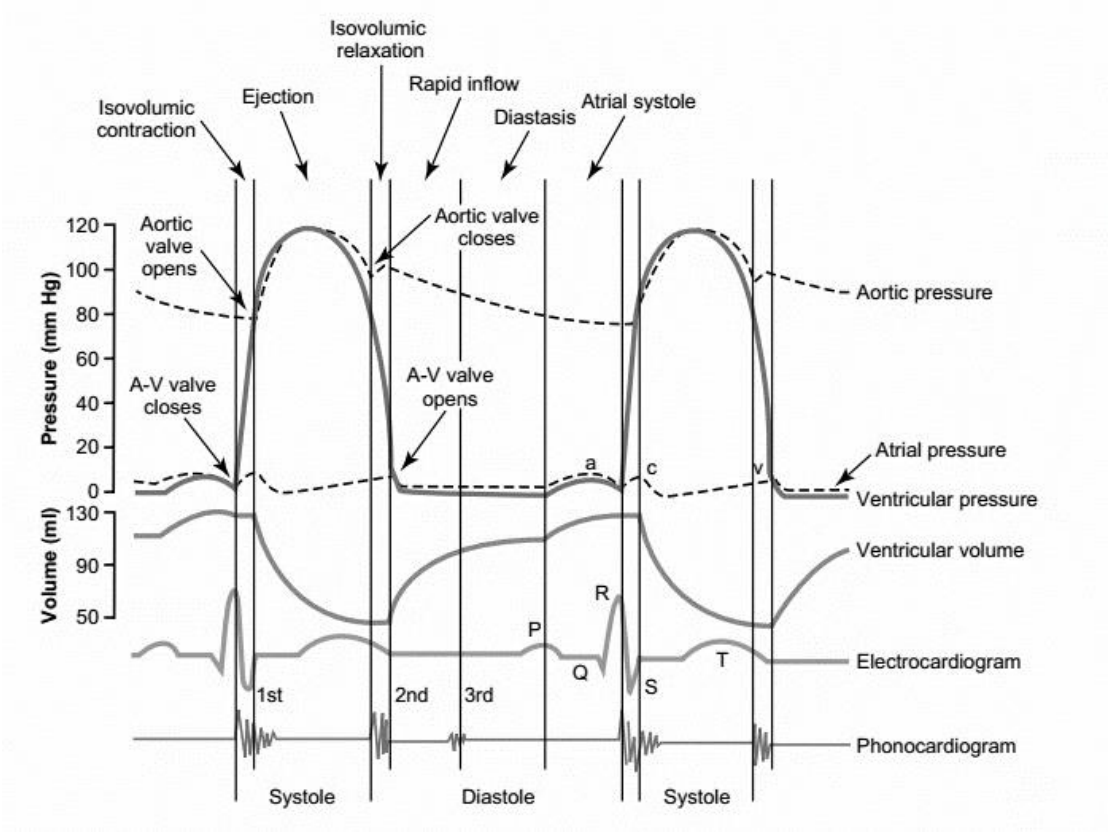

Figure 2.2: Events in the cardiac cycle of the left heart (adapted from [16]).

also steadily decreases. The ventricles repolarize, and this event is associated with the T wave in the ECG. The left ventricle pressure starts falling. As it becomes lower than the aortic pressure, the aortic valve closes, ending the period of ejection. The second heart sound is caused by the closure of the semilunar valves. It is a quick snap and it lasts for a shorter time than the first heart sound. The period when the ventricles are relaxing with both the valves closed is known as the isovolumic relaxation period. During this period, a notch known as incisura occurs in the aortic pressure curve. It is caused by the accumulation of the blood in the aorta, which presses on the walls of the aortic valve causing the blood to flow back into the left ventricle. This flow is suddenly stopped by aortic valve closure. The slight rise in the atrial pressure curve marked as the 'v' wave occurs due to the storage of the blood in the left atrium, before the mitral valve is opened. When the AV valve is opened, the accumulated blood in the left atrium starts flowing into the left ventricle. Generation of the next cardiac impulse in the SA node causes the contraction of the atriums and beginning of the next cardiac cycle [16]. The relaxation period in the cardiac cycle when the ventricles are filled with the blood is known as the diastole, while the contraction period when the ventricles are pumping the blood is known as the systole.

The contraction and relaxation of the atrium and ventricle muscles normally occur in a repeated rhythmic pattern that may be disturbed due to some diseases like ischemia. The abnormal heart rhythm is known as arrhythmia. The heart rate exceeding 100 beats per minute (bpm) is known as tachycardia. It is known as bradycardia if the heart rate is less than 60 bpm. Sometimes, the contraction sequence of the atriums and ventricles may be abnormal, significantly affecting the effectiveness of the heart [16], [18].

The pressure of the blood in the aorta and other arteries varies during the cardiac cycle. The minimum pressure is known as the diastolic pressure (DP) and the maximum pressure is known as the systolic pressure (SP). These two values measured noninvasively in the brachial artery are considered clinically important. The DP and SP values for adults with normal health are around 80 and 120 mmHg, respectively [16].

2.2 Blood pressure measurement techniques

The BP measurement techniques can be grouped as invasive and noninvasive. For invasive BP measurement, a probe is inserted into the artery. It gives accurate readings, but the probe carries the risk of causing infection. Noninvasive measurement, although less accurate, is preferred for routine BP checking. It is usually carried out using the sphygmomanometer technique. A cuff is wrapped around the arm rested at the level of the heart. The cuff is inflated so that the pressure inside the cuff is higher than the pressure of the blood inside the brachial artery and the blood flow is stopped. The cuff is slowly deflated, the blood flows in a turbulent way after heartbeats. As the cuff is deflated further, the blood flow increases and becomes more

turbulent. The turbulence decreases and eventually the flow becomes laminar. The value of the pressure in the cuff at the moment the blood starts flowing again is taken as the SP value. The value when the flow has the highest turbulence is taken as the value of the mean arterial pressure (MAP), which represent the mean of the BP over one cardiac cycle. The value when the blood flow becomes laminar is taken as the DP value. There are two commonly used methods to detect these three events for BP measurement: the auscultatory and the oscillometric methods.

2.2.1 Auscultatory method

This method is mostly used for manual BP measurements. The cuff of the instrument is wrapped around the arm and it is inflated by squeezing a bulb or using an electric pump. The pressure in the cuff is measured using a mercury manometer, or a pressure gauge with a dial. A stethoscope is used to detect the sound that is generated due to the turbulence in the blood flow inside the artery, which is known as the Korotkoff sound [19], [20]. The first Korotkoff sound is heard at the first heartbeat after the cuff pressure falls below SP. The Korotkoff sounds get louder with further decrease in the cuff pressure, with the loudest sound corresponding to the MAP value. The loudness of the sounds decreases as the cuff pressure is further decreased. The DP value is the cuff pressure when the last Korotkoff sound is heard before the sound disappears and the blood flow becomes laminar [20], [21]. Figure 2.3 shows the variation of Korotkoff sound with cuff deflation and Figure 2.4 shows the variation in the amplitude and wave shape of the Korotkoff sound.

It may be noted that the measured values could be erroneous if the cuff is deflated too fast because the heartbeat may not occur when the cuff pressure is near the actual SP or DP. Too slow deflation may cause discomfort to the subject or may even alter the pressure values. A period of diminished Korotkoff sounds known as the auscultatory gap [22] may occur during the BP measurement, requiring palpation of the radial pulse in place of detection of the Korotkoff sound. This method is highly subjective, as it depends on the manner of cuff deflation and it is also affected by the hearing acuity of the person making the measurement. With decrease in the blood pressure, the spectrum of the Korotkoff sound shifts to lower frequencies, causing failure of the auscultatory method in hypotensive patients due to lower sensitivity of the human ear in this frequency band [23].

2.2.2 Oscillometric method

In this method, a pressure transducer is used to monitor the pressure in the cuff. The cuff is first inflated to a value higher than the SP and then gradually deflated. When the cuff pressure falls just below the SP, the turbulent flow of the blood causes the walls of the artery to vibrate with every heartbeat. These oscillations are detected by the transducer of the system monitoring the cuff pressure. As the cuff pressure decreases further, the oscillations increase in amplitude.

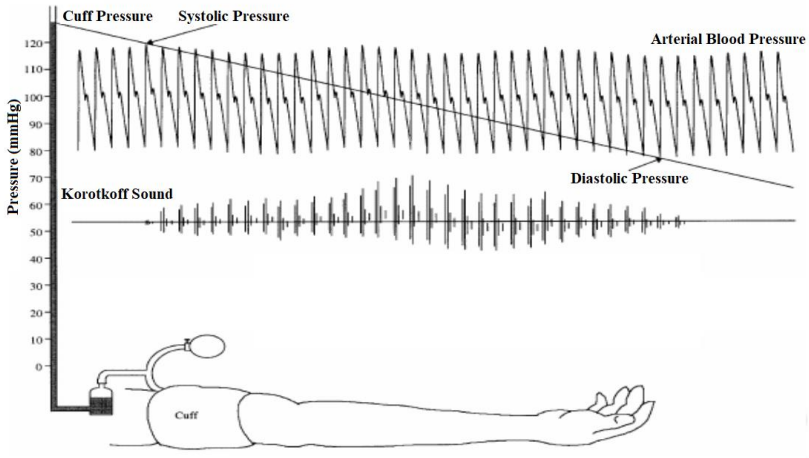

Figure 2.3: Arterial pressure and Korotkoff sound during deflation of the cuff in the auscultatory method, (adapted from [24]).

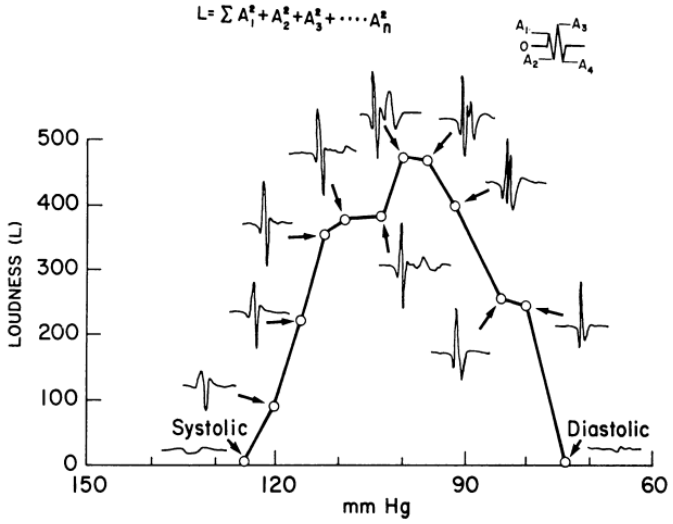

Figure 2.4: Korotkoff sound loudness and wave shape as a function of the cuff pressure (source: [23]).

The cuff pressure at which the oscillations have the maximum amplitude, correspond to the MAP. With further deflation of the cuff, the amplitude of the oscillations decreases. Figure 2.5 shows arterial blood pressure and the oscillations in the cuff during its deflation and Figure 2.6 shows the cuff pressure and oscillations. It may be noted that the walls of the artery continue to expand even when the cuff pressure falls below the DP and the oscillations do not disappear when the cuff pressure reaches the DP. The artery is completely occluded when the cuff pressure is higher than the SP, but oscillations with small amplitude appear in the cuff due to the pulsation of the artery near the upper edge of the cuff. Thus, the SP and DP values are not marked by absence of the oscillations. The MAP value is the only robust BP parameter that can be directly measured by the oscillometric method. Algorithmic methods are used in automatic BP monitors for obtaining the SP and DP values from the variations in the amplitude envelope of the oscillations as a function of the cuff pressure [20], [21]. Features like the envelope height

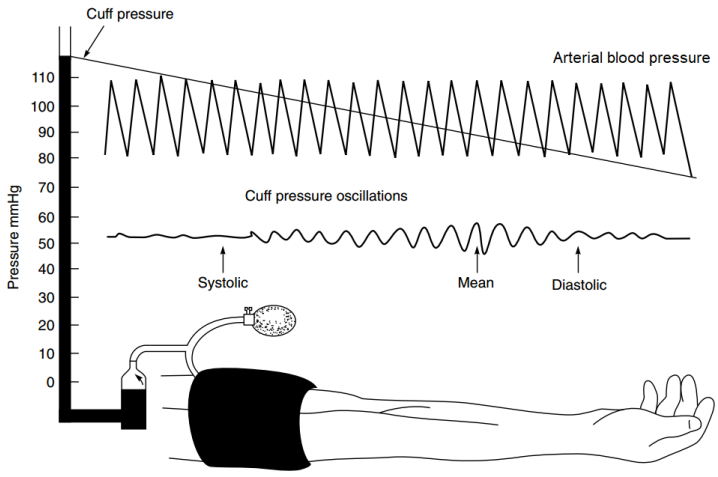

Figure 2.5: Arterial blood pressure and the oscillations in the cuff pressure during the cuff deflation in the oscillometric method (adapted from [20]).

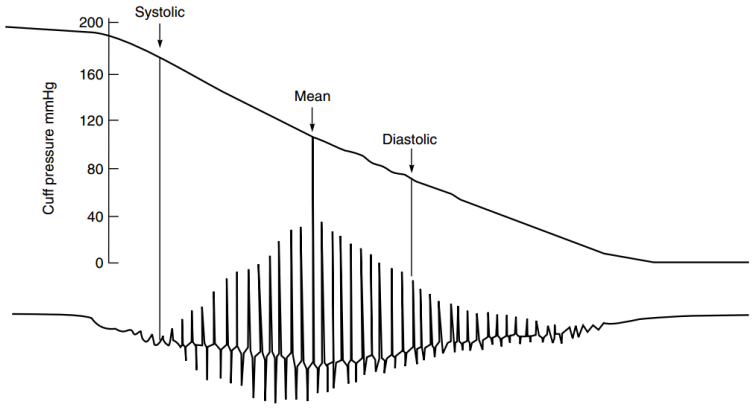

Figure 2.6: Cuff pressure and oscillation during cuff deflation (source: [20]).

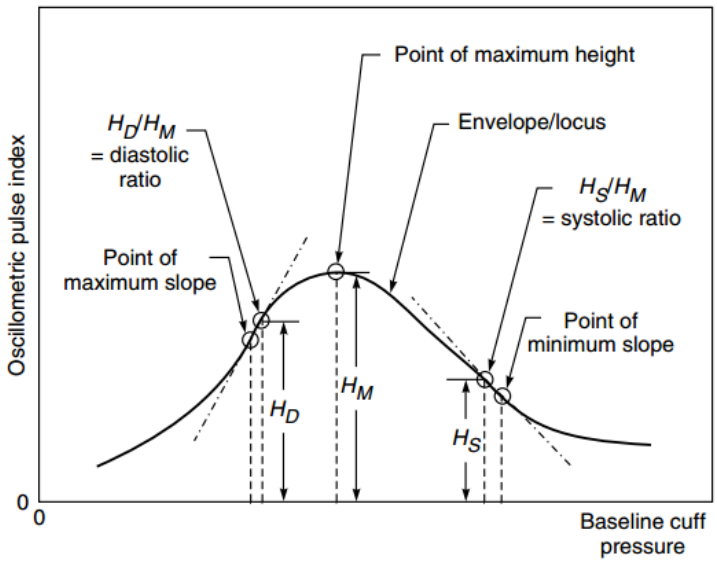

Figure 2.7: Features for estimation of SP and DP from the envelope of the oscillations (adapted from [20]).

and the slope of the envelope of the oscillations are used for estimation of the SP and DP [20], [23] as shown in Figure 2.7. The peak of the envelope corresponds to the MAP. The cuff pressure lower than the MAP value and with the envelope height as 80% of the maximum height is recorded as the DP value. The pressure higher than the MAP value and with the envelope height as 50% of the maximum height is recorded as the SP value. In another method, the pressure lower than the MAP value and with the highest envelope slope is recorded as the DP value. The pressure higher than the MAP value and with the lowest envelope slope is recorded as the SP value.

In an automatic BP measuring instrument, a single pressure transducer is used for sensing the cuff pressure. The low-pass filtered output is used for measuring the cuff pressure and the high-pass filtered output after amplification is used for monitoring the oscillations. Unlike the auscultatory method, no sound detection is used in the oscillometric method and hence it is not affected by the environmental noise. However, excessive movement or vibration may lead to inaccurate readings.

2.3 BP arm simulators

For BP measurement to be accurate, the healthcare worker making the measurement should be well trained and the instrument should be calibrated and tested. The traditional training method for auscultatory BP measurement involves measuring the BP of normotensive adults. It does not give a trainee enough exposure to abnormal cardiac conditions like abnormally low and high BP or arrhythmias. Further, the accuracy of each BP reading cannot be verified. The instructor may take a reading immediately after the trainee, but the instructor's reading cannot be used to determine the accuracy of the trainee's reading due to the possibility of change in the BP values [1]. A stethoscope with dual headsets could be used by both the trainee and the instructor so that the instructor would monitor the Korotkoff sound simultaneously. However, only one of the two will be controlling the cuff deflation. In a study on BP measurement reported in 2013 [3], 116 pharmacy students were trained in a span of two years and asked to measure the BP twice using an arm simulator [15], which was set to pre-specified high and normal BP values. Accuracy of the high BP readings was considerably less than that of the normal BP readings, indicating a need for more experience in measurement of the high BP.

Like any other medical measurement, it is necessary to develop a systematic way for evaluating new BP monitors and confirming the performance of existing ones. Several protocols have been developed for standardizing this process, e.g., those by the American National Standards Institute (ANSI) [25], the British Hypertension Society (BHS) [26], and the European Society of Hypertension (ESH) [2]. These protocols are based on comparing the readings taken from a large number of subjects using the test monitor with those using the reference monitor. The reference readings could be taken either by using the manual

auscultatory method or the intra-arterial method where the BP is continuously monitored by inserting a cannula needle inside the artery. In addition to the errors due to the imperfections of the reference monitor and the operator related variation in the readings, there could be errors if the two measurements are not performed simultaneously and at the same body part location [1]. Measurements from a large number of subjects with different ages and BP values are required to average out these errors. For example, in the case of the ESH protocol, 33 subjects of age 25 years or higher are required, with at least 10 of each gender and 10 – 12 in each one of the low, medium, and high BP ranges. Subjects with sinus heart rhythm are considered sufficient for testing and the protocol does not test the ability of the BP monitor to accurately measure the BP in the presence of abnormal cardiac conditions like arrhythmia [2]. It has been reported that the evaluation results using this method may not be repeatable [1].

In summary, evaluation of BP measurement monitors using human subjects is time-consuming, impractical for routine performance checking of BP measuring monitors, and insufficient for covering all cardiac conditions. Several arm simulators that mimic the behavior of the human arm have been developed as an alternative to the use of human subjects for training of BP measurement and also for evaluation of the noninvasive blood pressure (NIBP) monitors. Most of them are developed for BP monitors using the oscillometric method. Some of the simulators are reviewed in the following subsections.

2.3.1 Dynamic arterial BP simulator by Klein (1975)

This simulator [4] is shown in Figures 2.8. It simulates the arterial BP variation during the cardiac cycle. The pressure inside the chamber is controlled by the bulb. Figure 2.8 (a) shows the instrument setup. The pressure waveform is shown in Figure 2.8 (b). A manometer is used to monitor the pressure inside the chamber. A cam, with the shape as shown in Figure 2.8 (c) is used to press the platen. The pressure inside the chamber changes depending on which point of the cam is pressing against the platen at that specific moment. A DC motor with a controllable speed, using a variable resistor, is used to control the speed of rotation of the cam. Every cycle of the cam represents one cardiac cycle. Therefore, the speed of the motor represents the heart rate. The device is bulky and power consuming. The change of the SP and DP requires changing the cam, and it is difficult to simulate abnormal conditions like arrhythmia.

2.3.2 Arm simulator for an oscillometric BP monitor by Glover and Medero (1984)

This simulator [5] is for BP by the oscillometric method. As shown in Figure 2.9, the simulator consists of a pressure sensor to monitor the pressure inside the cuff. The output of the simulator depends on the user-settable values of the heart rate, SP, MAP, and DP. The heart rate is used to set the time interval between pressure pulses generated by the pulse generator.

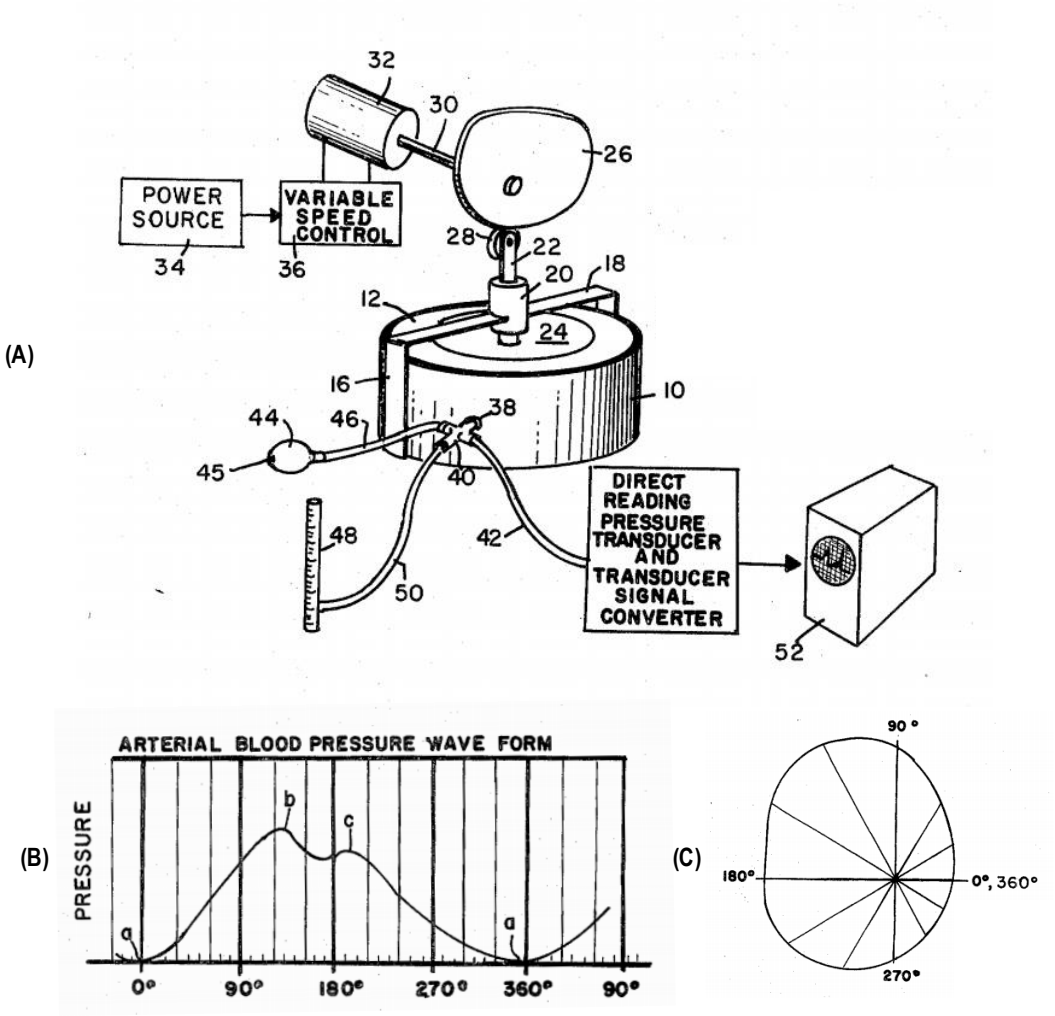

Figure 2.8: Arterial BP simulator by Klein: (a) the instrument, (b) Arterial BP waveform, and (c) cam shape (adapted from [4]).

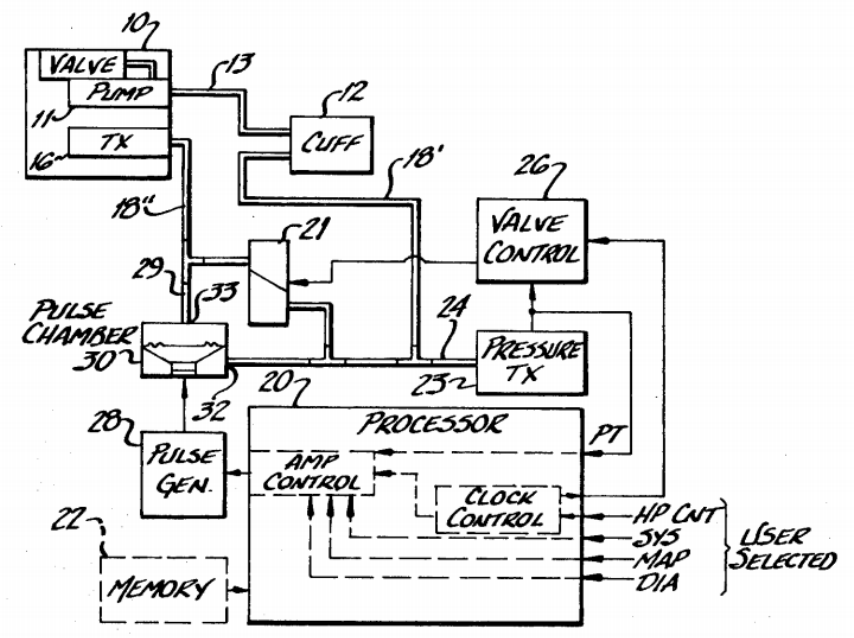

Figure 2.9: Arm simulator by Glover & Medero for oscillometric method (source: [4]).

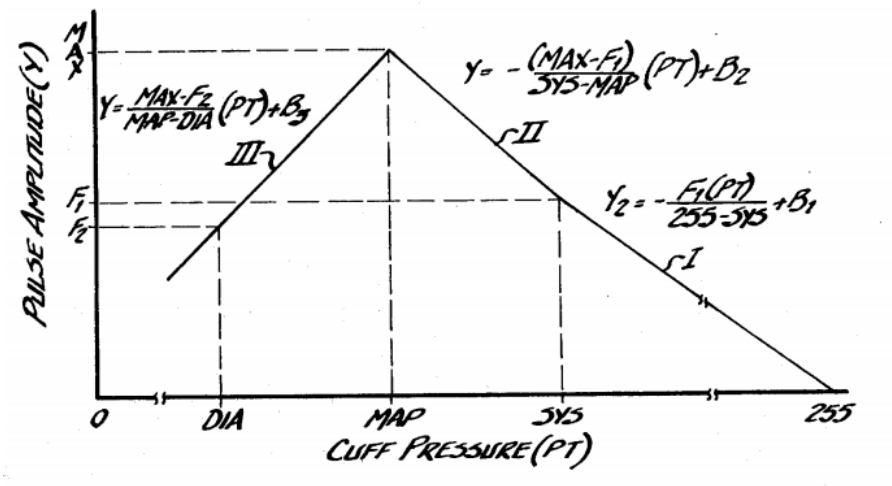

Figure 2.10: Pulse amplitude vs cuff pressure in the simulator by Glover and Medero (source: [5]).

The pressure pulses are started when the cuff pressure just equals the SP value and stopped when the cuff pressure reaches the DP value. During this interval, the amplitude of the pulses is increased with every pulse until it reaches the maximum at the point where the cuff pressure is equal to the MAP value, then it decreases until the pulses disappear at the moment when the cuff pressure is equal to the DP value. Figure 2.10 shows the pulse amplitude changing with the change of the cuff pressure. A valve placed between the cuff and the pressure sensor of the monitor is controlled by the processor. The valve closes right before the pressure pulse is produced by the pulse generator so that only the tube connecting the pulse generator and the monitor is affected, therefore eliminating the need for a larger pulse chamber that requires high power to change the pressure in the whole cuff. Although a small amount of power is required to generate the pulses, additional power is required to control the valve with every generated pulse. Unlike the simulator by Klein [4], the SP and DP values can be changed without the need to replace any part of the device. This simulator, is like that in [4], invasive to the BP measuring instrument in the sense that a T-connector has to be inserted between the cuff and the pressure monitor. Also, it can only simulate regular heartbeats, where the time between every two consecutive heartbeats is constant. Abnormal conditions like arrhythmias are not simulated.

2.2.3 Oscillometric non-invasive BP simulator by Costello (1991)

The simulator [8] is for evaluation and calibration of oscillometric BP measuring instruments. The simulator has three embodiments shown in Figures 2.11, 2.12, and 2.13. In the first embodiment, the pressure of the cuff is sensed by the pressure transducer of the simulator that is connected to the cuff through a T-connector inserted in the tubing between the cuff and the BP monitor under test. The pressure oscillations are generated using a pneumatic pulse generator that is formed of a linear actuator and a piston coupled to the tubing of the BP monitor. When the piston is moved, it presses the air inside the cuff producing the desired pressure pulse. The simulation parameters including the SP, DP, MAP, and the heart rate are

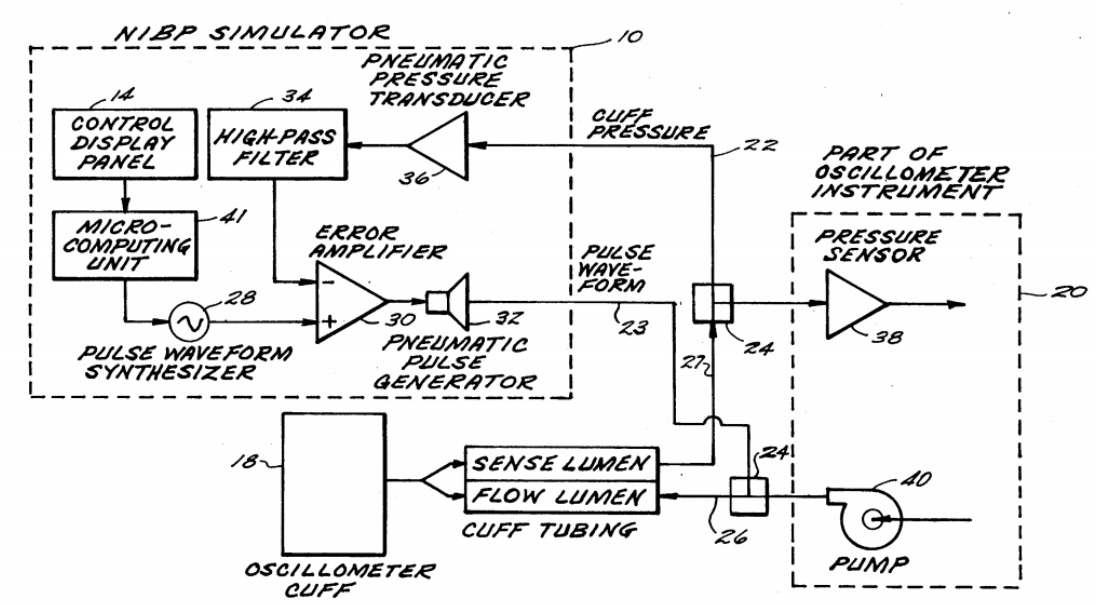

Figure 2.11: The embodiment of BP simulator by Costello with pneumatic pulse generator and a feedback loop (source: [8]).

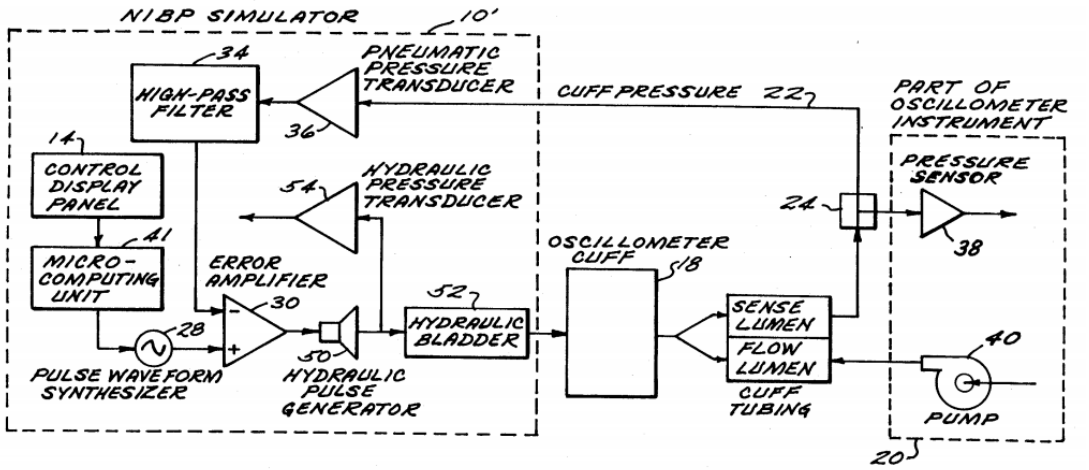

Figure 2.12: The embodiment of BP simulator by Costello with hydraulic pulse generator and feedback loop (source: [8]).

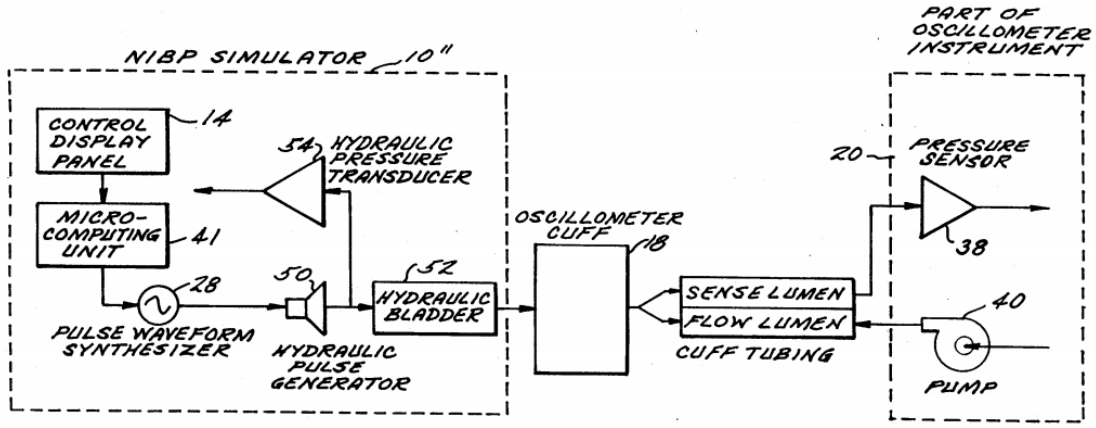

Figure 2.13: The embodiment of BP simulator by Costello with hydraulic pulse generator and no feedback (source: [8]).

selected by the user through a control display unit containing switches and alphanumeric display. The amplitude of the generated pulses is controlled, by a microcomputing unit, based on the user-set parameters and in accordance with the sensed cuff pressure to produce the desired oscillation envelope. A pulse waveform synthesizer is used to convert the digital value of the desired amplitude of the generated pulse to analog value that is fed to the linear actuator of the pneumatic pulse generator. To compensate for the nonlinearities in the pneumatic pulse generator and the load of cuff and tubing, the high-pass filtered component of the sensed cuff pressure is used as a feedback that is fed to an error amplifier to correct the value of the voltage sent to the pneumatic pulse generator.

The BP pressure of different subjects is measured invasively using a catheter-tip medical transducer and noninvasively using manual auscultation. The oscillation envelope has also been recorded separately. Various parameters including the MAP, SP, and DP have been calculated from the recorded arterial pressure signal. Various envelope parameters like the location of the MAP, SP, and DP, ratios of amplitude for SP and DP, and envelope slope for MAP, SP, and DP, have been calculated from the recorded envelope and the parameters of the recorded arterial pressure signal. Multi-linear regression and standard statistical analysis techniques are used to correlate the dependent envelope parameters to the independent physiological parameters set by the user.

Another embodiment of the simulator is shown in Figure 2.12. A hydraulic pulse generator is used instead of the pneumatic pulse generator. The feature of feedback is retained. Yet another embodiment of the simulator is shown in Figure 2.13. In this design, the simulator is completely noninvasive, which allows for testing the BP monitor without the need for dismantling it. The DC component of the cuff pressure is sensed using a bladder. However, the feature of the feedback has been removed, which adversely affect the accuracy of the generated oscillations.

The simulator has the advantage of producing physiologically correct envelopes unlike the simulator in [5] where linear envelope is produced. The simulator is invasive to the BP monitor, and when it is not invasive, the produced envelope is not accurate. In addition to the lack of closed-loop control, the source of error may be that the pressure sensed by the bladder is not identical to the cuff pressure, as the sensed pressure depends on the stiffness of the material of the cuff and the bladder.

2.3.4 Compact oscillometric BP simulator by Ruiter and Ruiter (2010)

The simulator [9] is for generating pressure oscillations for testing and calibration of BP measuring instruments as shown in Figure 2.14. the simulator consists of a bidirectional actuator that is generating the pressure pulse by pressing against a pneumatic conduit made from elastomeric material and coupled to the cuff through an extension hose and a T-connector.

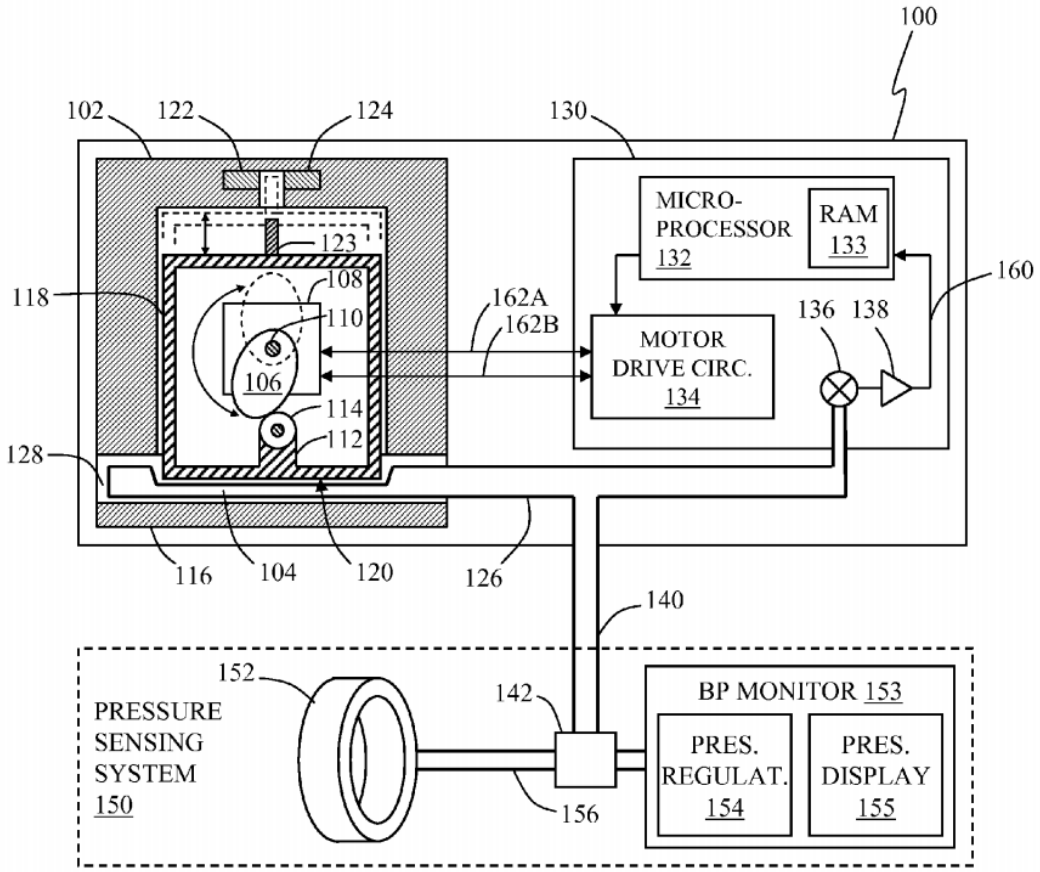

Figure 2.14: Compact oscillometric BP simulator by Ruiter and Ruiter (source: [9]).

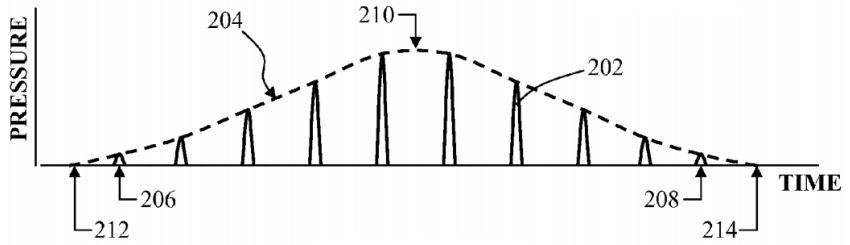

Figure 2.15: The envelope of the oscillations produced by the simulator (source: [9]).

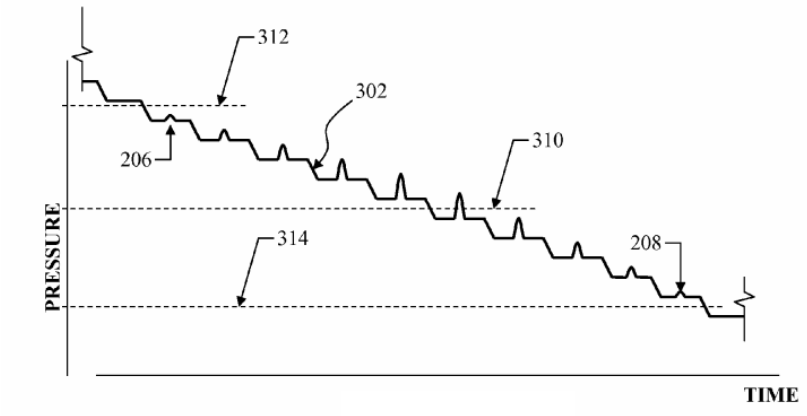

Figure 2.16: Variation of cuff pressure with cuff deflation (source: [9]).

The simulator has a pressure sensor that is also coupled to the cuff to monitor the value of the cuff pressure. The bidirectional actuator is formed of a stepper motor with its shaft fixedly attached to a cam. The cam drives a cam follower through bearing. The cam follower is attached to a slider that acts as a piston with its movement restricted to be only in the vertical direction. For generating a pressure pulse, the cam is turned to move the slider down and press against the pneumatic conduit. When the peak pressure pulse is reached, the direction of the cam is reversed. The amplitude of the generated pulse is controlled by a microprocessor in accordance with the dynamically sensed cuff pressure to generate the desired envelope set by the user. The amplitude and the shape of the generated pulses can be stored in the memory. The cuff pressure is first increased to a value higher than the simulated SP then it is deflated in a step-wise manner. When the cuff pressure reaches the simulated SP, the first pulse is produced. The amplitude of the pulses increase as the cuff is deflated further till it reaches the maximum at the MAP. As the cuff pressure decreases to values lower than the MAP, the amplitude of the pulses starts decreasing. The last pulse is produced when the cuff pressure equals the DP. Figure 2.15 shows an example of the oscillations envelope that is produced by the simulator and Figure 2.16 shows the variations in the cuff pressure as the cuff is deflated. A light source and a light detector are used to ensure that the slider has reached the initial position before the start of every new pulse. The opaque blade, attached to the slider, interrupts the light beam received by the light detector indicating that the slider has reached the initial position.

The simulator provides more flexibility as the desired envelope of the oscillations can be stored in the memory and reproduced as needed. Unlike the simulator developed by Glover and Medero [5], this simulator consumes more power as the oscillations are generated in the whole cuff. Abnormal conditions like arrhythmias are not implemented.

2.3.5 “Universal sphygmomanometer simulator” by Olmstead et. Al (2014)

The simulator reported in [10] is for training and evaluation of medical professionals in manual auscultatory method. The simulator consists of a cuff that contains a rigid-wall vessel, a pressure sensor, a cuff controller, and a speaker as shown in Figure 2.17. The rigid-wall vessel is coupled to a bulb with a valve to control the pressure inside the vessel. A pressure gauge is controlled by the cuff controller to show the value of the pressure inside the vessel. A removable user interface unit is provided for the trainee to set the simulation parameters. The objective of the simulator is to provide a more realistic approach for training of medical professionals. The cuff is wrapped around the arm of a simulated patient which can be a live subject or a manikin. The material of the vessel inside the cuff is chosen to be rigid to make sure that the artery of the subject is not occluded while the pressure inside the vessel is increased. The pressure inside the rigid-wall vessel is sensed by the pressure sensor inside the cuff.

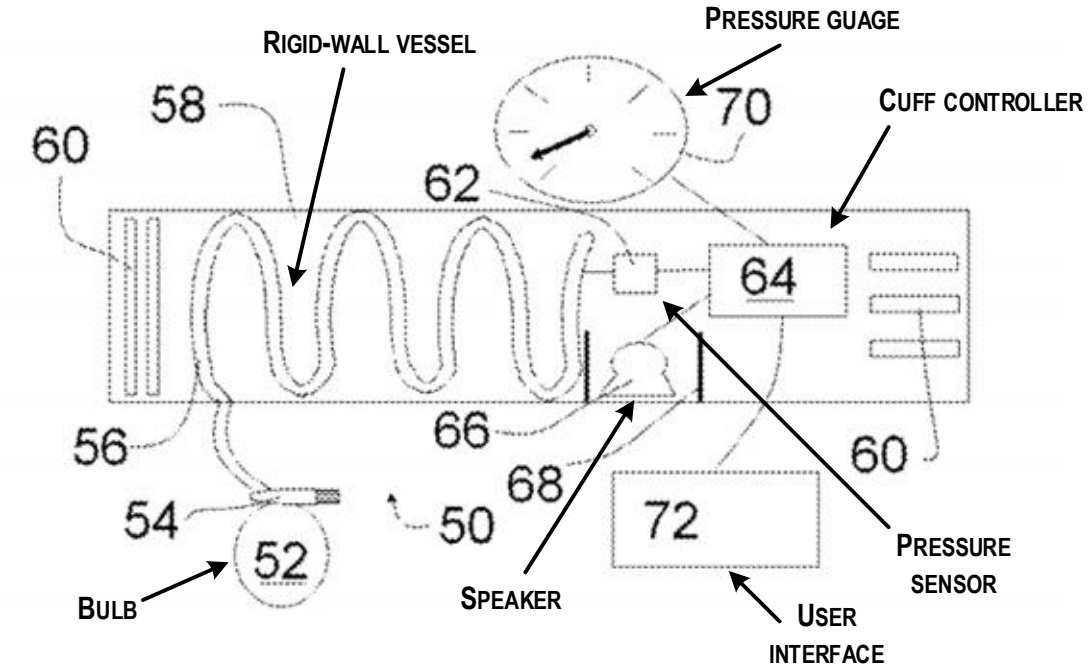

Figure 2.17: Universal sphygmomanometer simulator (adapted from [10]).

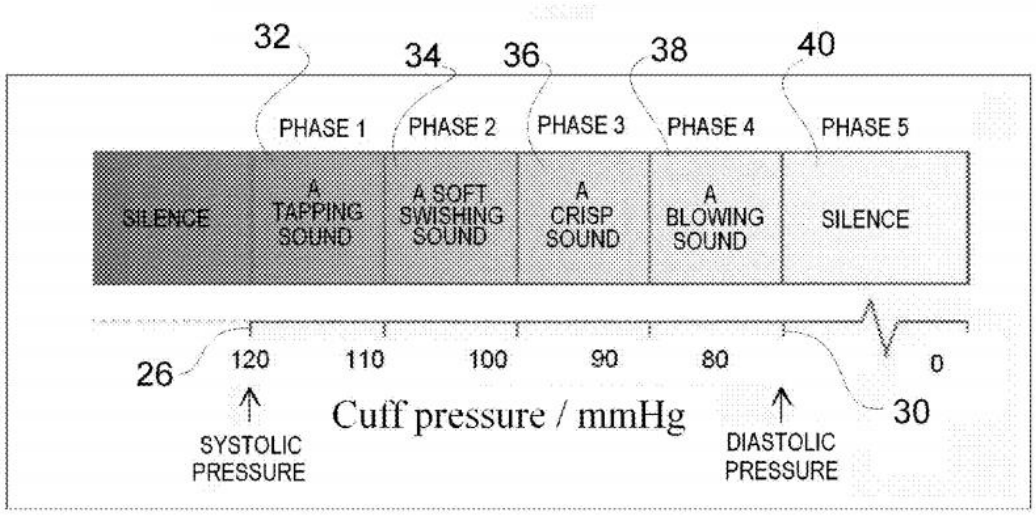

Figure 2.18: Variation of Korotkoff sounds as the cuff is deflated from SP to DP (source: [10]).

The simulation parameters are set and the user interface unit is removed so that the trainee does not know the simulated BP values. The cuff is wrapped around the arm of the simulated patient and a stethoscope is placed on the brachial artery of the arm of the simulated patient to listen the Korotkoff sounds produced by the speaker. Note that the rigid-wall vessel does not expand to occlude the artery of the simulated patient, therefore, no Korotkoff sounds are generated from the simulated patient and the trainee listens to only those sounds generated by the speaker inside the cuff. The trainee inflates the cuff to a value well above the simulated SP. The pressure is then released slowly till the pressure inside the rigid-wall vessel reaches the simulated SP, that is when the first Korotkoff sound is produced by the speaker. The trainee

records the pressure value, shown in the gauge, as the SP. As the cuff pressure is decreased further the characteristics of the generated Korotkoff sounds varies, as shown in Figure 2.18, until they disappear at the simulated DP. In addition to the generated Korotkoff sounds, the needle of the gauge is controlled by the cuff controller to simulate the gauge pumps that occur in the actual BP measurement because of the oscillations of the brachial artery as the cuff is deflated from the SP to the DP.

The simulator offers a more realistic approach for training of medical professionals, it can be used with live subjects or with manikins. However, Korotkoff sounds will be generated from both the arm of the live subject and the speaker inside the cuff if the cuff is wrapped tightly enough to partially occlude the artery of the subject. Abnormal conditions like arrhythmias are not implemented.

2.3.6 Commercially available BP simulators

There are many BP simulator available in the market for purposes of training of health care workers, and evaluation of automatic BP measuring instruments. The following is a list with some them:

i. BP pump 2 NIBP simulator from Fluke Biomedical [11].
ii. BP-SIM handheld NIBP simulator from Rigel Medical [12].
iii. Life/form® blood pressure simulator arm from Global technologies [13].
iv. Blood pressure training system from Gaumard [14].
v. Blood pressure training arm from Laerdal Medical Corporation [15].

Appendix D provides a brief description of these simulators.

2.3.7 Arm simulator for blood pressure measurement developed at IIT Bombay

In 2011, Gothwal [7] developed an arm simulator for use with the auscultatory method of BP measurement. In 2013, Tanvar developed an arm simulator [6] for use also with the oscillometric method. In this design, a microcontroller based circuit board is used along with a pressure sensor and actuators to generate the Korotkoff sounds and the oscillations in the cuff as if the cuff is wrapped around a human arm. The instrument, shown in Figure 2.19, is in the form of a vertical wooden cylinder with a horizontal support, for the cuff to be wrapped around it. The circuit board uses a microcontroller with on-chip ADC and DAC. The cuff pressure is sensed using a pressure sensor connected to a T-connector inserted in the tube between the cuff and the BP monitor. For the auscultatory method, a loudspeaker is used to produce the Korotkoff sounds. For this purpose, the waveforms stored in the microcontroller memory are scaled in accordance with the dynamically sensed cuff pressure and output through the DAC, audio amplifier, and loudspeaker to generate the sounds. A linear actuator located inside the

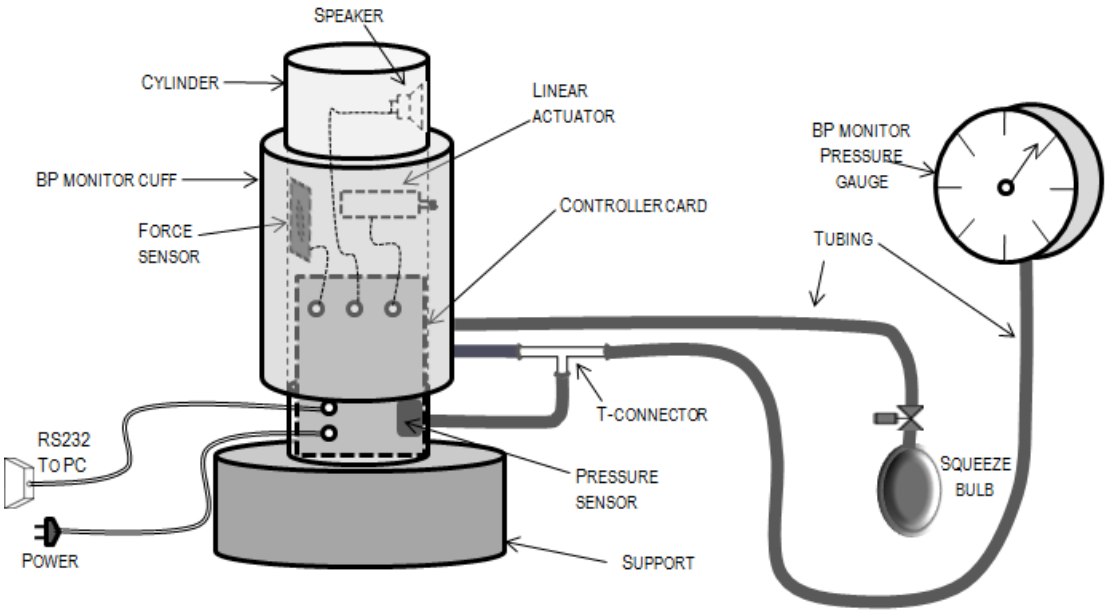

Figure 2.19: Instrument setup of Tanvar's arm simulator (source: [6]).

cylinder and pressing against the cuff through a hole in the cylinder wall is controlled through one of the port pins of the microcontroller for generating the oscillations inside the cuff for the oscillometric method. The heart pulse volume is controlled by scaling the signal sent to the DAC of the microcontroller. Arrhythmia is implemented by introducing a jitter in the time period between successive pulses using a pseudo-random number generator. The simulation parameters including SP, DP, heart rate, arrhythmia level, and pulse volume, are set using a PC-based GUI software and sent to the controller through the serial port. Due to power requirements for the linear actuator used to generate the oscillation in the cuff for oscillometric method, the simulator was designed as a mains-powered instrument. When a BP monitor with oscillometric method was used, heart rate was detected correctly. However, SP and DP were sometimes underestimated or overestimated.

Left blank

Chapter 3

DESIGN APPROACH AND HARDWARE DESCRIPTION

3.1 Design approach

This simulator is designed as an improvement of the simulator developed by Tanvar [6]. It is in the form of a vertical cylinder fixated on a horizontal base as shown in Figure 3.1. The linear actuator along with the controller board, the Bluetooth transceiver, the pressure sensor and speaker, are located inside the cylinder and to be powered from a battery. The cuff pressure is sensed using a pressure sensor connected to a T-connector inserted in the tube between the cuff and the BP monitor. For auscultatory method, the stored Korotkoff sound pulse waveforms are scaled and output to a speaker through an audio amplifier in accordance with the dynamically sensed cuff pressure. Arrhythmia is implemented by introducing a jitter in the time period between successive pulses using a pseudo-random number generator. For the oscillometric method, pressure pulses are generated in the cuff using a linear actuator located inside the cylinder. Simulation parameters including SP, DP, heart rate, arrhythmia level and pulse volume, are set using a PC-based or Android-based GUI software and a wireless link with the controller through Bluetooth. This approach for user interface rather than an instrument with its own keys and display, has been used to simplify the packaging and to reduce the development cost without adversely affecting the functionality.

The block diagram of the arm simulator is shown in Figure 3.2, the period between each two consecutive simulated beats is calculated based on the values of the heart rate (HR) and arrhythmia level (AL) received from the GUI software. The amplitude of both the generated Korotkoff sound (K-sound) for auscultatory method, and the pressure pulse signal for oscillometric method are calculated based on the values of the dynamically sensed cuff pressure (CP), SP, DP, and the pulse volume (PV). The generated sound is then amplified and output by the speaker and the generated pulse signal is sent to the linear actuator.

3.1.1 Heartbeat with specified heart rate and arrhythmia

In case of regular heartbeats, the heartbeat interval T_B is constant and is equal to T_{B0} = 60/HR, with T_{B0} in s and HR in beat/minute. In case of arrhythmia, the successive values have a random variation with a mean value of T_{B0}. For simulation, T_B can be obtained using a random variable *r*, as the following:

$$T_B = T_{B0}(1 + ra) \tag{3.1}$$

where *r* is uniformly distributed over the range [–1, 1] and *a* is the arrhythmia level, representing the maximum deviation as a fraction of the mean interval T_{B0}. Thus, the maximum variation in T_B is $|\Delta T_{B0}| \leq aT_{B0}$ and *a* can be in the range [0, 0.5]. The heartbeat interval T_B is modeled as consisting of two subintervals, a fixed on-period T_{on} during which the K-sound is

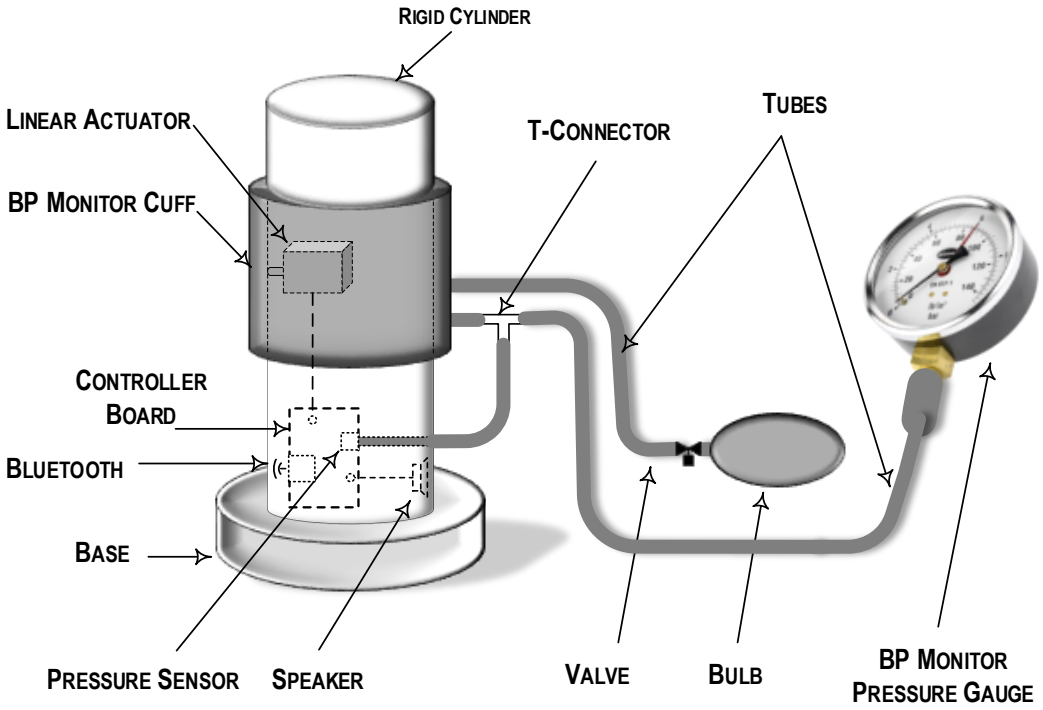

Figure 3.1: Arm simulator setup.

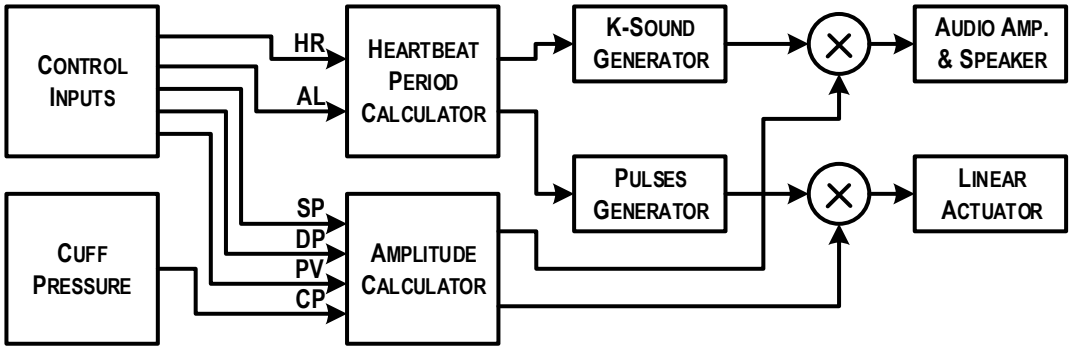

Figure 3.2: Conceptual block diagram of the arm simulator.

output, and a variable off-period T_{off} during which no sound is produced. Thus $T_B = T_{on} + T_{off}$, with T_{off} varied to vary T_B. The on-period T_{on} is kept constant and the off-period for each heartbeat is calculated as $T_{off} = T_B - T_{on}$. Figure 3.3 shows examples of heartbeat intervals with increased and decreased T_{off} related to arrhythmia.

The random variable r can be generated using a pseudo-random generator [27]. A computationally simple approach in integer arithmetic is to use a feedback shift register with maximum-length sequence generator as shown in Figure 3.4 with 8-bit shift register. The output of the XOR gate with the 4^{th}, 5^{th}, 6^{th} and 8^{th} bits as inputs is used for feedback so that maximum-length sequence of 255 is achieved. If all bits in the register are zeros, the output of the XOR gate would always be 0. To avoid this possibility, the register is initialized with 0xff. The most significant bit represents the sign S and the remaining bits represent the magnitude R of the integer random number with the range [–127, 127]. This number is related to the variable r as

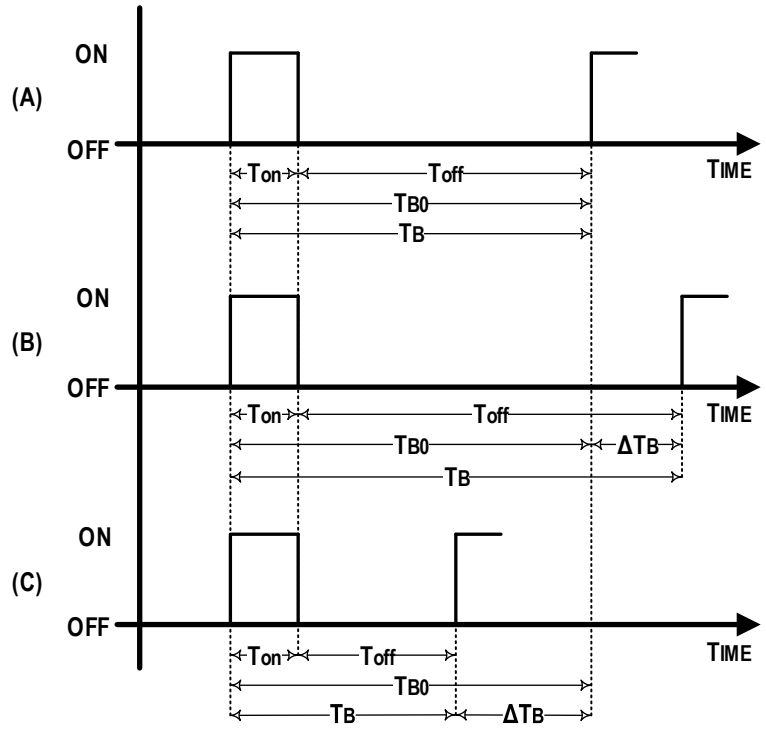

Figure 3.3: Examples of heartbeat intervals: (a) heartbeat with $T_B = T_{B0}$, (b) increased heartbeat interval with increased T_{off}, and (c) decreased heartbeat interval with decreased T_{off}.

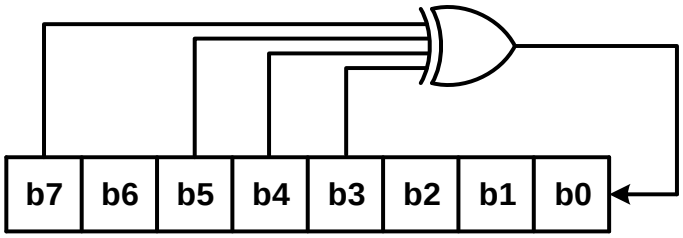

Figure 3.4: Feedback shift register with maximum-length sequence for pseudo-random sequence generation (adapted from [27]).

$$r = SR/128 \tag{3.2}$$

The arrhythmia level a can be represented as a percentage $A = 100a$ with a range of [0, 50]. Therefore, the value of T_B in terms of S, R, and A can be given as

$$T_B = T_{B0}(1 + ASR/12800) \tag{3.3}$$

For the K-sound pulse waveform, stored in memory, with the sampling frequency of 8 kHz, the mean interval T_{B0} in number of samples is calculated as

$$N_{TB0} = 480{,}000/\mathrm{HR} \tag{3.4}$$

Therefore, the variable heartbeat interval T_B is calculated in number of samples, using 16-bit integer arithmetic as

$$N_{TB} = (4{,}800/\mathrm{HR})(100 + (ASR)/128) \tag{3.5}$$

3.1.2 Generation of Korotkoff sound

The Korotkoff sound, recorded during BP measurement, was downloaded from [28] and ten sound pulses were extracted as shown in Figure 3.5. For each waveform, 1500 samples are stored.at a sampling frequency of 8 kHz. As the cuff pressure is decreased from the SP to the DP, the waveform of the output Korotkoff sound is changed as shown in Table 3.1. The amplitude of the waveform is scaled down according to the dynamically sensed CP using the scaling factor F_1, with the range 0 – 1, as shown in Figure 3.6 and calculated as the following:

$$F_1 = \begin{cases} 0, & \mathrm{DP} > \mathrm{CP} \\ \mathrm{Min} + (1 - \mathrm{Min})(\mathrm{CP} - \mathrm{DP})/(\mathrm{MAP} - \mathrm{DP}), & \mathrm{MAP} > \mathrm{CP} \geq \mathrm{DP} \\ \mathrm{Min} + (1 - \mathrm{Min})(\mathrm{SP} - \mathrm{CP})/(\mathrm{SP} - \mathrm{MAP}), & \mathrm{SP} > \mathrm{CP} \geq \mathrm{MAP} \\ 0, & \mathrm{CP} \geq \mathrm{SP} \end{cases} \quad (3.6)$$

The minimum value 'Min' of F_1 is set so that the output sound from the speaker is loud enough to be heard.

3.1.3 Generation of pressure pulses

The pressure pulses are generated by introducing a change in the pressure inside the cuff by pushing the shaft of a linear actuator against the outer wall of the cuff for a specific amount of time. The maximum heart rate is taken as 150 bpm, which corresponds to 0.4 s between two consecutive pulses. If arrhythmia is introduced, that number can be further reduced to 0.2 s. To ensure that the pulses are detectable, the on-time of the pulse is set to be 0.125 s. The amplitude of the pulse depends on the distance that the shaft of the linear actuator goes against the wall of the cuff, the further the distance the higher the amplitude of the pulse. The oscillation amplitude is scaled in accordance with the change in the sensed cuff pressure using the scaling factor F_2 with the range 0 – 1 as shown in Figure 3.7 and calculated as the following piecewise linear relationship:

$$F_2 = \begin{cases} 0, & \mathrm{DP} - 20 > \mathrm{CP} \\ 0.025\big(\mathrm{CP} - (\mathrm{DP} - 20)\big), & \mathrm{DP} > \mathrm{CP} \geq \mathrm{DP} - 20 \\ (0.2(\mathrm{CP} - \mathrm{DP}) + 0.8(\mathrm{MAP} - \mathrm{DP}))/(\mathrm{MAP} - \mathrm{DP}), & \mathrm{MAP} > \mathrm{CP} \geq \mathrm{DP} \\ 0.5(\mathrm{CP} + \mathrm{MAP} - 2\mathrm{SP})/(\mathrm{MAP} - \mathrm{SP}), & \mathrm{SP} > \mathrm{CP} \geq \mathrm{MAP} \\ 0.5, & \mathrm{SP} + 20 > \mathrm{CP} \geq \mathrm{SP} \\ 0, & \mathrm{CP} \geq \mathrm{SP} + 20 \end{cases} \quad (3.7)$$

The sharp transitions in the amplitude are introduced to identify the DP, while the interval with the slope of zero is introduced to identify the SP. The ratio of the amplitude of the oscillations at the SP and DP to the maximum amplitude is set to 0.5 and 0.8, respectively, as mentioned in

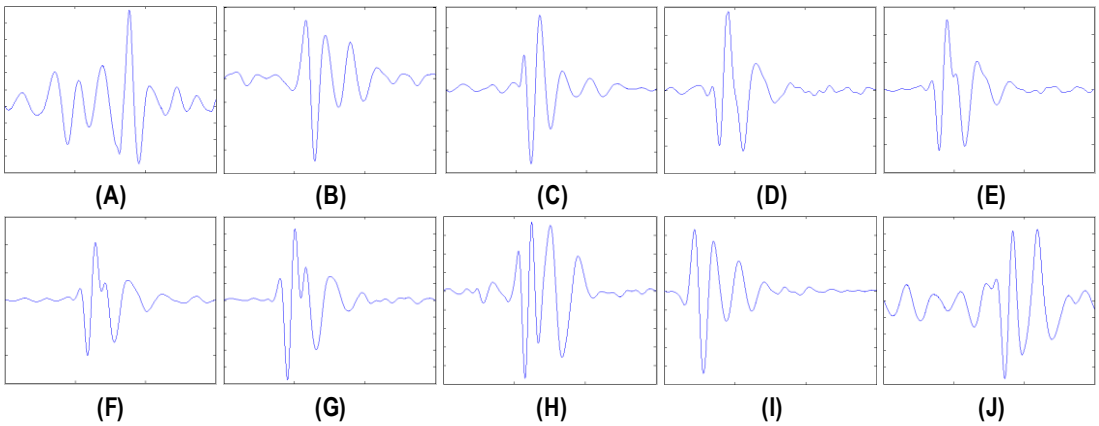

Figure 3.5: Ten K-sound waveforms as extracted from the sound in [28]: (a) waveform1, (b) waveform2, (c) waveform3, (d) waveform4, (e) waveform5, (f) waveform6, (g) waveform7, (h) waveform8, (i) waveform9, (j) waveform10.

Table 3.1: Relation between CP and K-sound waveform selection

Cuff pressure range	K-sound waveform
$DP \leq CP < DP + 1/3(0.95MAP - DP)$	Waveform1
$DP + 1/3(0.95MAP - DP) \leq CP < DP + 2/3(0.95MAP - DP)$	Waveform2
$DP + 2/3(0.95MAP - DP) \leq CP < 0.95MAP$	Waveform3
$0.95MAP \leq CP < 1.05MAP$	Waveform4
$1.05MAP \leq CP < 1.05MAP + 1/6(SP - 1.05MAP)$	Waveform5
$1.05MAP + 1/6(SP - 1.05MAP) \leq CP < 1.05MAP + 2/6(SP - 1.05MAP)$	Waveform6
$1.05MAP + 2/6(SP - 1.05MAP) \leq CP < 1.05MAP + 3/6(SP - 1.05MAP)$	Waveform7
$1.05MAP + 3/6(SP - 1.05MAP) \leq CP < 1.05MAP + 4/6(SP - 1.05MAP)$	Waveform8
$1.05MAP + 4/6(SP - 1.05MAP) \leq CP < 1.05MAP + 5/6(SP - 1.05MAP)$	Waveform9
$1.05MAP + 5/6(SP - 1.05MAP) \leq CP < SP$	Waveform10

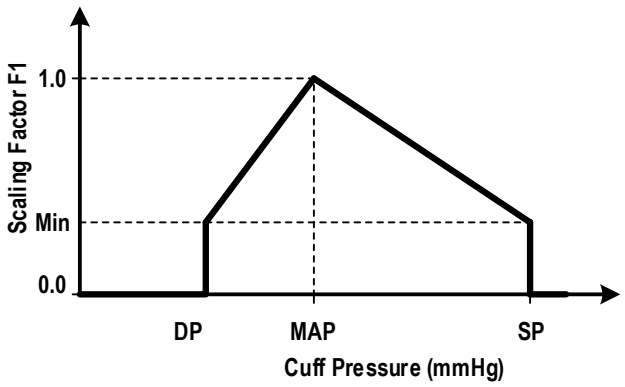

Figure 3.6: Scaling factor for the generated K-sound as a function of CP.

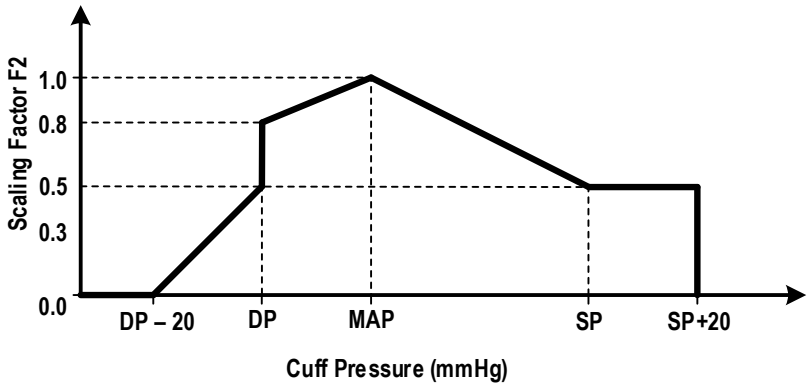

Figure 3.7: Scaling factor for the generated oscillations as a function of CP.

the literature [23]. This relation between the scaling factor F_2 and the cuff pressure CP provides oscillation magnitude that can be correctly detected by the slope method as well.

3.2 Hardware description

Figure 3.8 shows the detailed hardware block diagram of the arm simulator, for realizing the functional blocks of the conceptual block diagram shown in Figure 3.2. The control inputs are set wirelessly through Bluetooth using a PC-based or an Android-based GUI. The period of the simulated heartbeat and the amplitude of both the K-sound waveforms and the pressure oscillations is calculated by a microcontroller in accordance with the cuff pressure read by the on-chip ADC of the microcontroller from a pressure sensor connected to the tubing of the BP measuring instrument via a T-connector. The signals of the K-sound are generated by the DAC of the microcontroller and output to the Audio amplifier. The pressure oscillations are generated using a linear actuator controlled by a pulse width modulated (PWM) signal from the microcontroller. The simulator board is powered by a 5 V supply, which can be a battery or a USB power. The power circuit provides 3.3 V to power the microcontroller, and 5 V to power the Bluetooth transceiver, the pressure sensor, and the audio amplifier.

3.2.1 Microcontroller circuit

The 16-bit DSPIC33FJ128GP802 microcontroller [29] (from Microchip) labeled as U1 in Figure 3.9, is used as the processor, with the program in its on-chip flash memory. The micro controller is powered by 3.3 V. It has an internal fast RC oscillator with a nominal clock of 7.37 MHz [30], and an internal phase-locked loop (PLL) to scale the operating frequency to higher values. An external clock or crystal oscillator could also be used to clock the system. The internal fast RC oscillator with PLL is used to set the device instruction clock at 40 MHz. The controller has two ports, Port A, which has 5 pins (RA0 to RA4) and Port B with 16 pins (RB0 to RB15). Each pin of these two ports can be used as a general-purpose input/output pin, or it can be configured to have some specific special functions, the unused pins are configured as output pins and connected to ground [29].

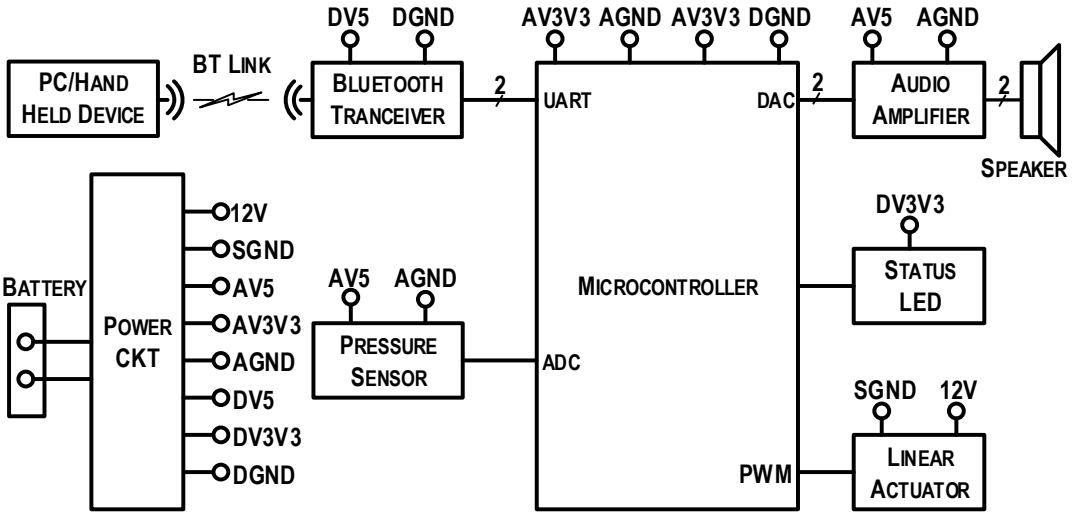

Figure 3.8: Detailed hardware block diagram of the arm simulator.

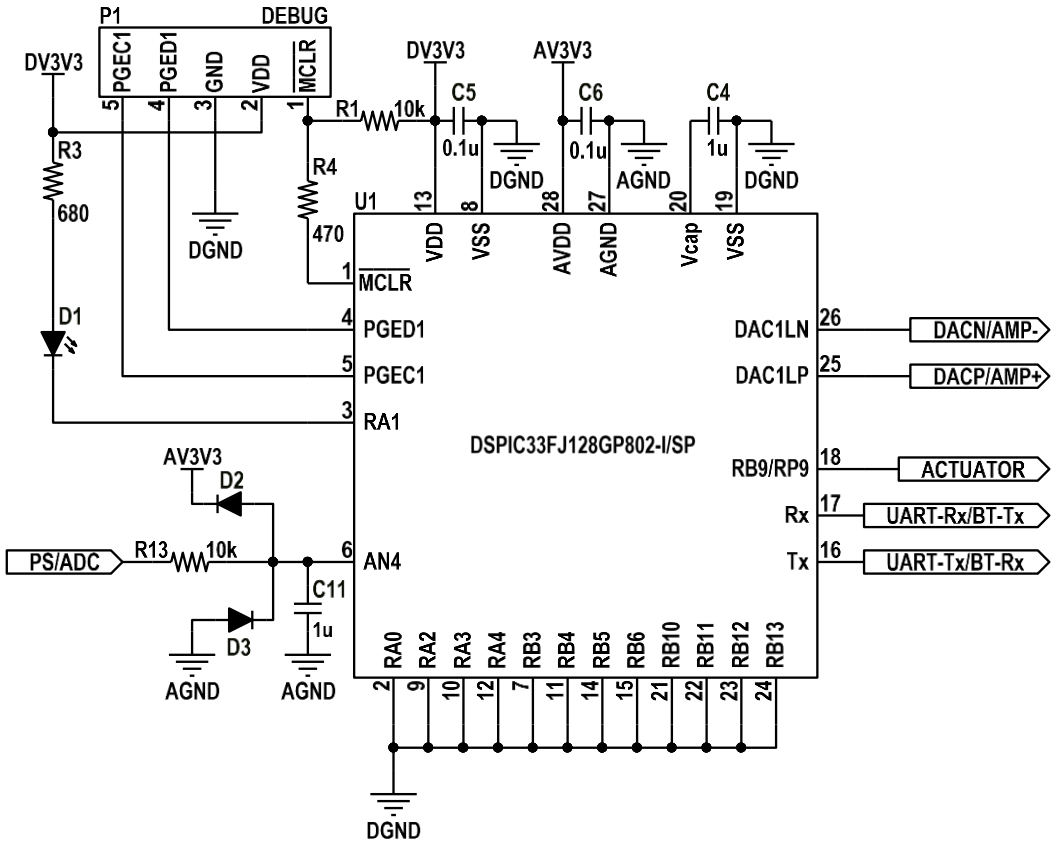

Figure 3.9: Microcontroller circuit.

The pressure sensor output is acquired through the ADC input. The Korotkoff sounds are output through the DAC output. The control for linear actuator is generated through PWM output pin. It also controls the status indicator through its port pin. The Bluetooth transceiver, used for user setting, is interfaced to the universal asynchronous receiver-transmitter (UART) port of the processor.

The microcontroller has an on-chip ADC, which can be used with either 12-bit or 10-bit

resolution. The ADC has 4 channels, if more than one channel is sampled simultaneously, only10-bit resolution can be used. In this case, only one input signal from the pressure sensor is to be read. Hence, the ADC is used in single channel 12-bit resolution mode. Pin 6 (RB2/AN4) is configured to be used as the ADC input pin that is connected to the output of the pressure sensor. The resistor R13 and the diodes D2 and D3 are used for protection of the ADC. The capacitor C11 of 1 nF is connected across the ADC pin to filter out the noise from the sensor and the noise introduced by the charging/discharging of the internal sample-hold capacitor of the ADC.

For the sake of monitoring the progress of the program execution in the microcontroller, the green light emitting diode (LED) labeled as D1 is connected from the 3.3 V supply to the microcontroller through the current limiting resistor R3 of 680 Ω to make sure that the current sunk by the microcontroller pin does not exceed the maximum current rating (4 mA). Pin 3 (RA1) is configured as an output pin to drive the LED.

The microcontroller has 5 internal 16-bits timers (Timer1 to Timer5). The sampling of the sensor signal is performed in the interrupt service routine (ISR) of Timer3, which has been configured to interrupt every 125 μs, corresponding to the sampling frequency of 8 kHz. The microcontroller also has a 16-bit audio DAC with sampling frequency up to 100 kHz. The DAC has two channels (the left and the right channels) with independent 4-word buffers. Each channel has two reserved pins, which can also be used as general-purpose I/O pins in case that channel is disabled. In our design, 1500 samples of a single heartbeat signal sampled at 8 kHz are stored in the memory of the microcontroller. The on-chip DAC is configured to output the stored signal through the left channel (pins 25 and 26); at sampling frequency of 8 kHz.

The PWM output is configured to work with Timer2 to produce the control for the linear actuator. Pin 18 (RB9/RP9) is configured as the output pin associated with the output compare module. The period of the PWM signal is set to be 16 ms. A new PWM period starts every time Timer2 reaches the maximum count and causes an interrupt.

The UART module of the microcontroller is used for communication with the Bluetooth module by assigning the pins 16 and 17 as TX and RX pins, respectively. The UART module is configured with 9600 baud, 8 bits, 1 stop bit, and no parity. The value of the sensed cuff pressure to the Bluetooth module is sent after each 25 interrupts of Timer2. Since the interrupt of Timer2 is configured to occur at 16 ms intervals, the most recent value of the sensed cuff pressure is sent every 0.4 s.

The 5-pin header P1 labeled as DEBUG is used for connecting the programmer/ debugger PICKIT3, for loading the flash memory and debugging the code execution. Pin 1 is for resetting the microcontroller. Depending on the setting of the configuration bits of the microcontroller, the data and clock pins of the PICKIT3 (Pins 4 and 5 respectively) could be connected to either

Pins 4 and 5 in the microcontroller (PGED1 and PGEC1, respectively), Pins 21 and 22 (PGED2 and PGEC2, respectively) or Pins 14 and 15 (PGED3 and PGEC3, respectively). Here pins 4 and 5 are used. Pin 3 of the header of the PICKIT3 is connected to ground, while Pin 2 is connected to 3.3 V. The 6-pin header, labeled as BT, is used to connect the Bluetooth module.

3.2.2 Bluetooth transceiver

The Bluetooth transceiver module ZC-HC-05 [31] with an integrated antenna is used to send and receive data from the GUI software on the PC or a handheld computing device. It is powered by 5 V. It has UART interface with programmable baud rate. It has 6 pins as shown in Figure 3.10, two pins for power (5 V and ground), transmitting pin TX and receiving pin RX with a voltage level of 3.3 V, an enable pin, and the operation mode set pin. The last pin is used to set the mode on: (i) configuration mode to adjust the parameters of the Bluetooth module like the baud rate, the password of the module, etc, or (ii) operation mode to send and receive data. The default setting is operation mode with a baud rate of 9600, and the password as '1234'.

3.2.3 Linear actuator

The 'mightyZap' mini linear servo from IR Robot [32] shown in Figure 3.11, is used to generate the pressure pulses. It has an embedded drive circuit and a position control with an accuracy of 100 µm. The default of the maximum stroke is 27 mm and it can be extended to 30 mm. The actuator has a speed of 90 mm/s at a force of 20 N. It is powered by 12 V and draws a maximum current of 2.3 A. The position of the shaft can be controlled through PWM signal or by sending the desired position to the actuator through UART. Figure 3.12 shows the change in the duty cycle to control position of the linear actuator.

3.2.4 Pressure sensor circuit

The piezoresistive pressure sensor MXPV5050GP [33] from Freescale, labeled as U3 in Figure 3.13, is used to sense the pressure of the air inside the cuff. It senses the difference in the pressure between the pressure of air in the tube connected to it and the atmospheric air pressure. The sensor can be powered by 5 ± 0.25 V, and it drains a maximum current of 10 mA. The temperature range of the sensor is from 0º to 80º C. The sensor has an input range of 0 – 50 kPa, i.e. 0 – 375 mmHg, and accuracy of ± 2.5% of the full-scale voltage span, i.e. the algebraic difference between the output voltage at full rated pressure and the output voltage at the minimum rated pressure. The sensor output is given in V as

$$V_{\text{out}} = V_{\text{s}}(0.018\,P + 0.04) \tag{3.8}$$

where P is the sensed pressure in kPa and V_{s} is supply voltage in V. The sensitivity of the sensor is 90 mV/kPa, and it has an offset voltage of 4% of V_{s}. For reducing the digital switching noise, the supply and ground tracks of the sensor are separated from those of the microcontroller. The

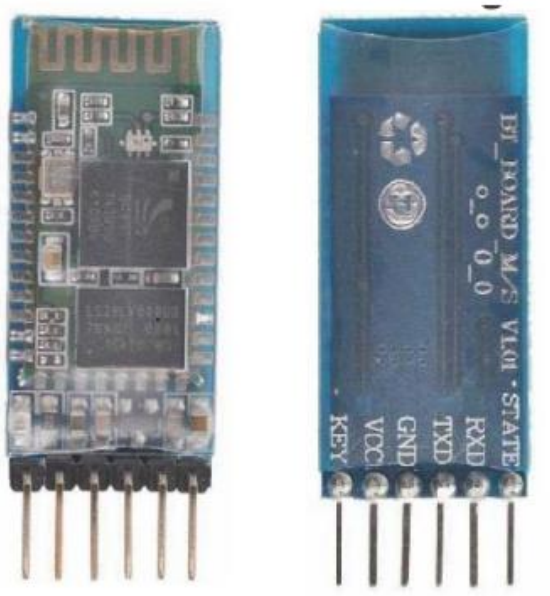

Figure 3.10: Bluetooth module (source: [31]).

Figure 3.11: MightyZap Linear actuator (source: [32]).

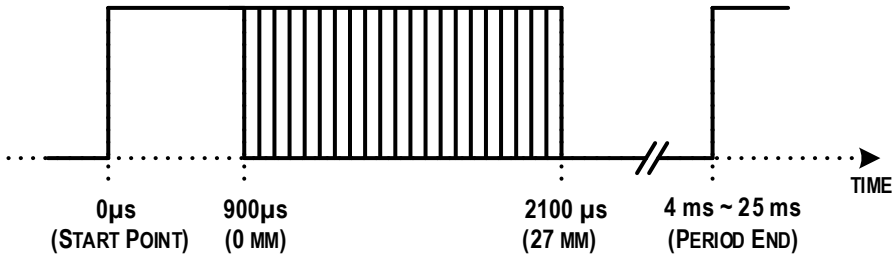

Figure 3.12: Change in duty cycle to control the position of the actuator (adapted from [32]).

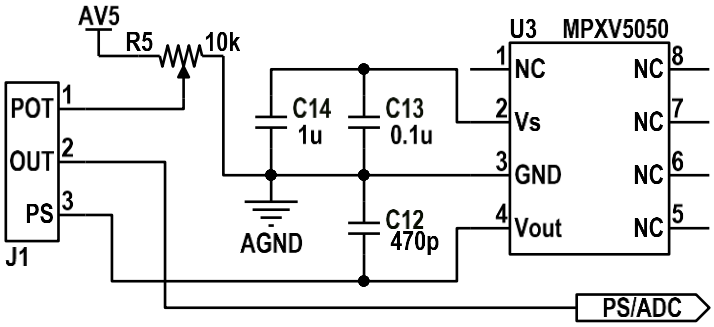

Figure 3.13: Pressure sensor circuit.

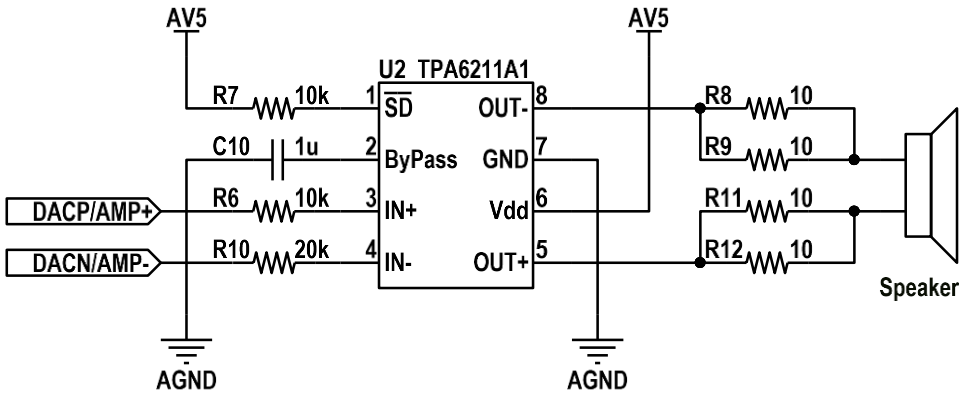

Figure 3.14: Audio amplifier circuit.

supply of the sensor is marked as AV5 and its ground is marked as AGND. The ground plane for the digital part of the circuit is marked as DGND. The capacitors C13 and C14 are used as decoupling capacitors, while C12 serves as an output filtering capacitor. A 10 kΩ potentiometer (R5) is connected along with the output of the sensor to a 3-pin header J1 for the purpose of testing. A jumper is used to deliver either the output of the sensor or the output of the potentiometer to the microcontroller.

3.2.4 Audio amplifier circuit

The audio power amplifier TPA6211A1 [34], labeled as U2 in Figure 3.14, is used to drive the speaker through a 3.5 mm jack. The amplifier is powered by AV5. The amplifier is a difference amplifier with internal fixed resistors values of 40 kΩ as shown in Figure 3.15. It has a bridge-tied load (BTL) output, avoiding the need for dc blocking capacitor and doubling the output voltage swing. The gain of the amplifier is adjusted by changing the value of the input resistors. In the simulator circuit, these resistors are set to 20 kΩ adjusting the gain to 2. The output signal from the DAC of the microcontroller is controlled so that it does not exceed the output voltage swing of the amplifier. The shutdown pin (Pin 1) acts as a low active enable of the amplifier. It is connected to 5 V through the resistor R7 of 10 kΩ to keep the amplifier permanently enabled. A minimum load resistance of 4 Ω is required for the amplifier to maintain the gain calculated. A parallel combination of two 10 Ω resistors is connected is series with each output terminal, providing a minimum load resistance of 10 Ω.

3.2.5 Power circuit

The simulator circuit is powered by a 5 V power source, which can be a power bank or USB power. A voltage of 3.3 V is required to power the microcontroller and the LED, 5 V is required to power the audio amplifier, the pressure sensor, and the Bluetooth transceiver, and 12 V is required to power the linear actuator. The charge pump labeled as U4 in Figure 3.16 is used to double the battery voltage so that the output voltage would be regulated by the ASM1117-5.0 regulators VR1 and VR3 to produce 5 V. The output of VR1 is used to power

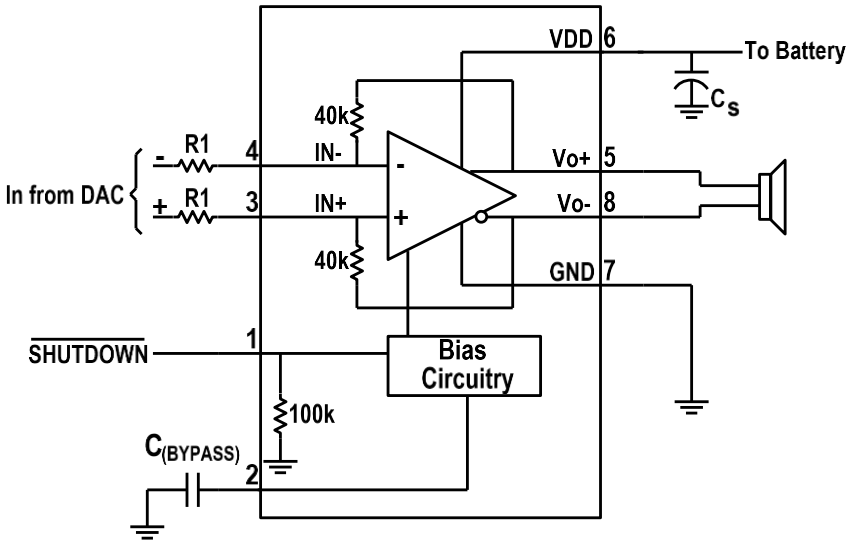

Figure 3.15: Internal circuit and typical application of the TPA6211A1 amplifier (adapted from [34]).

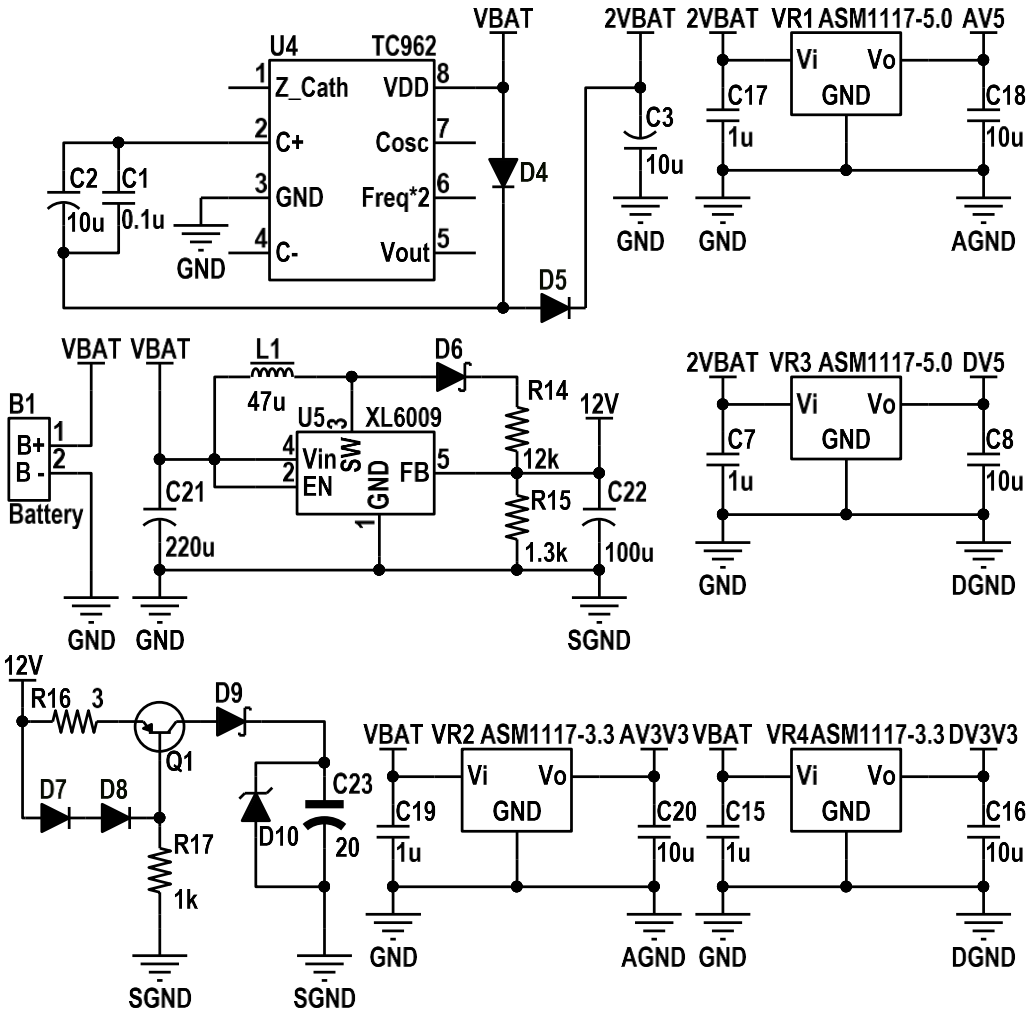

Figure 3.16: Power supply circuit.

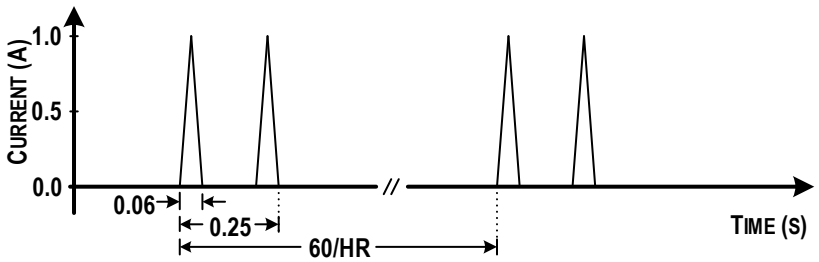

Figure 3.17: Waveform of the current drain by the linear actuator.

the analog part (pressure sensor and amplifier) and the output of VR3 is used for the digital part (Bluetooth transceiver). The battery voltage is regulated by the ASM1117-3.3 regulators, labeled as VR2 and VR4, to produce 3.3 V for the analog part (protection diodes) and digital part (microcontroller circuit) respectively. The ground planes of the analog and digital parts of the circuit are separated to eliminate the switching noise. Further details on the PCB layout are given in Appendix B.

The linear actuator is operated only when the heartbeat is simulated by making the actuator shaft push against the wall of the cuff and come back to its initial position after 125 ms. These two movements are accomplished within a period of 250 ms. The linear actuator is powered by 12 V and it requires a maximum current of 1 A only during the first and the last part of this period as shown in Figure 3.17. The XL6009 dc-dc convertor, labeled in Figure 3.17 as U5, is used to provide the 12 V from the 5V supply voltage. Considering some loss of power in the dc-dc boost converter, the current drawn from the battery when the heartbeat is simulated would be more than 2.5 A. To reduce the peak drain on the battery, a supercapacitor, labeled in the figure as C23, is used as an energy storage to be charged slowly from the battery with low current. The CK100 transistor, labeled in the figure as Q1, along with the resistors R16 and R17, and the diodes D7 and D8, is used the limit the charging current of the supercapacitor to 0.2 A. When the pulse is produced, the energy stored in the supercapacitor is delivered to the actuator. This way the actuator can be driven by high current without overloading the battery. The capacitance is calculated based on the maximum drop in the voltage of the capacitor. The actuator works properly if it is powered by a voltage in the range 9.5 – 12.5 V, otherwise, the movement of the shaft is unpredictable. With nominal charging to 12 V, the maximum drop allowed is 2.5 V. It also depends on the maximum number of heartbeats before the capacitor must be charged again. The maximum range of pressure simulated by the arm simulator is 220 mmHg. Assuming the cuff is deflated with a rate 3 mmHg/s, the total time needed to complete one measurement is 70 s. With the heart rate set to its maximum of 150 beat/min, the total number of heartbeats during one measurement is 175. The current drain by the actuator is for 120 ms for every heartbeat as shown in Figure 3.17. Therefore, the maximum time for which the actuator draws current in one measurement is 21 s.

With a drain current I_L, for a duration T_D, and permitted voltage drop ΔV, the capacitor value is given as

$$C = I_L T_D / \Delta V \tag{3.9}$$

with I_L = 1 A, T_D = 21 s, and ΔV = 2.5 V, the capacitor value turns out to be 88.4 F. In our design, 5 supercapacitors each with capacitance of 100 F and voltage rating of 2.7 V, are connected in series, providing the net capacitance of 20 F with voltage rating of 13.5 V. With this capacitor, the voltage drop is

$$\Delta V = I_L \, T_D / C = 1 \times 21/20 = 1.05 \text{ V} \tag{3.10}$$

Considering a charging current of 0.2 A, the time needed to charge the drop of 1.05 V is

$$T_{\text{Charge}} = C\Delta V / I_{\text{Charge}} = 20 \times 1.05/0.2 = 105 \text{ s} \tag{3.11}$$

The supercapacitor while supplying charge to the actuator, will also receive charge from the charger. Therefore, after each measurement, a maximum wait period of 70 s (total charging time of 105 – charging time during measurement of 35) is needed before starting the next measurement.

Chapter 4

SOFTWARE DEVELOPMENT

In this chapter, the microcontroller program, the PC-based GUI, and the Android-based GUI software are described with the help of flowchart diagrams.

4.1 Microcontroller program

The code of the microcontroller was written in C using the MPLAB X software, version 3.61, and loaded into the program memory of the microcontroller through the PICKIT3 programmer/debugger. The microcontroller program performs the following tasks:

i. Communication with the GUI software for sending the value of the cuff pressure and receiving the simulation parameters through UART.
ii. Continuously reading the output voltage of the pressure sensor via ADC with a sampling frequency of 8 kHz.
iii. Controlling the timing and frequency of the LED blinking according to the flow of the program execution.
iv. Outputting the Korotkoff sounds for auscultatory method and the linear actuator control for the oscillometric method, in accordance with the sensed cuff pressure and the simulation parameters.

These tasks are carried out through either the main program or through interrupt service routines (ISR) that interrupt the main program.

4.1.1 Main program

Figure 4.1 shows the flowchart of the main program, which is started at power-on. The first step in the program is to configure all the hardware modules and to initialize all the flags and variables. At the start-up, the microcontroller is configured to be clocked by the internal fast RC oscillator. It is configured to scale the system frequency F_{CY} to 40 MHz through PLL. The port pins are configured for specific tasks as the following:

i. Pin 3 (RA1) is configured as output to drive the LED with its initial value as 0, i.e. the LED is ON initially.
ii. Pin 6 (AN4/RB2) is configured as an analog input pin and used for reading the pressure sensor signal.
iii. Pins 25 and 26 (RB14 and RB15/DAC1LP and DAC1LN, respectively) are configured as output pins and used for outputting the DAC differential signal to the audio amplifier.

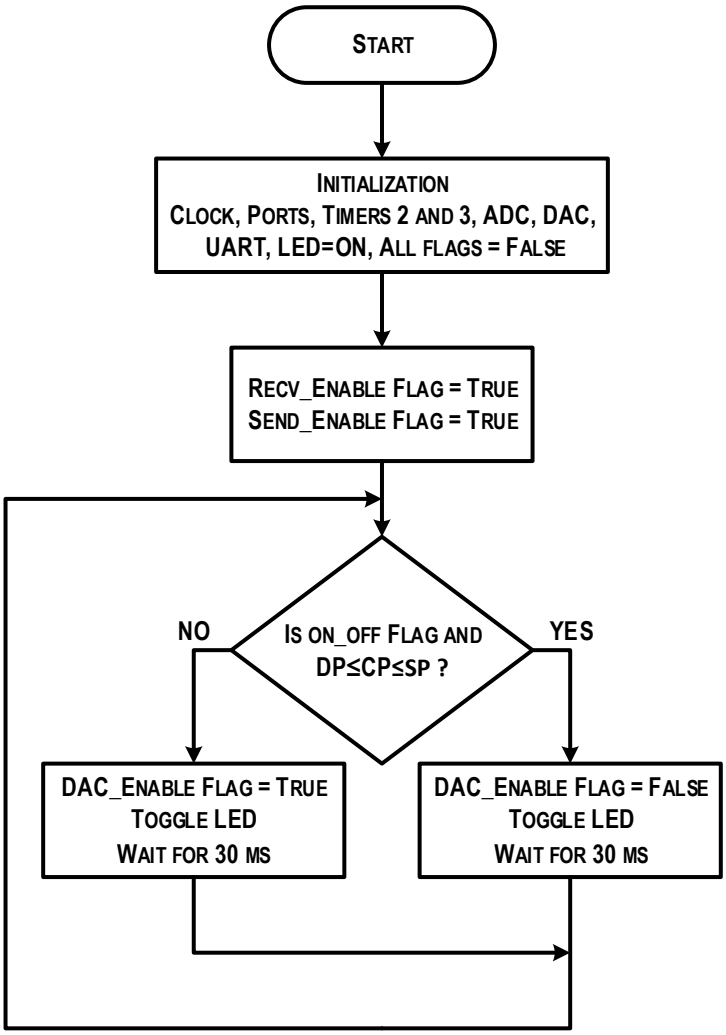

Figure 4.1: Flowchart diagram of the main program.

iv. Pin 16 (RB7) is configured as an output pin and allotted for the transmitting pin of the UART, while Pin 17 (RB8) is configured as an input pin and allotted for the receiving pin of the UART.

v. Pin 18 (RB9) is configured as an output pin and allotted to output the PWM signal for controlling the linear actuator.

The ADC module is configured to work with 12-bit resolution and single channel input. It is configured so that the sampling process starts automatically after the end of the last conversion. The ADC reference positive and negative voltages are set to be VDD and ground (3.3 V and 0 V). The clock of ADC is derived from the clock system F_{CY}. The sampling frequency of the ADC is set by the ISR of Timer3. The clock of Timer3 is driven from the system clock (F_{CY} = 40 MHz), and it is configured so that the interrupt occurs every 125 μs. The prescaler of Timer3 clock is set to be 64, and the interrupt occurs when the timer counting register reaches 78. The different values are given as the following:

$$T_{CY} = 1/F_{CY} = 1/(40\ \text{MHz}) = 25\ \text{ns} \tag{4.1}$$

$$T_{\text{Timer3}} = 64\,T_{\text{CY}} = 1.6\ \mu\text{s} \tag{4.2}$$

$$T_{\text{Interrupt}} = 78\,T_{\text{Timer3}} = 125\ \mu\text{s} \tag{4.3}$$

The DAC of the microcontroller is configured so that only the left channel is on. The clock for the DAC is driven from the PLL output (F_{VCO}= 160 MHz). The sampling frequency of the DAC is set to be 8 kHz. To achieve it, F_{VCO} is first scaled down by 16 to give the DAC clock ACLK. The prescaler of the DAC scales it further down by 5 to give the operating frequency of the DAC F_{DAC} as shown in Equation 4.4 and Equation 4.5. The sampling frequency is F_{DAC}/256 [29]. The calculations are as the following:

$$\text{ACLK} = F_{\text{VCO}}/16 = 10\ \text{MHz} \tag{4.4}$$

$$F_{\text{DAC}} = \text{ACLK}/5 = 2\ \text{MHz} \tag{4.5}$$

$$F_{\text{Sampling}} = F_{\text{DAC}}/256 = 7.812\ \text{kHz} \tag{4.6}$$

The UART module of the microcontroller is configured so that the baud rate is 9600. The clock of the UART is driven from the system clock F_{CY} with a prescaler of 260, and it is also configured so that every transmitted/received bit is 16 clock cycles length, as the following:

$$\text{Baud rate} = F_{\text{CY}}/(260 \times 16) = 9615\ \text{bits/s} \tag{4.7}$$

For the received data of the UART, an interrupt occurs every time a byte is received, while for the sent data, the interrupt of Timer2 is used to send the value of the cuff pressure every 0.25 s.

The interrupts of the UART receiving, DAC, and Timer2 are controlled by the flags ‘Recv_Enable’, ‘DAC_Enable’ and ‘Send_Enable’ respectively. If the flag value is false, the ISR is not executed. The used modules are configured, the ‘Recv_Enable’ and ‘Send_Enable’ flags are set as true, and the code goes into a wait loop as shown in Figure 4.1. When the ‘start’ byte is received, the ‘on_off flag’ is set as true, enabling the simulator circuit to produce output signals. When the cuff pressure is in the range between the set SP and DP, the ‘DAC_Enable’ flag is set to true and the heartbeat signal is output through the DAC, also the LED blinks indicating that the output is not zero. Otherwise, the ‘DAC_Enable’ flag is set to false and the LED is turned off. This cycle is repeated.

4.1.2 Timer2 interrupt service routine

Figure 4.2 shows the flowchart of the code executed when Timer2 interrupt occurs. It performs the following:

i. It continuously sends the ‘start’ byte at the beginning so that the GUI software can identify the COM port by scanning all the ports and chose the one from which the start byte is sent. The GUI responds by sending the ‘start’ byte back, when it is received, the code stops sending the ‘start’ byte.

ii. It continuously sends the value of the cuff pressure after the COM port is identified.

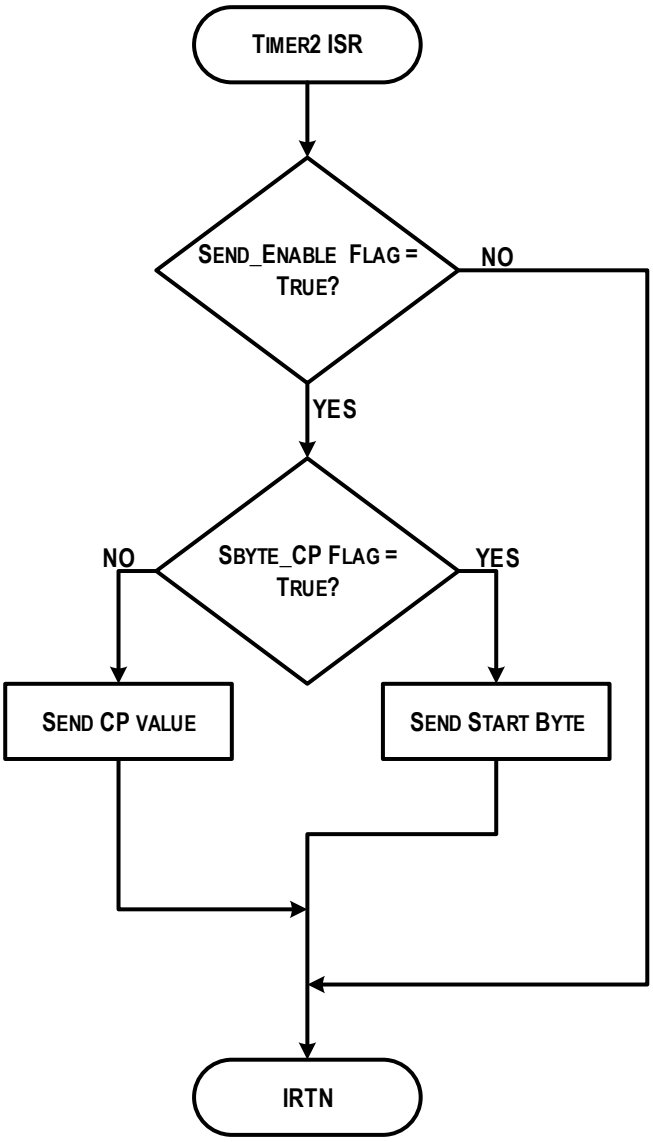

Figure 4.2: Flowchart diagram of Timer2 ISR.

The flag named 'Send_Enable' controls if any value is sent. If the value of this flag is false, the code exits the interrupt. Otherwise, it checks the value of the 'Sbyte_CP' flag. Initially the value of this flag is true, and the code sends the 'start' byte so that the GUI could identify the COM port. When the GUI replies by sending the same 'start' byte, the value of the 'Sbyte_CP' flag is changed to false, and the ISR stops sending the 'start' byte and sends the value of the cuff pressure instead.

4.1.3 Timer3 interrupt service routine

The task performed by this ISR is to set the sampling frequency of the ADC, calculate the value of the cuff pressure in mmHg, and store it in a global variable so that it could be used by the other parts of the code. Figure 4.3 shows the flowchart of the Timer3 ISR. The code stores the ADC value in a dummy variable, calculates the value of the cuff pressure and stores it in a

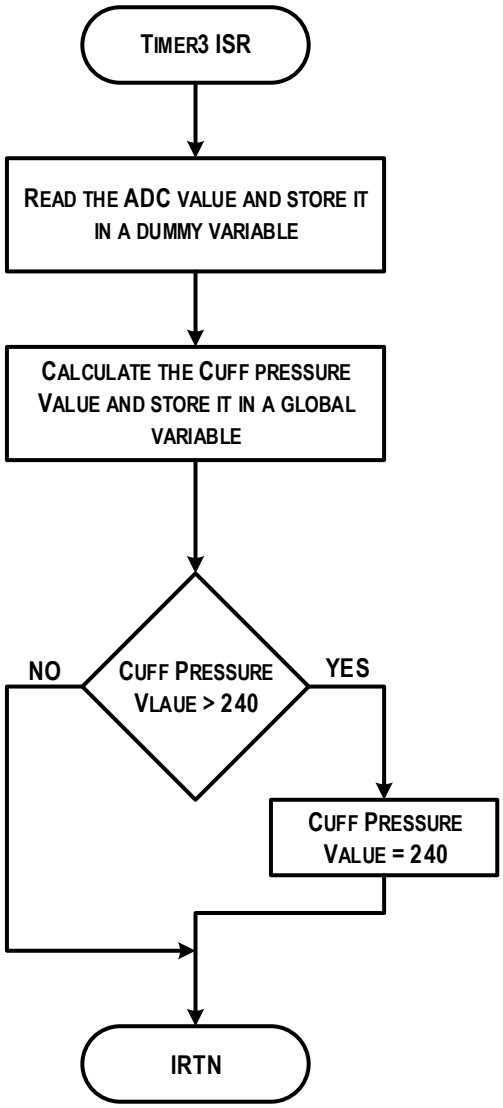

Figure 4.3: Flowchart diagram of Timer3 ISR.

global variable, and limits the cuff pressure value to 240, as the values from 241 to 255 are used for handshaking and communication between the GUI and the board.

4.1.4 DAC interrupt service routine

Figure 4.4 shows the flowchart diagram of the DAC ISR. The default value of the DAC output is set to be 1.8 V when there is no audio output. That is controlled by the 'DAC_Enable' flag. If it is false, the default value is output. Otherwise, the amplitude factor of the output audio signal is calculated according to Equation 3.5. The sampling frequency of the DAC is set as 8 kHz. The audio signal is stored as 1500 samples. the number of samples that represent the off period is controlled by the heartrate and the arrhythmia level. The samples of the audio signal are scaled by the amplitude factor and output and the sample count is incremented by one. When the count reaches 1500, the output voltage is fixed at 1.8 and samples count is incremented until it reaches the value of T_B. At that point the count is reset to 0 and a new random number is generated for calculating the length of the next period.

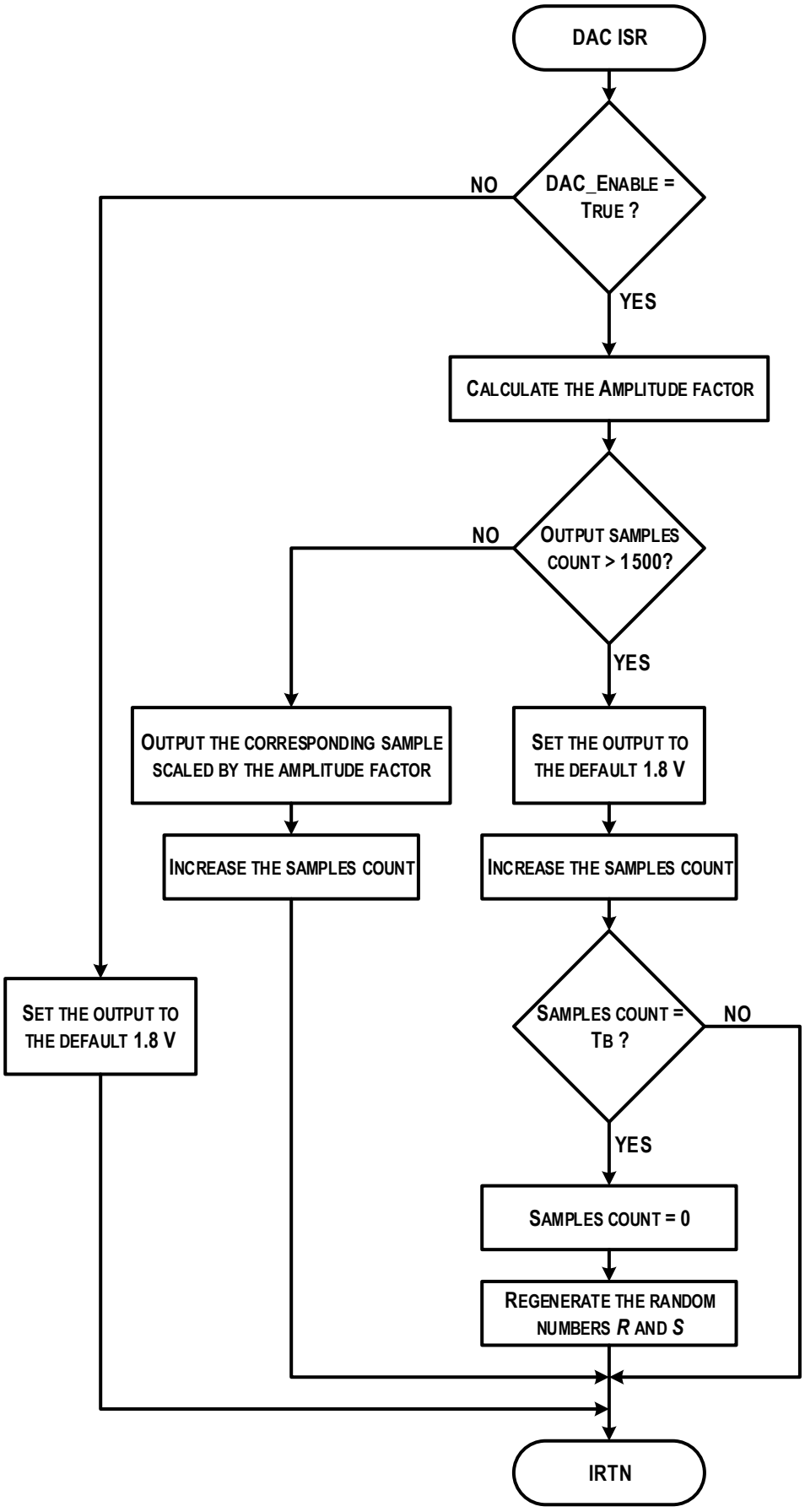

Figure 4.4: Flowchart diagram of DAC ISR.

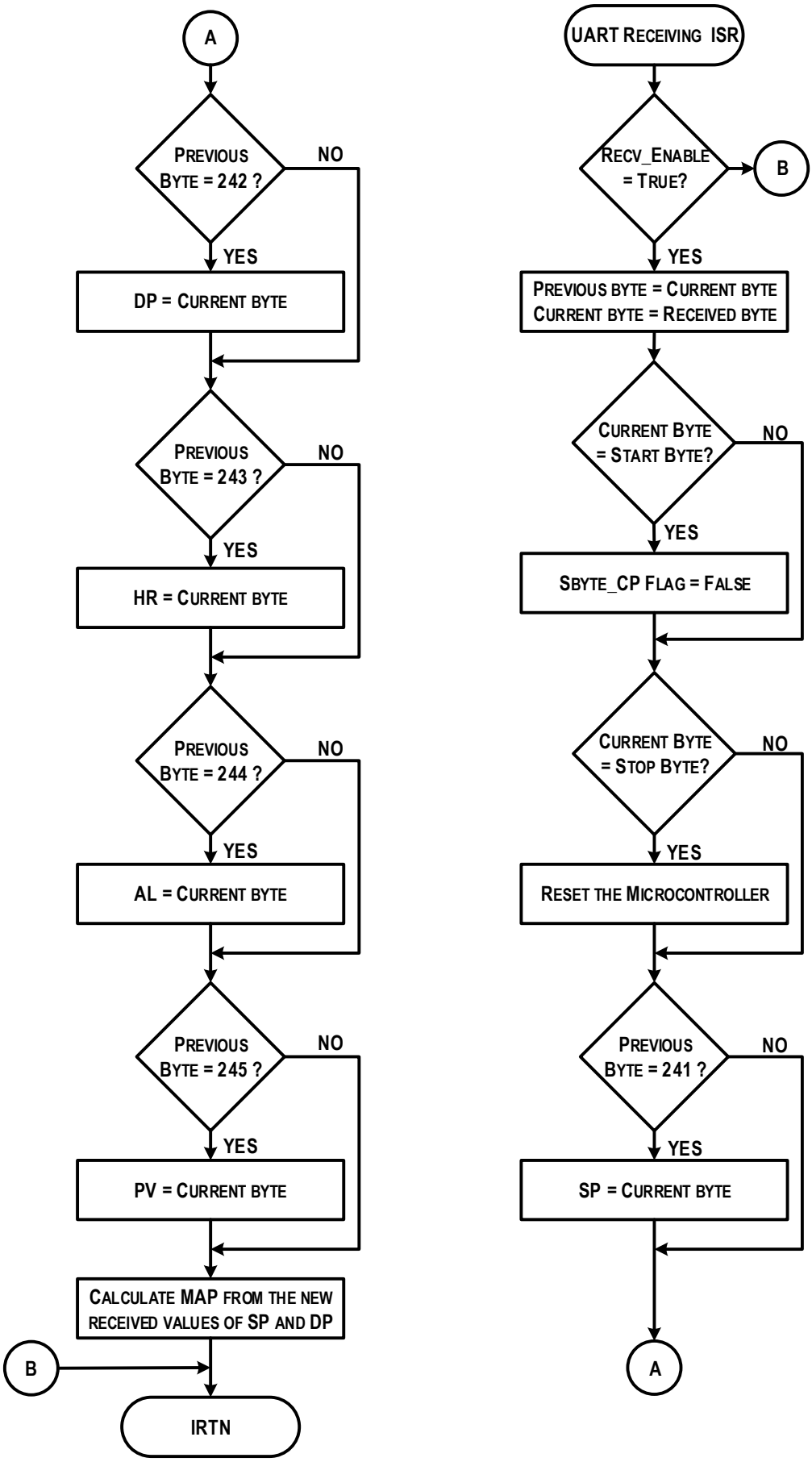

Figure 4.5: Flowchart diagram of UART ISR.

4.1.5 UART interrupt service routine

Figures 4.5 shows the flowchart of the code executed when a byte is received in the UART of the microcontroller. If the 'Recv_Enable' flag is true, the ISR is executed. The last received byte is saved in a variable named as the 'previous' byte and the new received byte is saved in a variable named as the 'current' byte. If the received byte is the 'start' byte, the 'Sbyte_CP' flag is set to false indicating that the COM port is recognized and the sending the 'start' byte is to be stopped and the cuff pressure value is to be sent. If the received byte is the 'stop' byte, the microcontroller is reset as it means that the GUI software is closed. If the 'previous' byte is equal to 241, the value of the 'current' byte is saved as the updated value of the SP, if it is equal to 242, the value of the 'current' byte is saved as the updated value of the DP, if it is equal to 243, the value of the 'current' byte is saved as the updated value of the HR, if it is equal to 244, the value of the 'current' byte is saved as the updated value of the AL, and if it is equal to 245, the value of the 'current' byte is saved as the value of the PV. The value of the MAP is then recalculated from the new received values of SP and DP before returning to the main code.

4.2 PC-based and Android-based GUI software

The PC-GUI interface was designed using XAML, and the operating code was written in C#, using Microsoft Visual Studio Community 2017, version 15.3.3. An EXE file was produced and installed on the PC. A Bluetooth dongle is connected to the PC to enable communication with the HC-05 Bluetooth module. Figures 4.6 shows a snapshot of the graphical interface of the PC-GUI. Figure 4.8 shows the flowchart of the code. When the software is opened, the 5 simulation parameters boxes are initialized with the default values as SP = 120, DP = 80, AL = 0, PV =50, and HR = 70. A list of all the available COM ports is obtained. The first COM port is opened and one byte is read from it. If the read byte is equal to the 'start' byte, the 'start' byte is sent back to the microcontroller indicating that the COM port is identified, the COM port is kept open, and the rest of the list is ignored. If no data are read or the read byte is not equal to the 'start' byte, the COM port is closed and the next port is opened. This process is repeated until the 'start' byte is received from one of the ports in the list. In case the 'start' byte is not received from any of the ports, a warning message with OK button is shown that either the simulator device is not powered on or the Bluetooth is not paired. When the user presses the OK button, the program is shut down. After the COM port is identified, the program stays in an idle mode waiting for an event to occur when the user presses one the buttons. The event could be user-driven by pressing a button on the GUI window, or it could be when a byte is received in the serial COM port.

Android-based GUI was designed using MIT app inventor website [35]. An APK file was produced and installed in a smart phone. The application is opened, a button shows with the

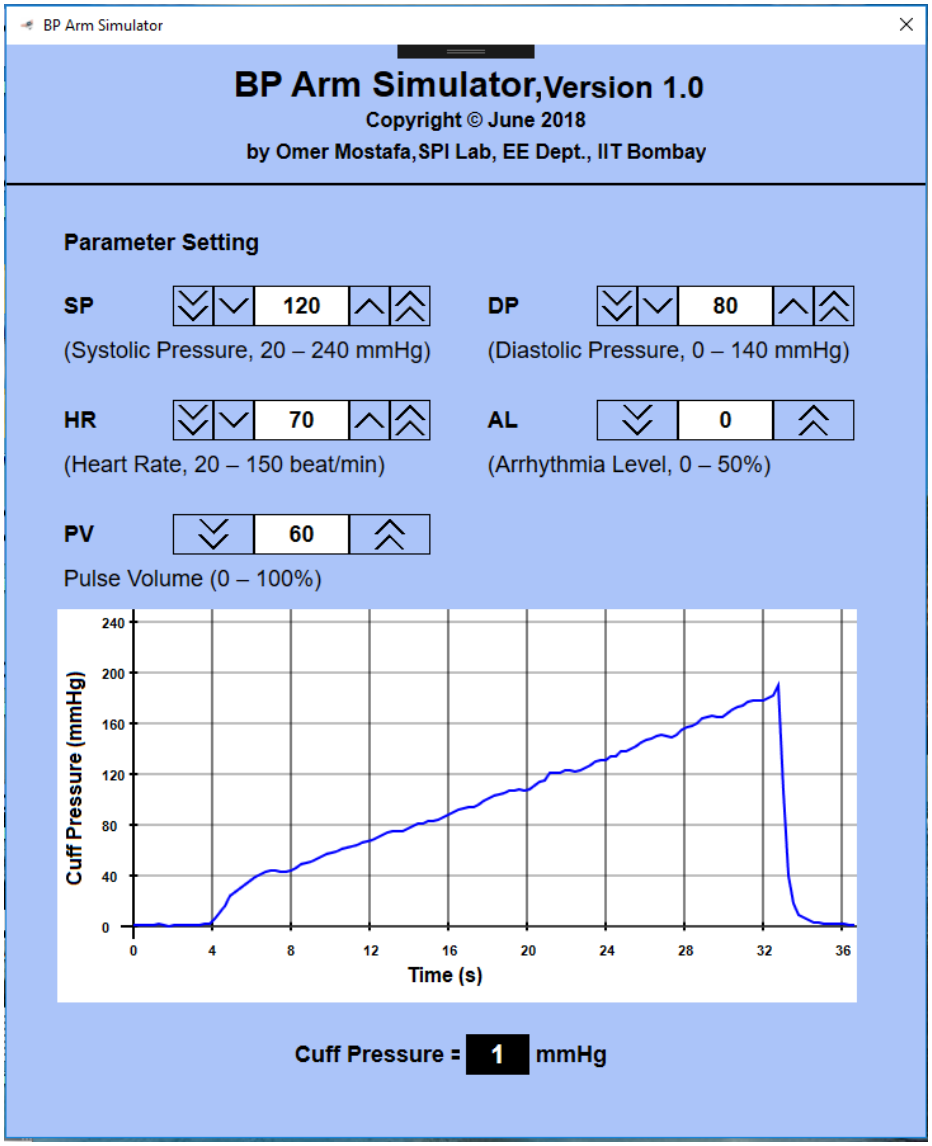

Figure 4.6: Snapshot of the PC-GUI.

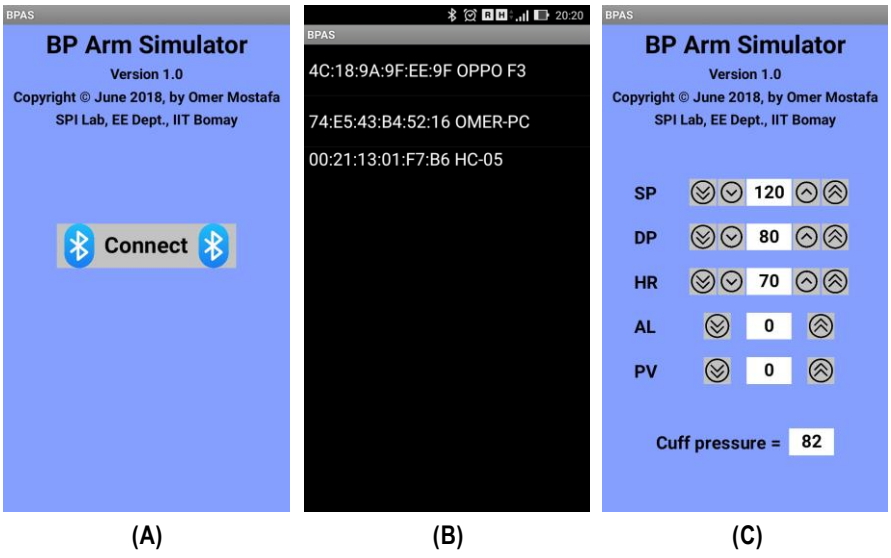

(A) (B) (C)

Figure 4.7: Snapshots of the Android-based GUI: (a) the screen when the application is opened, (b) the screen with the list of the paired devices, and (c) the screen with the editable simulation parameters.

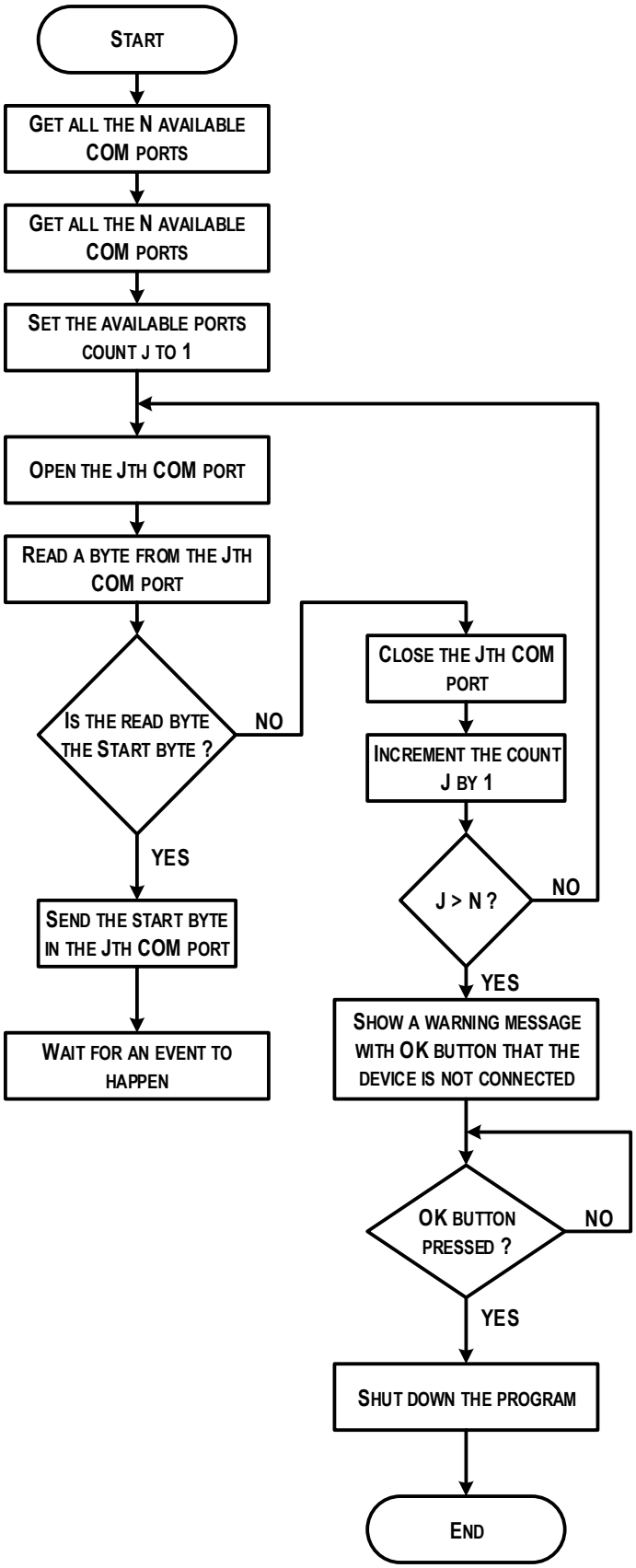

Figure 4.8: Flowchart of the PC-GUI code.

word ‘Connect’ written on it. When it is pressed, a list of all the paired Bluetooth devices is show. The Bluetooth device of the simulator is chosen and a graphical interface similar to the one in Figure 4.6 is shown. Figure 4.7 (a) shows a snapshot of the screen when the application is opened. Figure 4.7 (b) shows a snapshot of the screen with the list of the paired Bluetooth devices. Figure 4.7 (c) shows a snapshot of the screen with the editable simulation parameters.

Including the ‘x’ window-closing button in the PC-based GUI and the back button in the Android-based GUI, the screen contains 17 buttons. All the events that may occur are described in the following subsections.

4.2.1 SP coarse reduction event

When the button with the double down arrows of the SP is clicked, the SP value is reduced by 10, with the limits that it cannot be less than the DP value, and the minimum value is 20 mmHg. If the SP value does not satisfy the conditions $SP \geq (DP+10)$ and $SP \geq 30$, the program returns back to the idle mode. The flowchart of the code executed in this event is shown in Figure 4.9.

4.2.2 SP fine reduction event

When the button with the single down arrow of the SP is clicked, the SP value is reduced by 1, with the limits on its value as described earlier. If the SP value does not satisfy the conditions $SP > DP$ and $SP > 20$, the program returns back to the idle mode. The flowchart of the code executed in this event is shown in Figure 4.10.

4.2.3 SP fine increase event

When the button with the single up arrow of the SP is clicked, the SP value is increased by 1, with the limits that the SP value does not exceed the maximum value (240 mmHg). If the condition $SP < 240$ is not satisfied, the program returns back to the idle mode. The flowchart of the code executed in this event is shown in Figure 4.11.

4.2.4 SP coarse increase event

When the button with the double up arrows of the SP is clicked, the SP value is increased by 10, with the limit that $SP \leq 230$. Otherwise the program returns back to the idle mode. The flowchart of the code executed in this event is shown in Figure 4.12.

4.2.5 DP coarse reduction event

When the button with the double down arrows of the DP is clicked, the DP value is reduced by 10, with the limit that $DP>0$. The flowchart of the code executed in this event is shown in Figure 4.13.

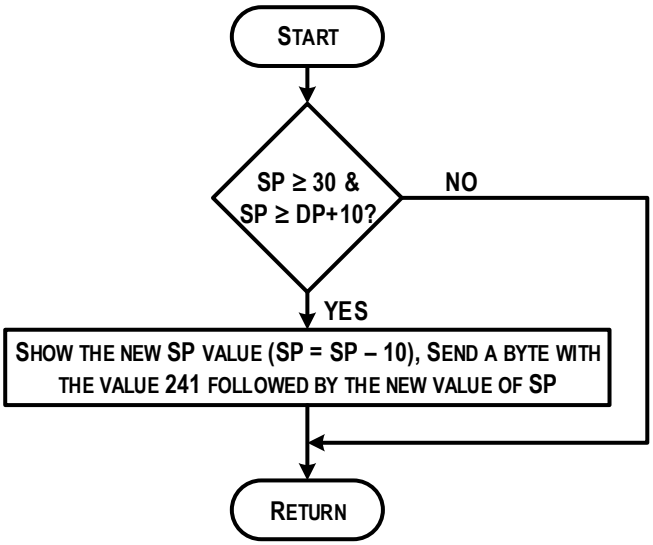

Figure 4.9: Flowchart of the SP coarse reduction event.

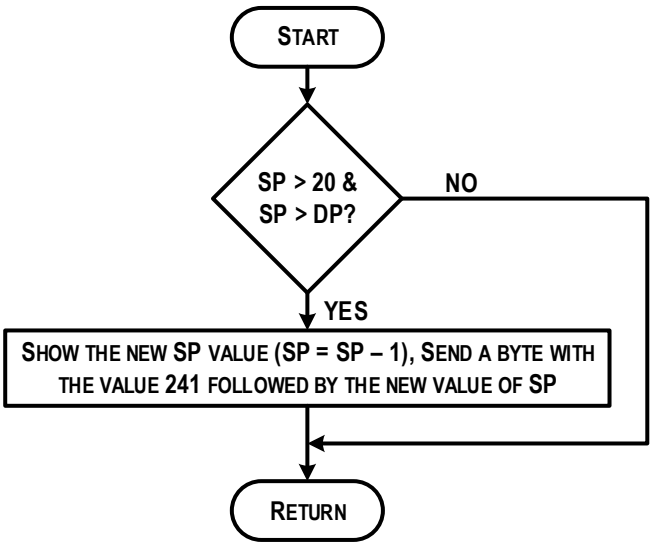

Figure 4.10: Flowchart of the SP fine reduction event.

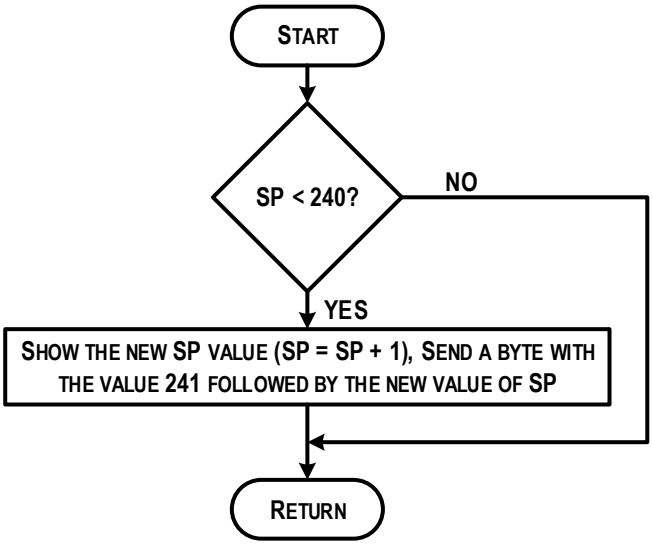

Figure 4.11: Flowchart of the SP fine increase event.

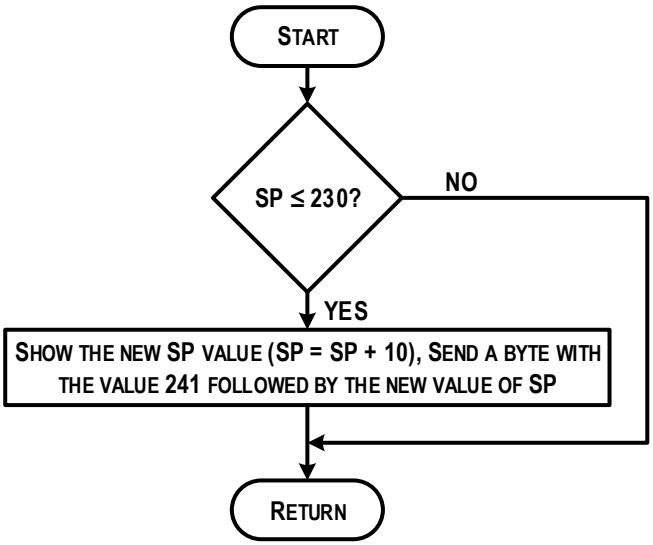

Figure 4.12: Flowchart of the SP coarse increase event.

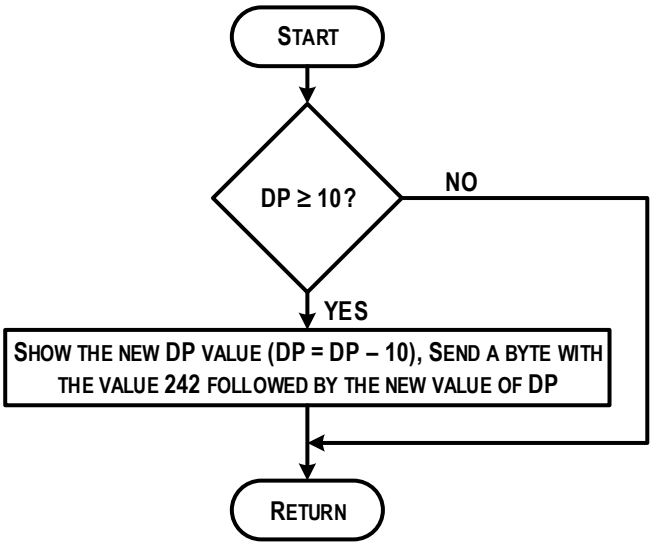

Figure 4.13: Flowchart of the DP coarse reduction event.

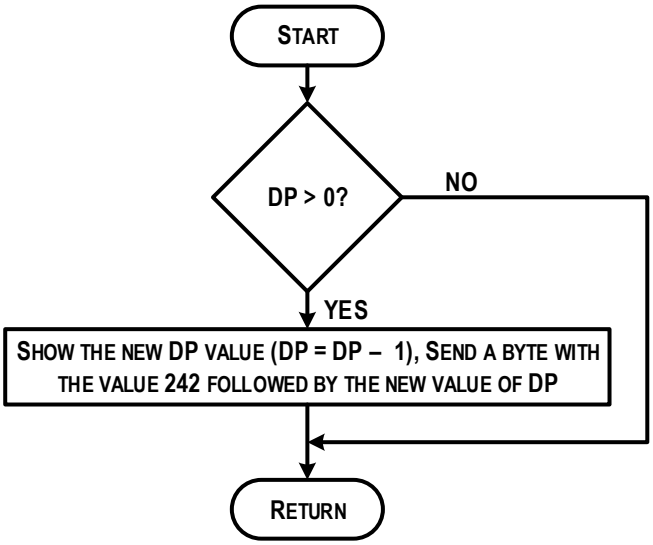

Figure 4.14: Flowchart of the DP fine reduction event.

4.2.6 DP fine reduction event

When the button with the single down arrow of the DP is clicked, the DP value is reduced by 1, with the limit that DP > 0. The flowchart of the code executed in this event is shown in Figure 4.14.

4.2.7 DP fine increase event

When the button with the single up arrow of the DP is clicked, the DP value is increased by 1, with the limits that DP < SP and DP < 140. The flowchart of the code executed in this event is shown in Figure 4.15.

4.2.8 DP coarse increase event

When the button with the double up arrows of the DP is clicked, the DP value is increased by 10, with the limits that DP ≤ SP –10 and DP ≤ 130. The flowchart of the code executed in this event is shown in Figure 4.16.

4.2.9 HR coarse reduction event

When the button with the double down arrows of the HR is clicked, the HR value is reduced by 10, with the limit that HR ≥ 30. The flowchart of the code executed in this event is shown in Figure 4.17.

4.2.10 HR fine reduction event

When the button with the single down arrow of the HR is clicked, the HR value is reduced by 1, with the limit that HR > 20. The flowchart of the code executed in this event is shown in Figure 4.18.

4.2.11 HR fine increase event

When the button with the single up arrow of the HR is clicked, the HR value is increased by 1, with the limit that HR < 150. The flowchart of the code executed in this event is shown in Figure 4.19.

4.2.12 HR coarse increase event

When the button with the single up arrow of the HR is clicked, the HR value is increased by 10, with the limit that HR ≤ 140.The flowchart of the code executed in this event is shown in Figure 4.20.

4.2.13 AL reduction event

When the button with the double down arrows of the AL is clicked, the AL value is reduced by 10, with the limit that AL > 0. The flowchart of the code executed in this event is shown in Figure 4.21.

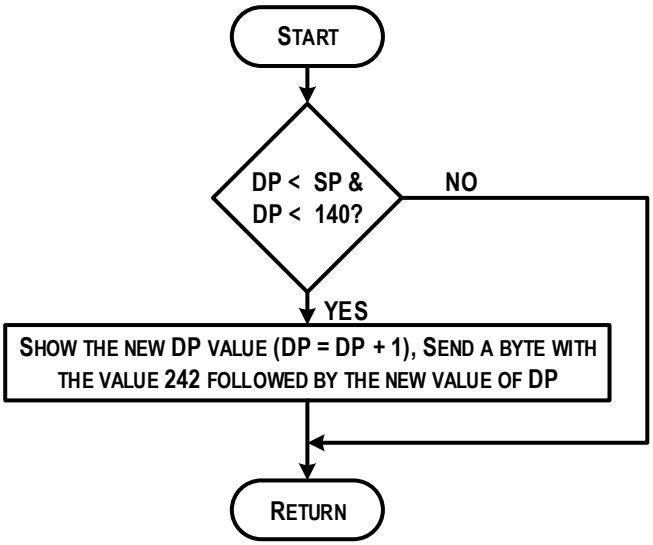

Figure 4.15: Flowchart of the DP fine increase event.

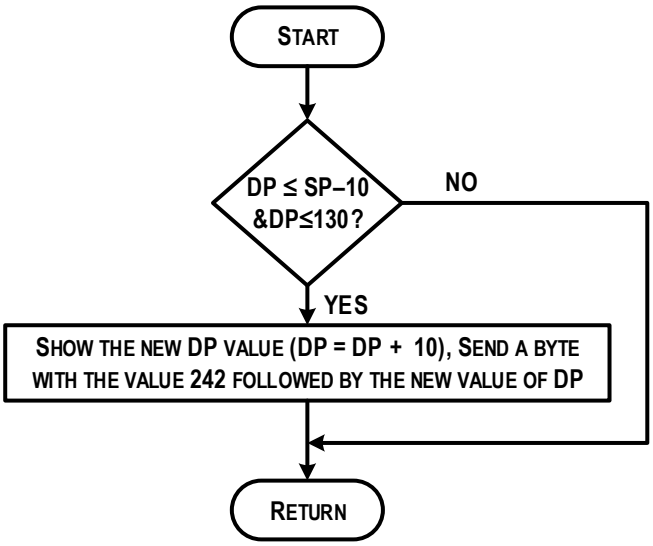

Figure 4.16: Flowchart of the DP coarse increase event.

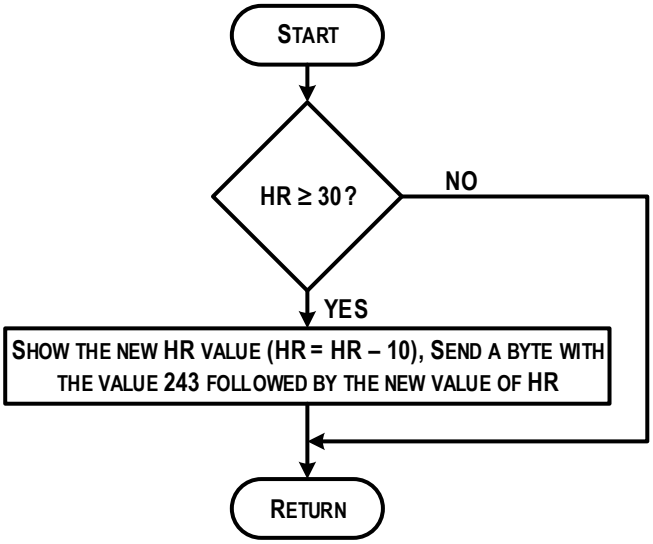

Figure 4.17: Flowchart of the HR coarse reduction event.

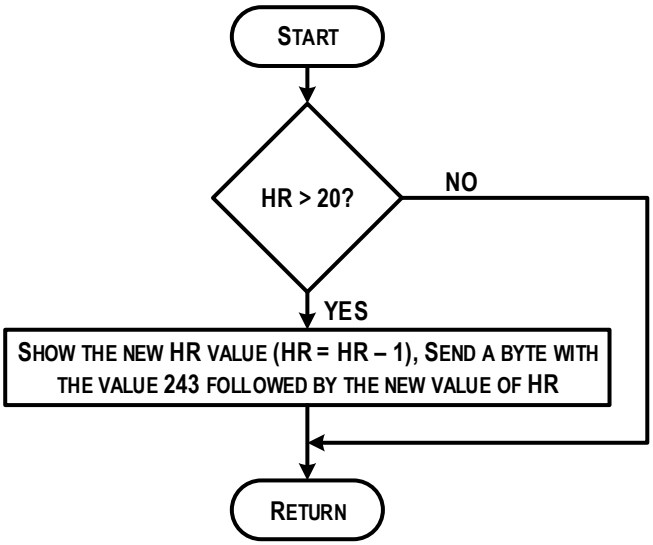

Figure 4.18: Flowchart of the HR fine reduction event.

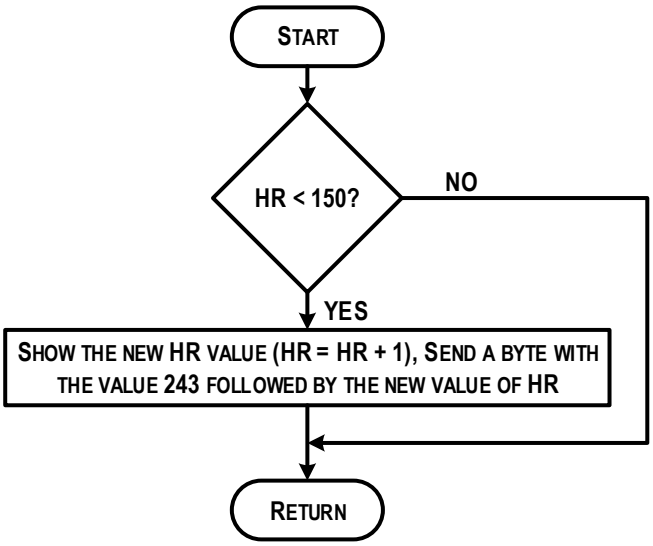

Figure 4.19: Flowchart of the HR fine increase event.

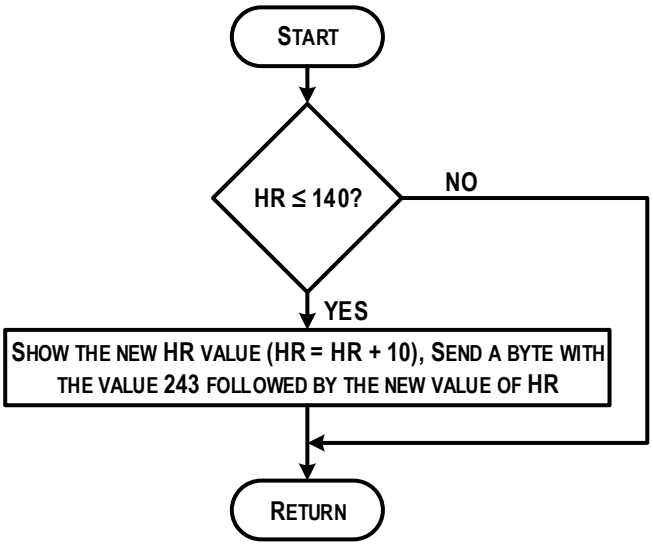

Figure 4.20: Flowchart of the HR coarse increase event.

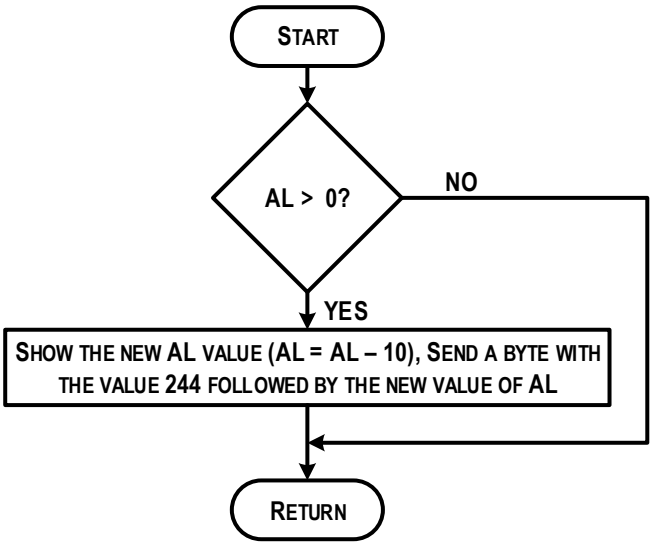

Figure 4.21: Flowchart of the AL reduction event.

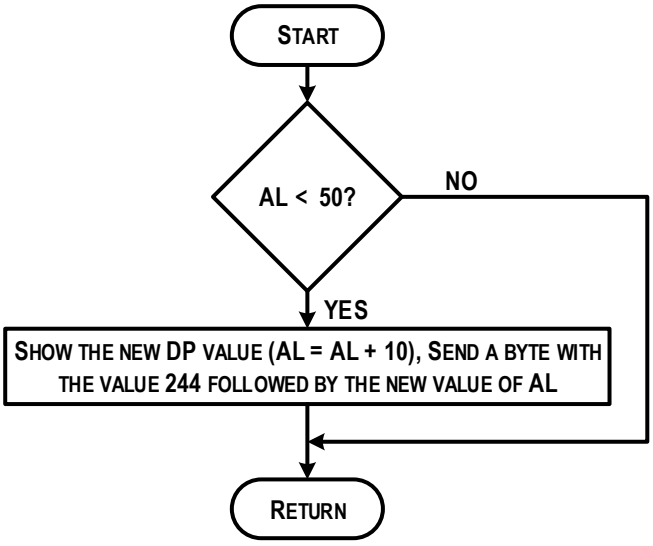

Figure 4.22: Flowchart of the AL increase event.

4.2.14 AL increase event

When the button with the double up arrows of the AL is clicked, the AL value is increased by 10, with the limit that AL < 50. The flowchart of the code executed in this event is shown in Figure 4.22.

4.2.15 PV reduction event

When the button with the double down arrows of the PV is clicked, the PV value is reduced by 10, with the limit that PV > 0. The flowchart of the code executed in this event is shown in Figure 4.23.

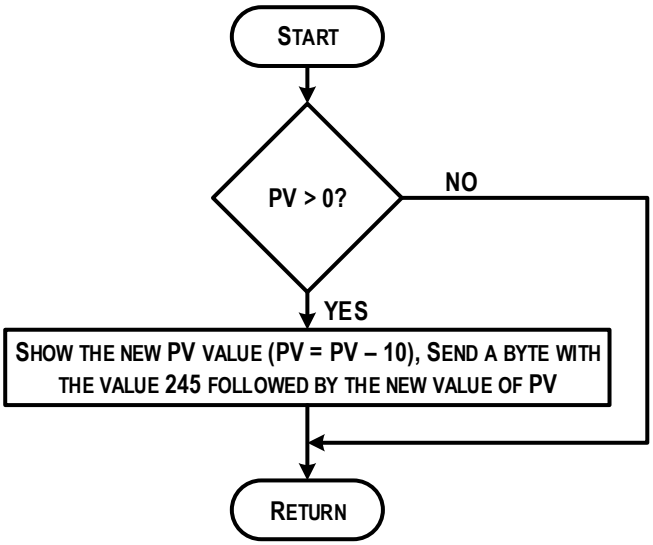

Figure 4.23: Flowchart of the PV reduction event.

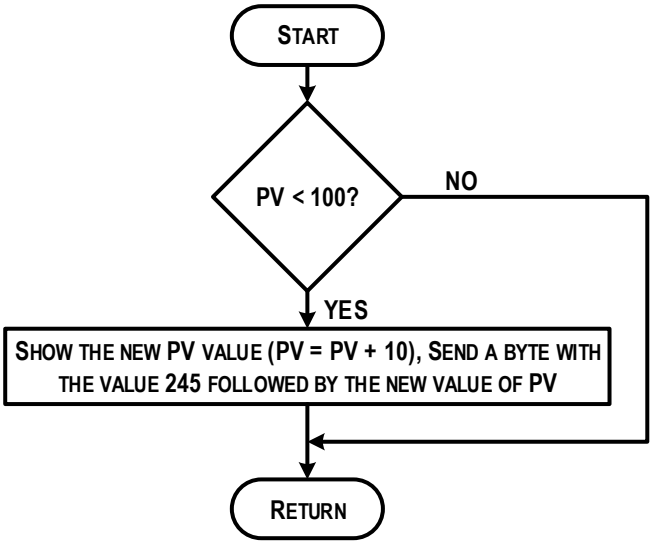

Figure 4.24: Flowchart of the PV increase event.

4.2.16 PV increase event

When the button with the double up arrows of the PV is clicked, the PV value is increased by 10, with the limit that PV < 100. The flowchart of the code executed in this event is shown in Figure 4.24.

4.2.17 Window-closing event

When the ‘x’ window-closing button in the PC-based GUI, or the back button in the Android-based GUI, is pressed, the program sends the ‘stop’ byte to microcontroller to be reset and closes the COM port. The window is closed, and the software is shutdown. The flowchart of the code executed in this event is shown in Figure 4.25.

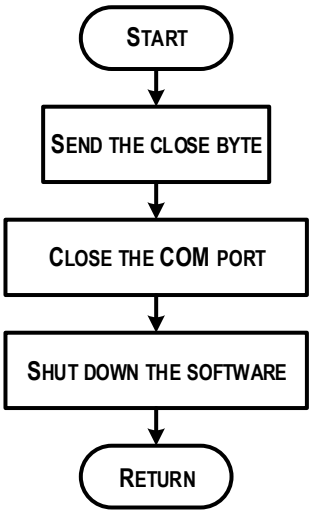

Figure 4.25: Flowchart of window-closing event.

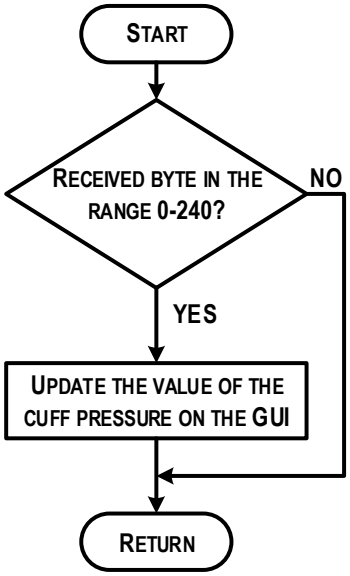

Figure 4.26: Flowchart of the serial port byte-receiving event.

Table 4.1: Protocol bytes and their values

Index	Byte name	Hex value	Decimal value
1	Previous byte of SP	0xF1	241
2	Previous byte of DP	0xF2	242
3	Previous byte of HR	0xF3	243
4	Previous byte of AL	0xF4	244
5	Previous byte of PV	0xF5	245
6	Start byte	0xFA	250
7	Stop byte	0xFC	252

Table 4.3: Summary of the events of the GUI

Event	Button clicked	Actions	Flow chart
SP coarse reduction	Double down arrows of SP	SP = SP – 10	Figure 4.9
SP fine reduction	single down arrows of SP	SP = SP – 1	Figure 4.10
SP fine increase	single up arrows of SP	SP = SP + 1	Figure 4.11
SP coarse increase	Double up arrows of SP	SP = SP + 10	Figure 4.12
DP coarse reduction	Double down arrows of DP	DP = DP – 10	Figure 4.13
DP fine reduction	single down arrows of DP	DP = DP – 1	Figure 4.14
DP fine increase	single up arrows of DP	DP = DP + 1	Figure 4.15
DP coarse increase	Double up arrows of DP	DP = DP + 10	Figure 4.16
HR coarse reduction	Double down arrows of HR	HR = HR – 10	Figure 4.17
HR fine reduction	single down arrows of HR	HR = HR – 1	Figure 4.18
HR fine increase	single up arrows of HR	HR = HR + 1	Figure 4.19
HR coarse increase	Double up arrows of HR	HR = HR + 10	Figure 4.20
AL coarse reduction	Double down arrows of AL	AL = AL – 10	Figure 4.21
AL coarse increase	Double up arrows of AL	AL = AL + 10	Figure 4.22
PV coarse reduction	Double down arrows of PV	PV = PV – 10	Figure 4.23
PV coarse increase	Double up arrows of PV	PV = PV + 10	Figure 4.24
Window-closing	The ‘X’ in PC-based GUI and back button in Android-based GUI.	Close serial port and shut down the software.	Figure 4.25

4.2.18 COM port byte-receiving event

When a byte is received in the COM port, the program checks if it is a protocol byte or it is a data byte that contains the cuff pressure value. If it is in the range from 0-240, it is a data byte, the program updates the value of the cuff pressure on the GUI. Otherwise, it is a protocol byte, the program does nothing and returns back to the idle mode. All the protocol bytes are listed in Table 4.1. The flowchart of the code executed in this event is shown in Figure 4.25.

Left blank

Chapter 5
TEST RESULTS

In this chapter, the instrument setup and the test results of the developed arm simulator, for both auscultatory and oscillometric methods are presented.

5.1 Instrument setup

The arm simulator is designed as a vertical cylinder with a horizontal square base. The cylinder represents the arm for the cuff to be wrapped around it as shown in Figure 5.1. The body of the simulator is designed using 'SolidWorks' and printed using a 3D printer. The material used is polylactic acid (PLA). The cylinder has a height of 15 cm and an outer diameter of 8 cm. The thickness of the wall of the cylinder is 7.5 mm. The cylinder is designed with a circular support on its transverse plane for the linear actuator to rest on as shown in Figure 5.1 (b). Two pieces in the shape of an inverted-U are used to restrict the movement of the linear actuator as shown in Figure 5.1(c). A hole is made in the cylinder wall for the shaft of the linear actuator to go through and push against the wall of the cuff as shown in Figure 5.1(a).

5.2 Test results of auscultatory method

Figures 5.2 to 5.6 show snapshots of signals recorded using a digital oscilloscope (DSO). Figure 5.2 shows a single heartbeat pulse when the cuff pressure is at the MAP, the SP is 120, DP is 80, HR is 70, AL is 0, and PV is 50.

To demonstrate that the circuit is working with different values of simulation parameters, the simulation was done three times. The signal of the sensor output voltage while decreasing the cuff pressure from SP to DP, along with the output of the amplifier, is shown in Figures 5.3 to 5.5. In Figure 5.3, the simulation parameters were set to the default values; the SP is 120, DP is 80, HR is 70, AL is 0, and PV is 50. In Figure 5.4, the parameters are set to give a wide range between SP and DP with a fast beating heart and high SP; the SP is 230, DP is 70, HR is 120, AL is 30 and PV is 70. In figure 5.5, the parameters are set to simulate low SP and DP pressures; the SP is 110, the DP is 50, the HR is 63, AL is 10, and PV is 100.

To test the circuit when arrhythmia is introduced, the simulation is performed with the default values and the cuff pressure is fixed at the value of the MAP to show the highest amplitude. The output signal of the amplifier is recorded several times with different settings of the AL. Figures 5.6 (a), 5.6 (b), 5.6 (c), and 5.6 (d) show the output signal with AL = 0, AL = 10, AL = 30, and AL = 50, respectively.

5.3 Test results of oscillometric method

The automatic BP monitor from 'AccuSure' with the model number 'TMB-1490-A' is used to demonstrate the working of the arm simulator. The monitor can measure the BP in the range

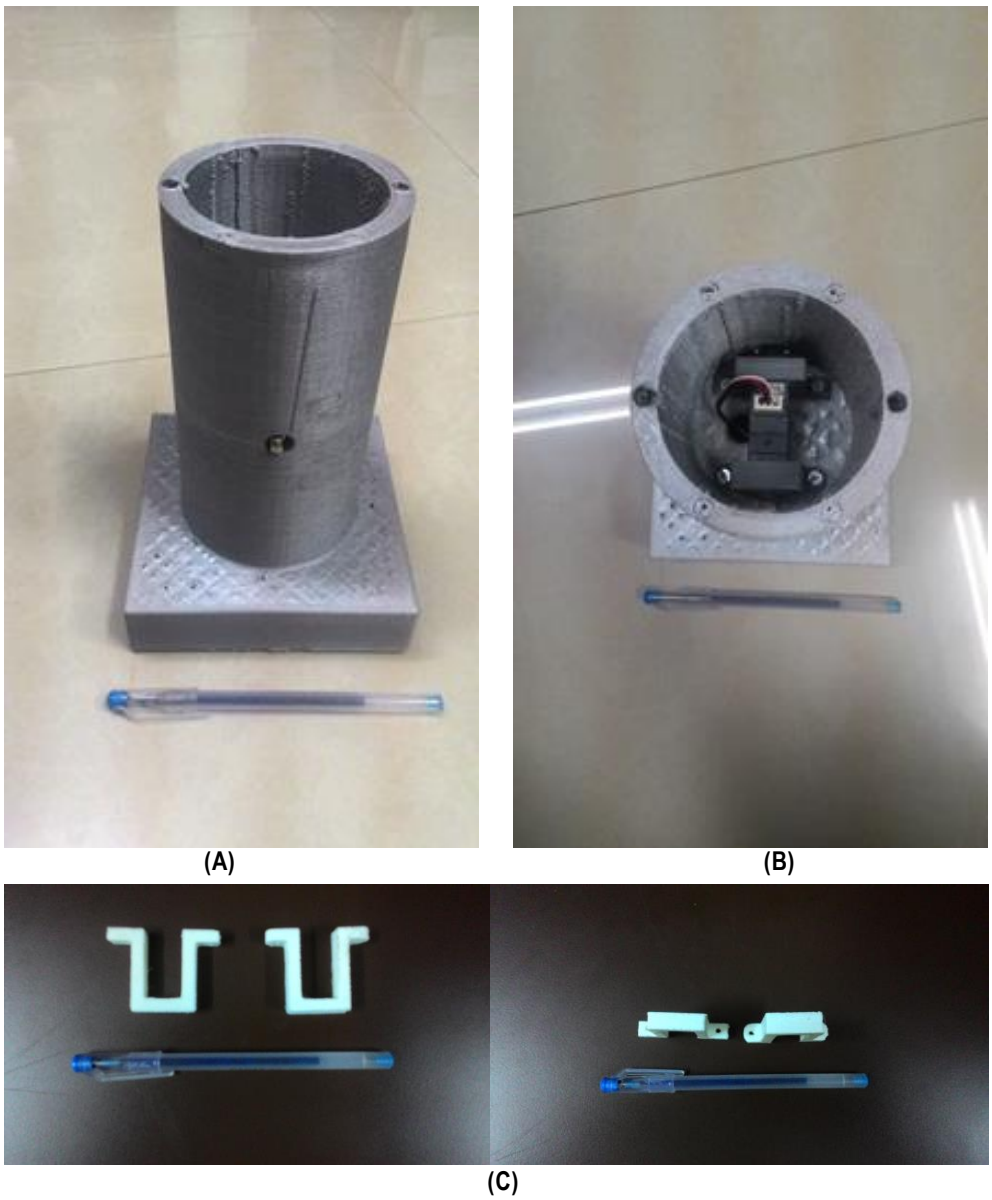

Figure 5.1: Instrument setup: (a) side view of the cylinder, (b) top view of the cylinder, and (c) the pieces used to restrict the motion of the linear actuator.

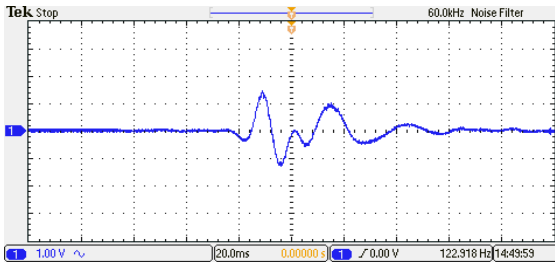

Figure 5.2: A single pulse of the heartbeat signal at the amplifier output with default parameters, as acquired using a DSO.

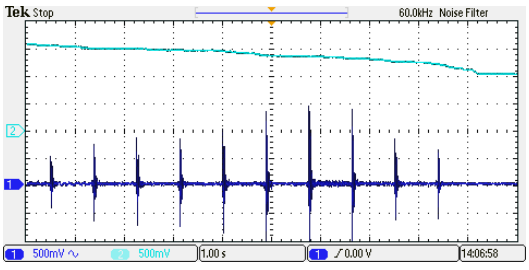

Figure 5.3: Ch1 (upper): voltage of the pressure sensor, Ch2 (lower): output signal of the amplifier while decreasing CP from SP to DP, with SP=120, DP=80, HR=70, AL=0, and PV=50.

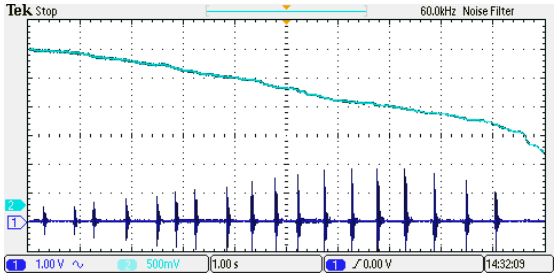

Figure 5.4: Ch1 (upper): voltage of the pressure sensor, Ch2 (lower): output signal of the amplifier while decreasing CP from SP to DP, with SP=230, DP=70, HR=120, AL=30, and PV=70.

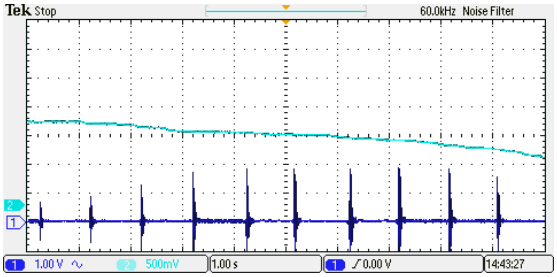

Figure 5.5: Ch1 (upper): voltage of the pressure sensor, Ch2 (lower): output signal of the amplifier while decreasing CP from SP to DP, with SP=110, DP=50, HR=63, AL=10 and PV=100.

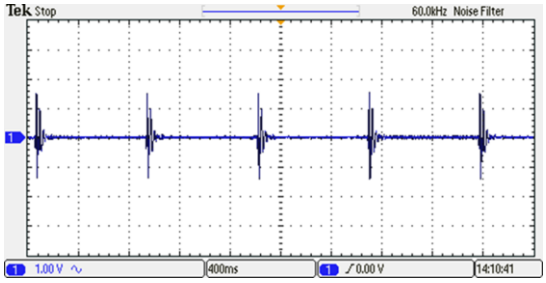

(a)

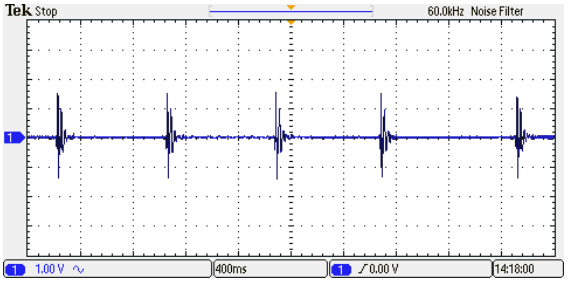

(c)

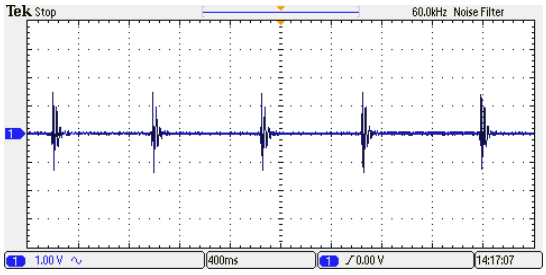

(b)

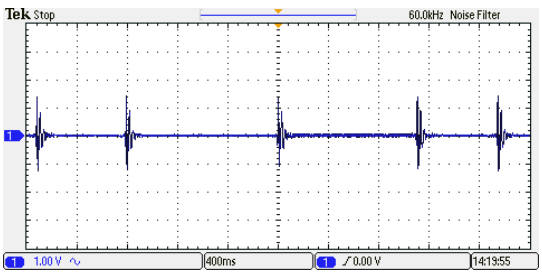

(d)

Figure 5.6: Amplifier output with CP=MAP, SP=120, DP=80, HR=70, and different arrhythmia levels: (a) AL=0, (b) AL=10, (c) AL=30, and (d) AL=50.

of 40 – 230 mmHg with an accuracy of ±3 mmHg. It can detect the heartrate in the range of 40 – 199 beat/min with an accuracy of ± 5%.

When the pressure pulses were produced according to the envelope shown in Figure 3.7, the readings of the BP monitor were different from the readings of the set simulation parameters. The readings of the BP monitor have a correlation with the maximum value of the amplitude of the pulses. When the maximum amplitude is increased, the SP is underestimated and the DP is overestimated, and vice versa. These readings could be explained that the BP monitor reads the envelope and based on that, predicts the values of the SP and DP. As shown in Figure 5.7 and 5.8, the SP and DP values estimated by the BP monitor vary with the value of the maximum amplitude of the generated pulses.

One possible source of the error in the readings maybe that the amplitude of the generated pulses in the cuff is not linear with the amount of displacement of the linear actuator. Figure

5.9 shows the change in the amplitude of pulses sensed by the pressure sensor with the amount of the shaft displacement of the linear actuator for different values of cuff pressures.

To make the pulses mimic the pulses that are produced by the human arm, the pressure pulses from 9 subjects, 4 females and 5 males with ages in the range 20 – 35 (25 ± 1.6) years, were recorded while measuring their BP using the automatic BP monitor. Figures 5.10 (a) to 5.10 (i) show the DSO recording of these pulses along with the values of SP, DP, and HR as measured by the automatic BP monitor.

After considering the variation of the amplitude of the generated pulses with the cuff pressure, reproduction of the envelope of the first subject shown in Figure 5.11 was attempted with doubling the amplitude of the pulses. The pulses generated by the arm simulator was read

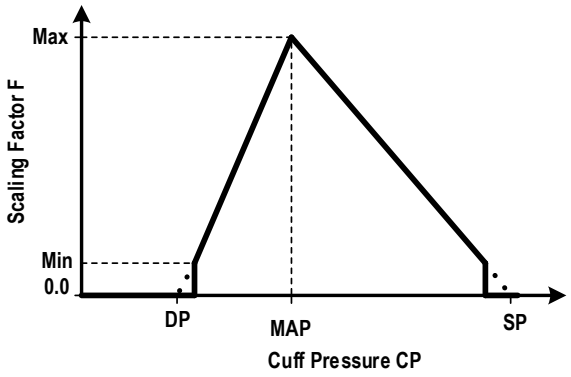

Figure 5.7: A narrow-generated envelope leading to overestimating of DP and underestimating of SP values read by the BP monitor.

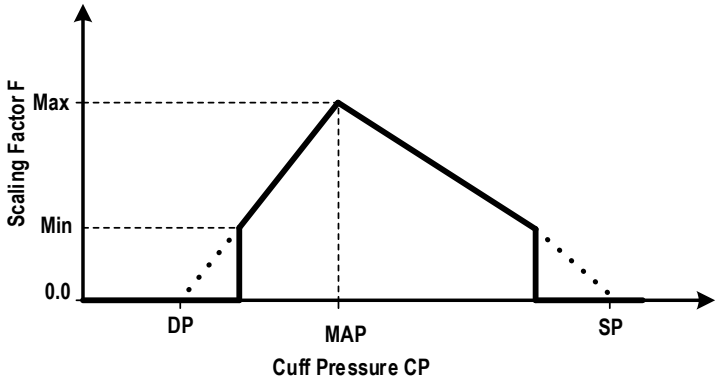

Figure 5.8: A wide-generated envelope leading to underestimating of DP and overestimating of the SP values read by the BP monitor.

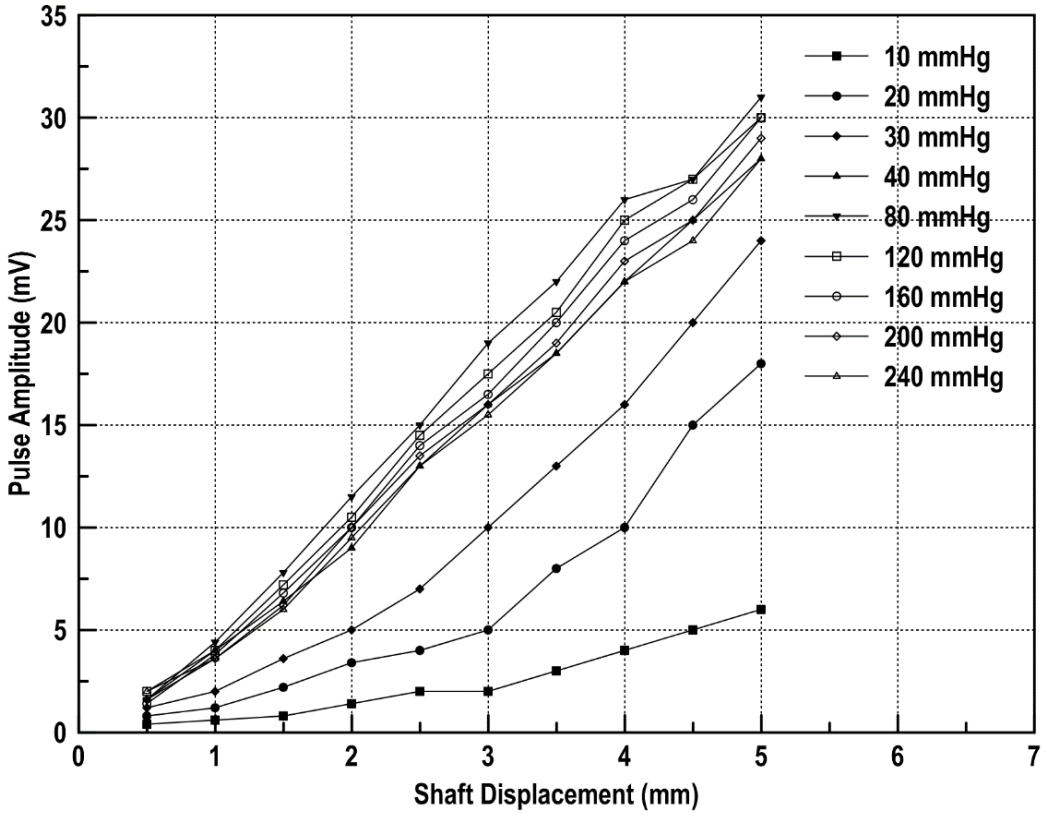

Figure 5.9: Change in the amplitude of the sensed oscillations with the amount of the shaft displacement of the linear actuator for different values of cuff pressure.

by the BP monitor and the simulation parameters were set to be similar to the readings of the subject (SP = 100, DP = 66, and HR =78). The readings of the BP monitor for the reproduced envelope were SP = 90, DP = 63, and HR = 77. Figure 5.12 shows envelopes for the subject and the simulator. The ratio of the amplitude of the simulated pulses to the amplitude of the pulses of the subject is reducing with the increase in the cuff pressure. That explains why the value of the SP for simulated envelope is less than the SP for envelope of the subject. The difference in the DP values is within the range of accuracy of the BP monitor.

To solve this issue, a closed loop control could be used instead of just sending the desired amplitude to the linear actuator in an open loop manner. The amplitude of the generated pressure pulses could be measured. The amplitude of each generated pulse would be used to recalculate the amplitude of the next one. This way, the generated envelope can be controlled to mimic the desired envelope.

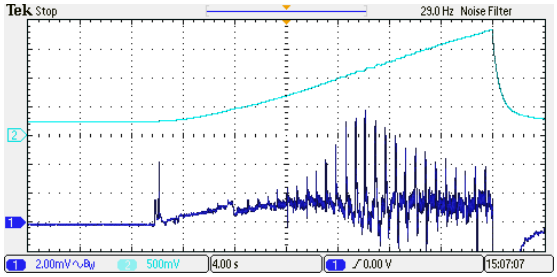

(a)

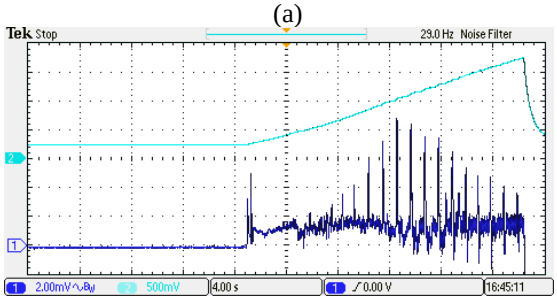

(b)

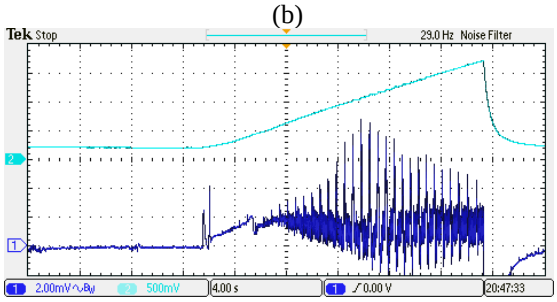

(c)

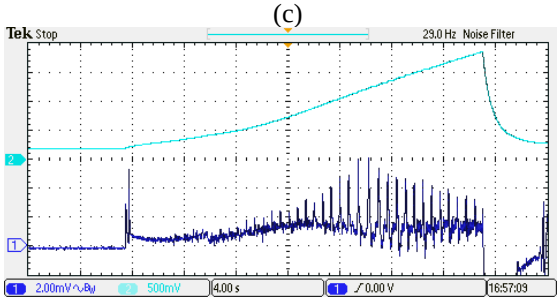

(d)

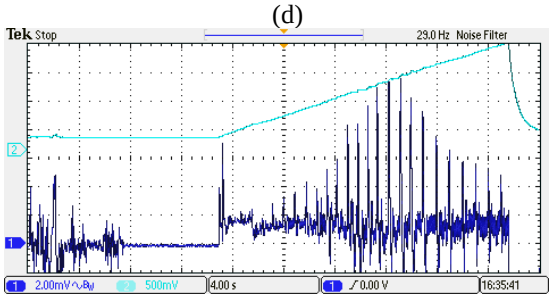

(e)

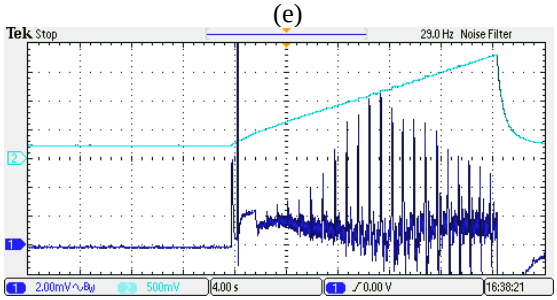

(f)

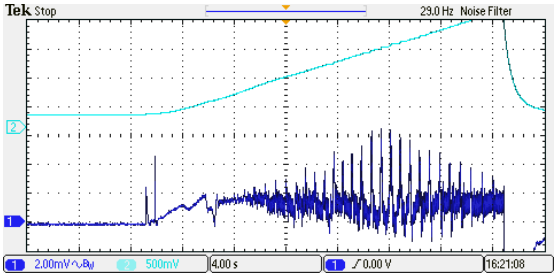

(g)

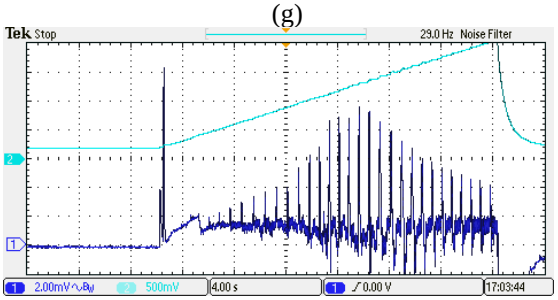

(i)

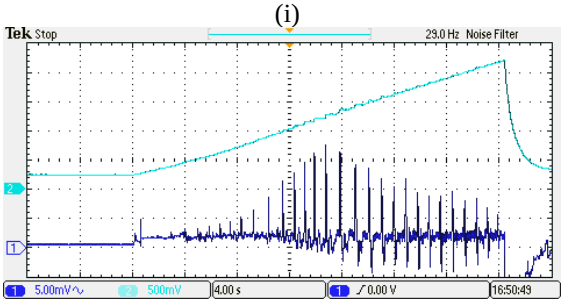

Figure 5.10: DSO recording, Ch1 (lower): ac coupled voltage signal of the pressure sensor, Ch2 (upper): dc-coupled voltage signal of the pressure sensor, of 9 subjects from both genders with different values of age, BP, and HR: (a) female with age =23, SP=100, DP=66, and HR=78, (b) female with age =22, SP=95, DP=61, and HR=57, (c) female with age =27, SP=109, DP=69, and HR=94, (d) female with age =24, SP=120, DP=75, and HR=89, (e) male with age =20, SP=114, DP=70, and HR=67, (f) male with age =20, SP=112, DP=67, and HR=69, (g) male with age =29, SP=122, DP=86, and HR=79, (h) male with age =35, SP=131, DP=81, and HR=75, and (i) male with age=25, SP=129, DP=74, and HR=65.

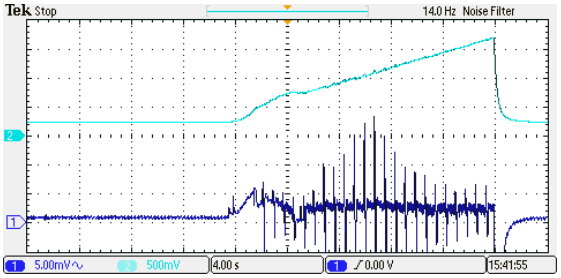

Figure 5.11: DSO recording of the reproduction of the envelope in Figure 5.10 (a) using the same simulation parameters (SP = 100, DP = 66, and HR = 78), Ch1 (lower): ac coupled voltage signal of the pressure sensor, Ch2 (upper): dc-coupled voltage signal of the pressure sensor.

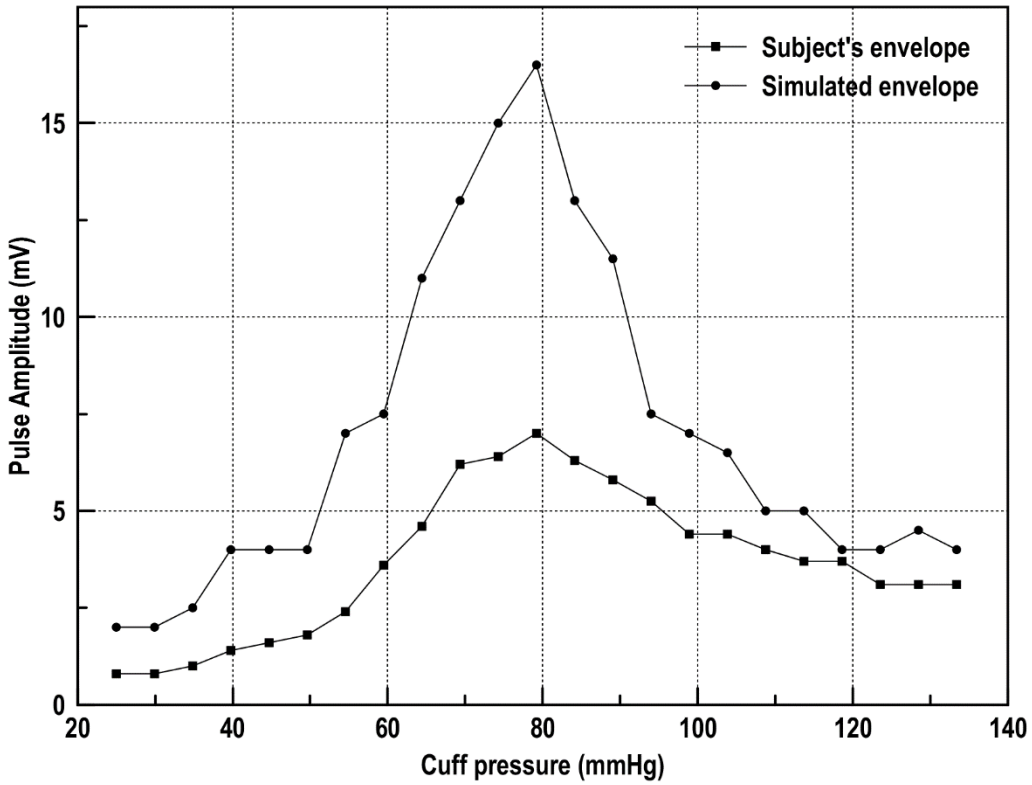

Figure 5.12: Amplitude of the oscillation envelopes from the subject and the simulator with.

Left blank

Chapter 6
SUMMARY AND CONCLUSION

An arm simulator for BP measurement using the auscultatory and oscillometric methods has been developed. It is in the form of a vertical cylinder with a horizontal base. The cuff pressure is measured using a pressure sensor, connected to the tube between the cuff and the monitor via a T-connector. A user-friendly PC-based and Android-based GUIs have been developed so that the simulation parameters are set wirelessly through Bluetooth.

The following has been accomplished:

i. An arm simulator circuit has been designed and tested for both auscultatory and oscillometric methods.
ii. PC-based and Android-based GUIs have been developed and tested.
iii. Bluetooth communication between the GUI and the simulator circuit has been implemented.

6.1 Future work

i. The PCB needs to be redesigned to include the part that controls the linear actuator for the oscillometric method and also to fit the board inside the base of the cylinder.
ii. Noninvasive measurement of the cuff pressure using a force sensor needs to be explored.
iii. Closed-loop control of the linear actuator is to be implemented for better accuracy of the generated envelope.
iv. Different models of BP measuring instruments are to be tested using the developed simulator.
v. Larger number of envelopes need to be recorded from subjects with various cardiovascular conditions.

Left blank

Appendix A

SCHEMATIC OF THE ARM SIMULATOR WITH AUSCULTATORY METHOD

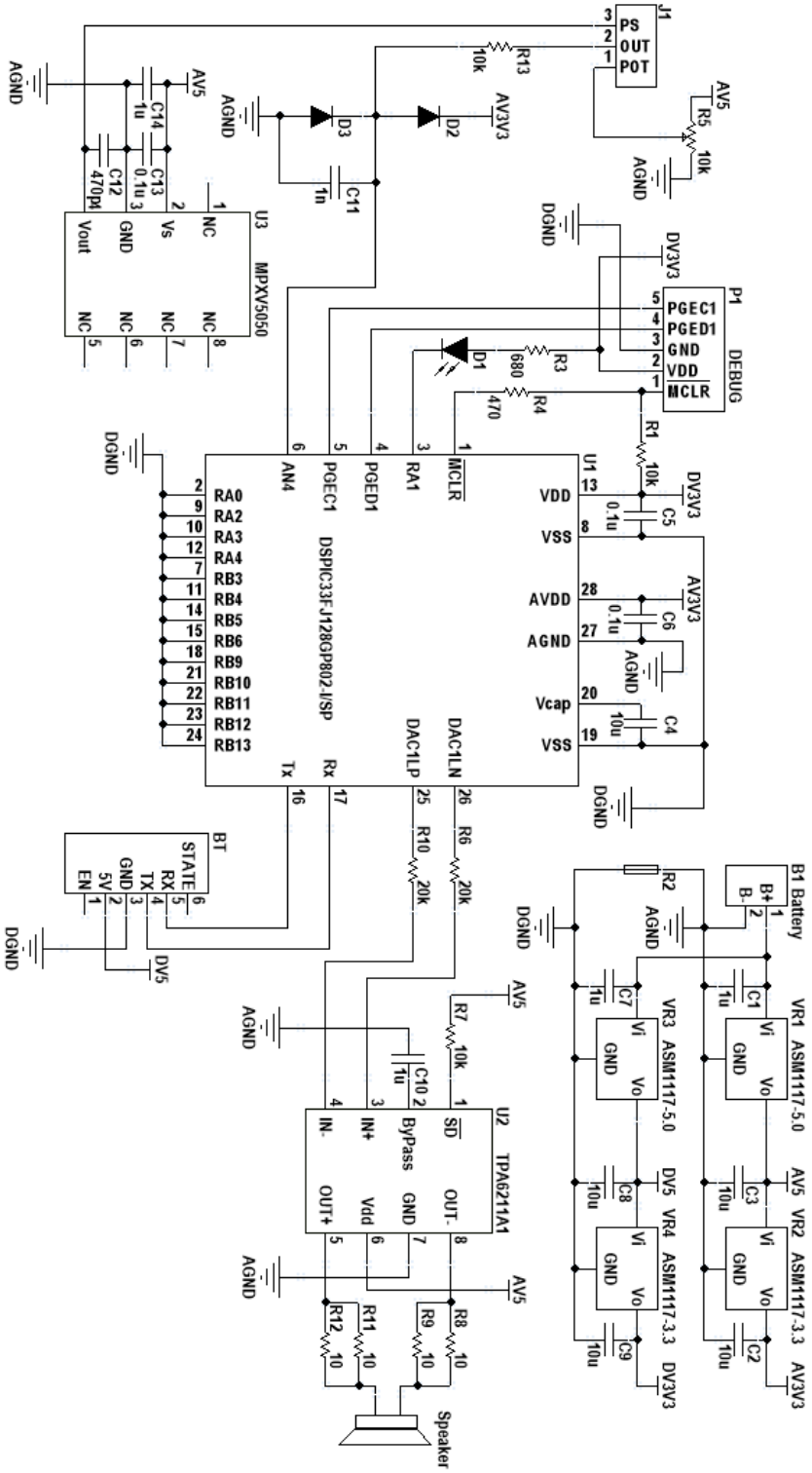

Figure A.1: Full circuit diagram of the arm simulator

Left blank

Appendix B

COMPONENT LIST OF THE ARM SIMULATOR CIRCUIT WITH AUSCULTATORY METHOD

Table B.1: Component list of the arm simulator circuit

Component designator	Component description	Part Number / Value	Quantity
C1, C7, C10, C14	Capacitor, ceramic, 0508 package	1 μF	4
C2, C3, C4, C8, C9	Capacitor, tantalum, 0508 package	10 μF	5
C5, C6, C13,	Capacitor, ceramic, 0508 package	0.1 μF	3
C11	Capacitor, ceramic, 0508 package	1 nF	1
C12	Capacitor, ceramic, 0508 package	470 pF	1
R1, R7, R13	Resistor, 0508 package	10 kΩ	3
R3	Resistor, 0508 package	680 Ω	1
R4	Resistor, 0508 package	470 Ω	1
R6, R10	Resistor, 0508 package	20 kΩ	2
R8, R9, R11, R12	Resistor, 0508 package	10 Ω	4
R5	Potentiometer, through hole	10 kΩ	1
D1	LED, 0508 package	--------	1
D2, D3	Diode, 0508 package	0.7 V	2
U1	Microcontroller, IC, SOIC package	DSPIC33FJ128GP802	1
U2	Differential amplifier, IC, MSOP-8 package	TPA6211A1	1
U3	Pressure sensor, IC	MPXV5050 GP	1
VR1, VR3	5V regulator, IC, SOT-223 package	ASM7111-5.0	2
VR2, VR4	3.3V regulator, IC, SOT-223 package	ASM7111-3.3	2

BT	Header, 6 pins, male	2.54 mm	1
P1	Header, 5 pins, female	2.54 mm	1
Speaker	Jack connector	3.5 mm	1
J1	Jumper, 2 Pins	2.54 mm	1

Appendix C

PCB LAYOUT OF THE SIMULATOR WITH

AUSCULTATORY METHOD

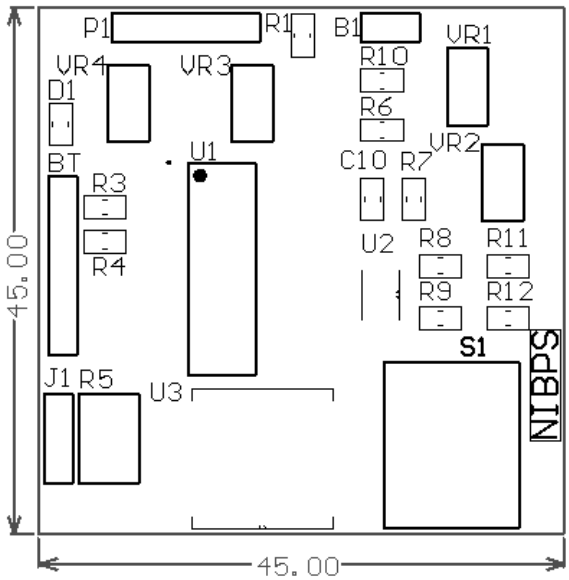

Figure C.1: Top overlay and keep out layers

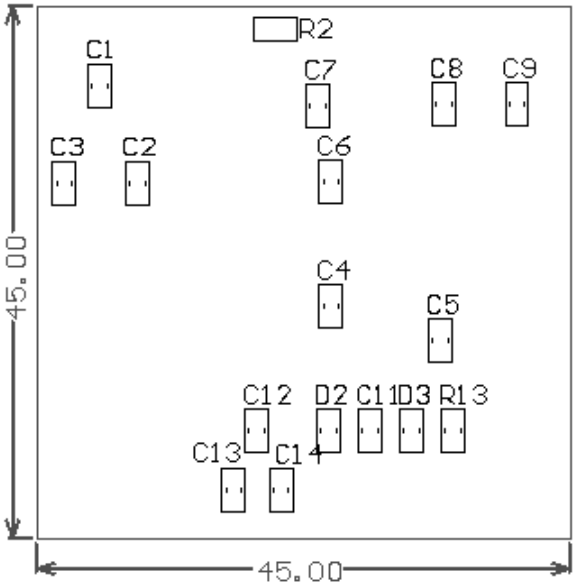

Figure C.2: bottom overlay and keep out layers

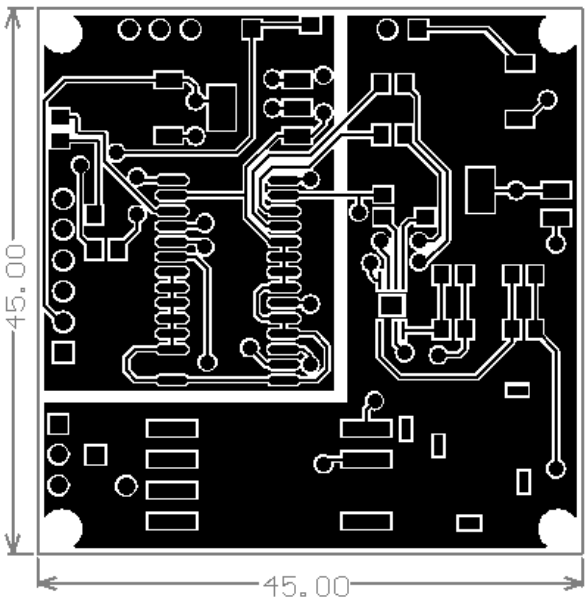

Figure C.3: Top copper and keep out layers

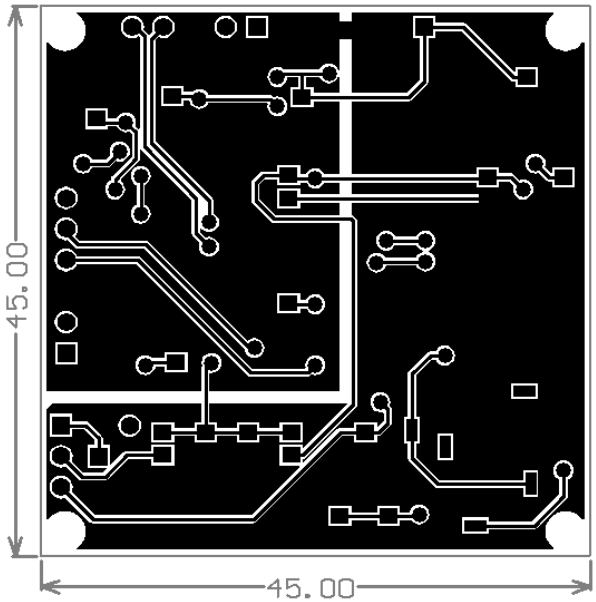

Figure C.4: bottom copper and keep out layers

Figure C.5: A picture of the top layer assembled PCB board

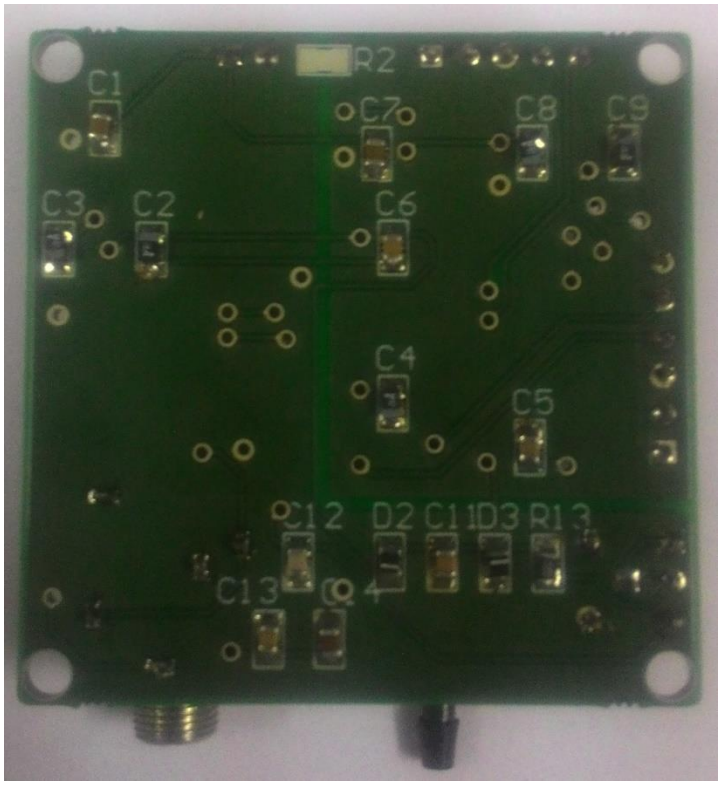

Figure C.6: A picture of the bottom layer assembled PCB board

Appendix D

COMMERCIALLY AVAILABLE BP SIMULATORS

In this appendix, some of the commercially available BP simulators are briefly described. In these simulators, the cuff pressure is sensed through a T-connector inserted in the tubing between the cuff and the measuring instrument.

D.1 Fluke Biomedical "BP pump 2 NIBP simulator"

The simulator [11] provides BP simulation for the oscillometric method for testing noninvasive BP monitors that are for adults and neonatal including both arm and wrist types. It comes in two models: the standard BP pump 2L and the BP pump 2M which features a high-accuracy pressure transducer. BP Pump 2 also includes an optional five-lead ECG test capability. The systolic pressure (SP), diastolic pressure (DP), heart rate (HR) and pulse volume (PV), are user defined. The simulator can simulate respiratory artifacts, including spontaneous breathing and controlled ventilation. The simulator can also simulate arrhythmia, including premature atrial contractions, atrial fibrillation, and premature ventricular contractions. The user can set the simulation parameters including the SP, DP, HR and PV. The SP range is 20 – 250 mmHg, DP range is 10 – 200 mmHg, HR range is 30 – 250 beat/min, and PV range is 0.1 – 2.4 cc. The standard 2L model has pressure accuracy of 1 mmHg + 0.5% in the range of 0 – 300 mmHg, and the accuracy is 2 mmHg if the pressure is in the range of 301 – 400 mmHg. For the high-accuracy 2M model, the accuracy is ±0.7 throughout the full range. The accuracy of the heart rate is 1 beat/min. The simulator is mains powered.

D.2 Rigel Medical "BP-SIM handheld NIBP simulator"

The simulator [12] is used for testing the performance of oscillometric BP monitors. The device is powered by a rechargeable battery which can last for 100 test sessions. It is a handheld device with keyboard and screen for entering the simulation parameters. It has an internal pump for leakage testing. Envelopes of the generated pulses are stored in the device memory. The envelope includes information about the SP and DP values. The stored envelopes are not general, a set of envelopes is stored for every BP monitor from a list of some commercial BP monitors like Omron and Criticare. The heart rate is settable in the range 1 – 300 beat/min. the accuracy of pressure measurement is ± 0.5%.

D.3 Global technologies "Life/form® blood pressure simulator arm"

The simulator [13] is used for training of medical professionals in auscultatory method. The device is powered by a battery. The simulator is form of a manikin of the human arm with a speaker inside it to produce the Korotkoff sounds. The simulation parameters including the SP, DP and HR can be set using a keyboard and a screen on the device. The five phases of Korotkoff sounds are simulated while the cuff is deflated from SP to DP. Auscultatory gap is also

simulated. A palpable pulse at the radial location is also simulated for training the medical professional in the cases where the auscultatory gap is present. Abnormal conditions like arrhythmias are not implemented.

D.4 Gaumard "Blood pressure training system (S415)"

The simulator [14] is a full size-adult adult left arm. It is developed to assist training health professionals to learn the skills required to perform BP measurement using auscultatory method. The device is mains-powered. The simulation parameters including SP, DP, HR and PV are settable using a keyboard and a screen. A stethoscope is needed to auscultate the Korotkoff sounds from a speaker embedded inside the arm. Auscultatory gap and a palpable pulse are simulated. Abnormal conditions like arrhythmias are not implemented.

D.5 Laerdal Medical Corporation "Blood pressure training arm"

The simulator [15] is a manikin of the human arm. It is used for training of medical professionals in auscultatory method. SP, DP, HR, PV is settable by the user through a keyboard and a screen. Auscultatory gap and radial palpable pulse are simulated. Abnormal conditions like arrhythmias are not implemented. The device is mains-powered.

REFERENCES

[1] K. Ng and C. Small, "Review of methods and simulators for evaluation of noninvasive blood pressure monitors," *Journal of Clinical Eng*, vol. 17, no. 6, pp. 469-479, Nov/Dec 1992.

[2] E. O'Brien, N. Atkins, G. Stergiou, N. Karpettas, G. Parati, R. Asmar, Y. Imai, J. Wang, T. Mengden, and A. Shennan, "European society of hypertension international protocol revision 2010 for the validation of blood pressure measuring devices in adults," *Blood Pressure Monitoring*, vol. 15, no. 1, pp. 23 – 38, Feb. 2010.

[3] M. Bottenberg, G. Bryant, S. Haack, and A. North, "Assessing pharmacy students' ability to accurately measure blood pressure using a blood pressure simulator arm," *American Journal of Pharmaceutical Education*, vol. 77, no. 5, Article 98, 2013.

[4] B. Klein, "Dynamic arterial blood pressure simulator," US Patent Application No. 3868844, 4 Mar 1975.

[5] W. Glover and R. Medero, "Arm simulator for an oscillometric blood pressure monitor," US Patent Application No. 4464123, 7 Aug 1984.

[6] P. Tanvar, "Arm simulator for BP measurement," *M. Tech. dissertation*, EE Dept., IIT Bombay, 2013.

[7] P. Gothwal, "Arm simulator for BP measurement," *M. Tech. dissertation*, EE Dept., IIT Bombay, 2011.

[8] L. F. Costello, "Oscillometric non-invasive blood pressure simulator," US Patent Application No. 5027641, 2 July 1991.

[9] K. A. Ruiter and W. W. Ruiter, "Compact oscillometric blood pressure simulator," US Patent Application No. US20100076713A1, 25 Mar 2010.

[10] C. D. Olmstead, C. G. Miller, J. Woods, and S. Dhingra, "Universal sphygmomanometer simulator for live training and evaluation," US Patent Application No. US20140342332A1, 20 Nov 2014.

[[11] Fluke Biomedical, "BP pump 2 non-invasive blood pressure simulator and tester," Nov. 2010. [online]. Available: http://support.fluke.com/biomedical/Download/Asset/2817822_6150_ENG_D_W.PDF [Accessed: June 25, 2018].

[12] Rigel Medical, "BP-SiM NIBP Simulator," 2009. [online]. Available: http://www.rigelmedical.com/downloads/BP-SiM%20Data%20Sheet.pdf [Accessed: June 25, 2018].

[13] Global technologies, “Life/form blood pressure simulator arm,” 2003. [online]. Available: https://www.gtsimulators.com/v/vspfiles/downloadables/lf03204.PDF [Accessed: June 25, 2018].

[14] Gaumard, “Blood Pressure Training System (S415),” 2018. [online]. Available: https://www.gaumard.com/s415 [Accessed: June 25, 2018].

[15] Laerdal Medical Corporation, “SimPad Blood Pressure Trainer,”, “Blood Pressure Training Arm,” June 2018. [online]. Available: https://www.laerdal.com/in/nav/202/Skills-Trainers [Accessed June 19, 2018].

[16] C. Guyton and J. E. Hall, “The heart,” in *Medical Physiology,* 11th ed. pp. 103-115, Philadelphia, Pennsylvania: Elsevier Saunders, 2006.

[17] K. Sembulingam and P. Sembulingam, “Cardiovascular system,” in *Essentials of Medical Physiology*, 5th ed, pp. 500-504, New Delhi: Jaypee, 2010.

[18] American Heart Association, “About Arrhythmia,” Sept. 2016. [online]. Available: http://www.heart.org/HEARTORG/Conditions/Arrhythmia/AboutArrhythmia/About-Arrhythmia_UCM_002010_Article.jsp#.W0i4PdIzbcs [Accessed Oct. 16, 2017].

[19] G. M. Drzewiecki, J. Melbin, and A. Noordergraaf, “The Korotkoff sound,” *Annals of Biomedical Engineering*, vol. 17, pp. 325-359, 1989.

[20] R. S. Khandpur, “Patient monitoring systems,” in *Handbook of Biomedical Instrumentation,* 2nd ed., pp. 218–227, New Delhi: Tata McGraw Hill, 2003.

[21] J. G. Webster, “Blood pressure and sound,” in *Medical Instrumentation Application and Design,* 2nd ed., pp. 394-401, Boston: Houghton Mifflin 1992.

[22] J. M. Askey, “The auscultatory gap in sphygmomanometry,” *Annals of Internal Medicine*, vol. 80, No. 1, pp. 94-97, 1974.

[23] L. A. Geddes, “The indirect measurement of blood pressure,” in *Handbook of blood pressure measurement*, 1st ed., pp. 51 – 118, New York: Springer 1991.

[24] D. Ventzas, “Signal processing and knowledge acquisition in objective blood pressure measurement with conventional clinical sphygmomanometry,” in *Proc. 4th Int. Conf. WSEAS, Info. Sci. & Apps. (BIOHEMED 2004),* Miami, Florida, USA, 2004, pp. 1-10.

[25] American National Standards Institute, “ISO 81060-2/Cor1:2011 Non-invasive sphygmomanometers - Part 2: Clinical validation of automated measurement type - Corrigendum 1,” 2016. [online]. Available: https://webstore.ansi.org/RecordDetail.aspx?sku=ISO+81060-2%2fCor1%3a2011 [Accessed Nov. 22, 2017].

[26] E. O'Brien, J. Petrie, W. Littler, M. Swiet, P. Padfield, D. Altman, M. Bland, A. Coats, and N. Atkins "The hypertension society protocol for the evaluation of blood pressure measuring devices," *Journal of Hypertension*, vol. 11, no. 2, pp. 43 – 62, Mar. 1993.

[27] P. Horowitz and W. Hill, "Digital meets analog," in *Art of Electronics*, UK: Cambridge University Press, 2nd ed. pp. 655-657, 1995.

[28] Thinklabs, "Blood Pressure: Korotkoff Sounds," 2015. [online]. Available: https://www.thinklabs.com/heart-sounds [Accessed: July 4, 2018].

[29] Microchip Technology, "DSPIC33FJ128GP802 16-bit digital signal controller," Apr. 2011. [Online]. Available: http://ww1.microchip.com/downloads/en/DeviceDoc/70292G.pdf. [Accessed Nov. 22, 2017].

[30] Microchip Technology, "Oscillator (Part III) dsPIC33F FRM reference manual," Apr. 2011. [Online]. Available: http://ww1.microchip.com/downloads/en/DeviceDoc/70216D.pdf. [Accessed Nov, 25 2017].

[31] Electrónica 60 Norte, "Bluetooth to serial port module HC05," Nov. 2017. [online]. Available: http://www.electronica60norte.com/mwfls/pdf/newBluetooth.pdf [Accessed Nov. 25, 2017].

[32] IR Robot, "mightyZap user manual V.1.04," May 2018. [online]. Available: https://www.irrobotusa.com/pages/ir-robot-mannual-software-blueprint [Accessed May 21, 2018].

[33] Freescale Semiconductor, "MPXV5050GP Integrated silicon pressure sensor: on-chip signal conditioned, temperature compensated and calibrated," May 2017. [online]. Available: https://www.nxp.com/docs/en/data-sheet/MP3V5050.pdf [Accessed Nov. 25, 2017].

[34] Texas Instrument, "TPA6211A1 3.1-W Mono Fully Differential Audio Power Amplifier," Oct. 2017. [online]. Available: http://www.ti.com/lit/ds/symlink/tpa6211a1.pdf [Accessed: Oct. 2018].

[35] Massachusetts Institute of Technology, "MIT APP Inventor," 2017. [online]. Available: http://appinventor.mit.edu/explore/# [Accessed: June 26, 2018].

Left blank

ACKNOWLEDGEMENT

I would like to express my sincere gratitude towards my supervisor, Prof. P. C. Pandey, for his endless support, precious time, invaluable help, genuine concern, and kind words. I am thankful for Mr. Vidhyadar Kamble for his appreciated efforts in providing all the electronic components. I am grateful to Mr. Uttam for the detailed revision of my dissertation, all my lab mates, Vikas, Susmi, Nitya, Nataraj, and Hirak, for their helpful suggestions, Mr. Aalim M. Mustafa for helping me with the design of the 3D files, and to all the staff members in Tata Centre lab for helping me with the 3D-printing.